(3)
SLAC – PUB – 3747
August 1985
(M)
CONF-850179--1

APPLICATIONS OF QUANTUM CHROMODYNAMICS TO HADRONIC AND NUCLEAR INTERACTIONS*

STANLEY J. BRODSKY AND CHUENG-RYONG JI

Stanford Linear Accelerator Center
Stanford University, Stanford, California, 94305

SLAC-PUB--3747

DE86 000054

ABSTRACT

We review the application of perturbative QCD and light-cone Fock methods to the structure of hadrons and nuclei and their exclusive and inclusive interactions at short distances.

TABLE OF CONTENTS

* Work supported by the Department of Energy, contract DE-AC03-76SF00515.

Invited Lectures presented at the Stellenbosch Advanced Course in Theoretical Physics (Quarks and Leptons), January 21 – February 1, 1985.

1. INTRODUCTION

The basic premise of the lectures at this school is the validity of the Standard Model $SU(3) \times SU(2) \times U(1)$ as the theory of strong, electromagnetic, and weak interactions. In particular, we now have a fundamental theory of the basic interactions and degrees of freedom of both hadrons and nuclei. The postulated theory is quantum chromodynamics (QCD), the renormalizable theory of spin-1/2 quark fields and spin-1 gluon fields, based on an underlying SU(3)-color gauge symmetry.

In principle, QCD could give just as accurate a description of hadronic phenomena as quantum electrodynamics provides for the interactions of leptons, but because of its non-Abelian nature, calculations in QCD are much more complex. The central feature of the theory is, in fact, its non-perturbative nature which leads to the confinement of quarks and gluons in color-singlet bound states. Because of the confinement of the colored quanta, observables always involve the dynamics of bound systems; hadron-hadron interactions are thus at least as complicated as the Van der Waals and covalent exchange forces of neutral atoms.

Unlike atomic physics, the constituents of hadrons are highly relativistic; because the forces are non-static, a hadron cannot be represented as a state of fixed number of quanta at a fixed time. The vacuum structure of QCD relative to the perturbative basis is also complex; virtually every local color-singlet operator constructed from the product of quark and gluon fields has a non-zero vacuum condensate expectation value.

At large distances, the gluonic sector of QCD has been shown to be effectively equivalent to a non-linear sigma model of psuedoscalar mesons, at least for large number of colors.[1] The topological solitons (Skyrmions) can be consistently identified as baryons. The connection between this representation of hadrons at long wavelength and the intuitive concept of the mesons and baryons as composites of quark fields at short distances is at this time only vaguely understood.

Despite the complexity of the theory, QCD has several key properties which make calculations tractable and systematic, at least in the short-distance, high momentum-transfer domain. The critical feature is asymptotic freedom: the effective coupling constant $\alpha_s(Q^2)$ which controls the interactions of quarks and gluons at momentum transfer Q^2 vanishes logarithmically at high Q^2:

$$\alpha_s(Q^2) = \frac{4\pi}{\beta \log(Q^2/\Lambda^2_{\rm QCD})} \qquad (Q^2 \gg \Lambda^2)\,. \tag{1.1}$$

[Here $\beta = 11 - \frac{2}{3}n_f$ is derived from the gluonic and quark loop corrections to the effective coupling constant; n_f is the number of quark contributions to the vacuum polarizations with $m_f^2 \lesssim Q^2$.] The parameter $\Lambda_{\rm QCD}$ normalizes the value of $\alpha_s(Q_0^2)$ at a given momentum transfer $Q_0^2 \gg \Lambda^2$, given a specific renormalization or cutoff scheme. Recently α_s has been determined

fairly unambiguously using the measured branching ratio for upsilon radiative decay $\Upsilon(b\bar{b}) \to \gamma X$:[2]

$$\alpha_s(0.157\ M_\Upsilon) = \alpha_s(1.5\ \text{GeV}) = 0.23 \pm 0.03\ . \tag{1.2}$$

Taking the standard $\overline{MS}$ dimensional regularization scheme, this gives $\Lambda_{\overline{MS}} = 119^{+\ 52}_{-\ 34}$ MeV. In more physical terms, the effective potential between infinitely heavy quarks has the form $[C_F = 4/3$ for $n_c = 3]$,[3]

$$V(Q^2) = -C_F\,\frac{4\pi\alpha_V(Q^2)}{Q^2}$$
$$\alpha_V(Q^2) = \frac{4\pi}{\beta\log(Q^2/\Lambda_V^2)} \qquad (Q^2 \gg \Lambda_V^2) \tag{1.3}$$

where $\Lambda_V = \Lambda_{\overline{MS}}\, e^{5/6} \simeq 270 \pm 100$ MeV. Thus the effective physical scale of QCD is $\sim 1\ f_m^{-1}$. At momentum transfers beyond this scale, α_s becomes small, QCD perturbation theory becomes applicable, and a microscopic description of short-distance hadronic and nuclear phenomena in terms of quark and gluon subprocesses becomes viable.

Thus perturbative calculations for processes in which all of the interacting particles are forced to exchange large momentum transfer is justified. Complimentary to asymptotic freedom is the existence of factorization theorems for both exclusive and inclusive processes at large momentum transfer. In the case of exclusive processes (in which the kinematics of all the final state hadrons are fixed) the hadronic amplitude can be represented as the product of a hard-scattering amplitude for the constituent quarks convoluted with a distribution amplitude for each ingoing or outgoing hadron. The distribution amplitude contains all of the bound-state dynamics and specifies the momentum distribution of the quarks in ther hadron. The hard scattering amplitiude can be calculated pertubatively in powers of $\alpha_s(Q^2)$. The predictions can be applied to form factors, exclusive photon-photon reactions, photoproduction, fixed-angle scattering, etc.

In the case of high momentum transfer inclusive reactions (in which final state hadrons are summed over), the hadronic cross section can be computed from the product of a perturbatively-calculable hard-scattering subprocess cross section invoving quarks and gluons convoluted with the appropriate quark and gluon structure functions which incorporate all of bound-state dynamics.[4] Since the distribution amplitudes and structure functions only depend on the composition of the respective hadron but not the nature of the high momentum transfer reaction, the complicated non-perturbative QCD dynamics is factorized out as universal quantities which may be parameterized to give useful phenomenological predictions.

The general structure of QCD indeed meshes remakarbly well with the facts of the hadronic world, especially quark-based spectroscopy, current algebra, the approximate point-like structure

of large momentum transfer inclusive reactions, and the logarithmic violation of scale invariance in deep inelastic lepton-hadron reactions. QCD has been remakably successful in predicting the features of electron-positron and photon-photon annnihilation into hadrons, including the magnitude and scaling of the cross sections, the production of hadronic jets with patterns conforming to elementary quark and gluon subprocess, as well as phenomena associated with the production and decay of heavy hadrons. Recent Monte-Carlo studies incorporating some features of coherence (angle-ordering) have been very successful reproducing the detailed features of the two-jet ($q\bar{q}$) and three-jet ($q\bar{q}g$) reactions. All of the experimental measurements appear to be consistent with the basic postulates of QCD, that the the charge and weak currents within hadrons are carried by fractionally-charged quarks, and that the strength of the interactions between the quarks and gluons becomes weak at short distances, consistent with asymptotic freedom.

The central unknown in the QCD predictions is the composition of the hadrons in terms of their quark and gluon quanta. Recently several important tools have been developed which allow specific predictions for the hadronic wavefunctions directly from the theory. A primary tool is the use of light-cone quantization to construct a consistent relativistic Fock state basis for the hadrons in terms of quark and gluon quanta. The distribution amplitude and the structure functions are defined directly in terms of these light-cone wavefunctions. The form factor of a hadron can be computed exactly in terms of a convolution of initial and final light-cone Fock state wavefunctions.

A second important tool is the use of QCD sum rules to provide constraints on the moments of the hadron distribution amplitudes.[5] This method has yielded important information on the possible momentum space strucure of hadrons. A particularly important advance is the construction of nucleon distribution amplitudes, which together with the QCD factorization formulae, predicts the correct sign and magnitude as well as scaling behavior of the proton and neutron form factors.

Another recent advance has been the development of a formalism to calculate the moments of the distribution using lattice guage theory.[6] The initial results are extremely interesting – suggesting a highly structured oscillating momentum-space valence wavefunction for the meson. The results from both the lattice calculations and QCD sum rules also demonstrate that the light quarks are highly relativistic in the bound state wavefunctions. This gives further indication that while potential models are useful for ennumerating the spectrum of hadrons (because they express the relevant degrees of freedom), they are not reliable predicting wavefunction structure.

The plan of these lectures is then as follows. A brief introduction to the construction of a Fock representation of hadronic wavefunctions on the light-cone is given in Chapter 2. The explicit construction and quantization of field theories on the light cone including the application to QCD is given in Appendixes A and B. The application of this formalism to large momentum transfer

processes is presented in Chapter 3. The constraints imposed by QCD sum rules on the hadronic wavefunctions is reviewed. We also discuss the explicit predictions of QCD for the form factors of bound states of heavy quarks. In this case the distribution amplitude is fixed by non-relativistic constraints. An interesting prediction is an exact zero in the cross section for the production of two heavy psuedoscalar mesons at a predictable energy in electron-positron annihilation.

In Chapter 4 we discuss some novel applications of QCD to exclusive nuclear processes. The role of hidden color in multiquark systems is discussed in Chapter 5 as well as rigorous constraints on the short distance behavior of the nuclear force. The breakdown of the traditional impulse approximation and the emergence of reduced-amplitude scaling is demonstrated in Appendix C. Other limitations on traditional nuclear physics and conclusions are presented in Chapter 6.[7]

REFERENCES

1. E. Witten, Nucl. Phys. B223, 422,433 (1983). For a recent review of Skyrmion physics and further references see V. P. Nair, IAS Princeton preprint (1985).
2. C. Klopfenstein *et al.*, CUSB 83-07 (1983).
3. S. J. Brodsky, G. P. Lepage, P. B. Mackenzie, Phys. Rev. D28, 228 (1983). The problem of setting the scale of the argument of the running coupling constant is discussed in this paper.
4. For a review of these topics, see F. Close, this volume.
5. V. L. Chernyak and A. R. Zhitnitskii, Phys. Rept. 112, 173 (1984).
6. S. Gottlieb and A. S. Kronfeld, CLNS-85/646 (June 1985). A. S. Kronfeld and D. M. Photiadis, Phys. Rev. D31, 2939 (1985).
7. For additional discussion of applications of QCD to nuclear physics and references, see S. J. Brodsky, published in the proceedings of the conference "New Horizons in Electromagnetic Physics", University of Virginia, April 1982; S. J. Brodsky, T. Huang and G. P. Lepage, SLAC-PUB-2868 (1982) published in Springer Tracts in Modern Physics, Vol. 100, "Quarks and Nuclear Forces", ed. D. Fries and B. Zeitnitz (1982); S. J. Brodsky and G. P. Lepage, in the proceedings of the Eugene Few Body Conference 1980: 247C (Nucl. Phys. A363, 1981) and S. J. Brodsky, in the proceedings of the NATO Pacific Summer Institute Progress in Nuclear Dynamics, Vancouver Island (1982).

2. QCD ON THE LIGHT-CONE

A central problem in hadron (and nuclear) physics is how to represent analytically the wave function of a relativistic multi-particle composite system. In general, it is not possible to represent a relativistic field theoretic bound system with a single wave function limited to a fixed number of constituents at a given time since the interactions create new quanta. In principle, the Bethe-Salpeter formalism (or its covariant equivalents) can be used, but in practice such tools are intractable. For example, in order to derive the Dirac equation for the electron in a static Coulomb field from the Bethe-Salpeter equation for muonium with $m_\mu/m_e \to \infty$ one reqires an infinite number of irreducible kernel contributions to the QED potential. The calculation of the deep inelastic structure functions of a composite system requires Bethe-Salpeter amplitudes of an arbitrary number of fields. Matrix elements of currents and the wave function normalization also require, at least formally, the consideration of an infinite sum of irreducible kernels. The relative-time dependence of the covariant formalism adds further complexities. The difficulties are even worse in QCD for the multi-field degrees of freedom of hadrons and nuclei.

A different and more intuitive procedure would be to extend the Schrödinger wave function description of bound states to the relativistic domain by developing a relativistic many-body Fock expansion for the hadronic state. Formally this can be done by quantizing QCD at equal time, and calculating matrix elements from the time-ordered expansion of the S-matrix. For example, the calculation of a covariant Feynman diagram with n-vertices requires the calculation of $n!$ frame-dependent time-ordered amplitudes. Even worse, the calculation of the normalization of a bound state wave function (or the matrix element of a charge or current operator) requires the computation of contributions from all amplitudes involving particle production from the vacuum. (Note that even after normal-ordering the interaction Hamiltonian density for QED, $H_I = e : \overline{\psi}\gamma_\mu \psi A^\mu :$, contains contributions $b^+ d^+ a^+$ which create particles from the perturbative vacuum.)

Fortunately, there is a natural and consistent covariant framework, originally due to Dirac,[1] for describing bound states in gauge theory analogous to the Fock state in non-relativistic physics. This framework is the light-cone formalism in which

$$|\pi\rangle = |q\bar{q}\rangle\, \psi^\pi_{q\bar{q}} + |q\bar{q}g\rangle\, \psi^\pi_{q\bar{q}g} + \cdots$$
$$|p\rangle = |qqq\rangle\, \psi^p_{qqq} + |qqqg\rangle\, \psi^p_{qqqg} + \cdots \tag{2.1}$$

Each wave function component ψ_n, etc. describes a state of fixed number of quark and gluon quanta evaluated in the interaction picture at equal light-cone "time" $\tau = t + z/c$. Given the $\{\psi_n\}$, virtually any hadronic property can be computed, including anomalous moments, form factors, structure functions for inclusive processes, distribution amplitudes for exclusive processes, etc.[2]

The use of light-cone quantization and equal τ wave functions, rather than equal t wave functions, is necessary for a sensible Fock state expansion. It is also convenient to use τ-ordered light-cone perturbation theory (LCPTh) in place of covariant perturbation theory for much of the analysis of light-cone dominated processes such as deep inelastic scattering, or large-$p_\perp$ exclusive reactions. Light-cone quantization and perturbation theory are developed in detail in Appendices A and B.

In light-cone quantization, the Fock state vacuum is an eigenstate of the full light-cone Hamiltonian ($H_{LC} \equiv P^- = P^0 - P^3$, conjugate to τ), and also all of the bare quanta in an hadronic Fock state are associated with the hadron; none are disconnected elements of the vacuum. This follows because of four-momentum conservation and because all particles in LCPTh, just as in TOPTh, are on the mass shell. The momentum components $P^+ \equiv P^0 + P^3$ and $\vec{P}_\perp = (P^1, P^2)$ are conserved, and since each particle is on-shell, P^+ is positive. Furthermore, since all P_i^+ are positive and conserved, amplitudes for vertices with zero particles entering or leaving vanish.

An essential feature of the light-cone Fock state basis is its orthornormality, providing a convenient basis for expanding the physical states and physical observables in terms of quark and gluon degrees of freedom. For example the form factor of a general system can be written in a simple and elegant form directly in terms of the Fock state wavefunctions:[3] (a sum over Fock components ψ_n is understood)

$$F(\vec{q}_\perp^{\,2}) = \sum_{a=1}^{n} e_a \int [dx] \int [d^2\vec{k}_{\perp i}]\; \psi_n^*\left(x_i, \vec{k}_{\perp i} + (\delta_{ia} - x_i)\,\vec{q}_\perp\right)\; \psi_n(x_i, \vec{k}_{\perp i})\;, \tag{2.2}$$

where $\vec{q}_\perp$ is absorbed by a^{th} quark, $\vec{q}_\perp^{\,2} = Q^2$, and

$$\begin{aligned} [dx] &= \delta\left(1 - \sum_{i=1}^{n} x_i\right) \prod_{i=1}^{n} dx_i \quad , \\ [d^2\vec{k}_{\perp i}] &= 16\pi^3\,\delta^2\left(\sum_{i=1}^{n} \vec{k}_{\perp i}\right) \prod_{i=1}^{n} \frac{d^2\vec{k}_{\perp i}}{16\pi^3} \quad . \end{aligned} \tag{2.3}$$

This formula is easily derived from the matrix element of the current $\langle p|J^\mu(0)|p+q\rangle$ by choosing the $\mu = +$ component in a frame where $\vec{p}_\perp = 0$ and $q^+ = 0$. [See Fig. 1.] Since the current conserves the + component of the struck constituent and the interactions cannot create particles from the vacuum, the form factor takes on a simple local form of a convolution of light-cone wavefucntions. Similarily, the structure functions for inclusive reactions can be written down as a simple summation over the square of the light-cone Fock state wavefuctions. [See Table 3.1.] In the gauge $A^+ = 0$ there are no negative-norm ghost contributions even in non-Abelian gauge theory.

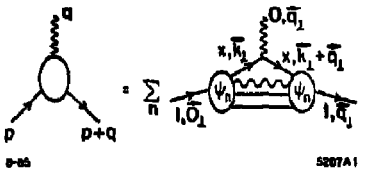

Fig. 1. Calculation of current matrix elements in light-cone perturbation theory.

As we show in Appendix B, the light-cone method in its descretized form for a finite x^- interval gives a block diagonal Hamiltonian for field theories in one space and one time dimension. This opens the possibility of an optimized numerical solution to a class of non-trivial theories.

The application of these methods to high momentum processes in QCD is discussed in the next Chapter.

REFERENCES

1. P. A. M. Dirac, Rev. Mod. Phys. 21, 392 (1949). Further references to light-cone quantization are given in Appendix A.
2. See, e.g. G. P. Lepage and S. J. Brodsky, Phys. Rev. D22, 2157 (1980).
3. S. D. Drell and T. M. Yan, Phys. Rev. Lett. 24, 181 (1970).

3. EXCLUSIVE PROCESSES IN QCD

Although we do not have complete information on the hadronic wave functions in QCD, it is still possible to make predictions at large momentum transfer directly from the theory. The results are rigorous and can be proved to arbitrary order in perturbation theory. The processes which are most easily analyzed are those in which all final particles are measured at large invariant masses compared to each other, i.e.: large momentum transfer exclusive reactions. This includes form factors of hadrons and nuclei at large momentum transfer Q and large angle scattering reactions such as photoproduction $\gamma p \to \pi^+ n$, nucleon-nucleon scattering, photodisintegration $\gamma d \to np$ at large angles and energies, etc. A key result is that such amplitudes factorize at large momentum transfer in the form of a convolution of a hard scattering amplitude T_H which can be computed perturbatively from quark-gluon subprocesses multiplied by process-independent "distribution amplitudes" $\phi(x,Q)$ which contain all of the bound-state non-perturbative dynamics of each of the interacting hadrons. To leading order in $1/Q$ the scattering amplitude has the form[1]

$$\mathcal{M} = \int_0^1 T_H(x_j,Q) \prod_{H_i} \phi_{H_i}(x_j,Q)[dx] \,. \tag{3.1}$$

Here T_H is the probability amplitude to scatter quarks with fractional momentum $0 < x_j < 1$ from the incident to final hadron directions, and ϕ_{H_i} is the probability amplitude to find quarks in the wavefunction of hadron H_i collinear up to the scale Q, and

$$[dx] = \prod_{j=1}^{n_i} dx_j \delta\left(1 - \sum_k^{n_i} x_k\right) \tag{3.2}$$

The key to the derivation of this factorization of perturbative and non-perturbative dynamics is the use of the Fock basis $\{\psi_n(x_i, \vec{k}_{\perp i}, \lambda_i)\}$ defined at equal $\tau = t + z/c$ on the light-cone to represent relativistic color singlet bound states. Here λ_i are the helicities; $x_i \equiv (k_i^0 + k_i^z)/(p^0 + p^z)$, $(\sum_{i=1}^n x_i = 1)$, and $\vec{k}_{\perp i}$, $(\sum_{i=1}^n \vec{k}_{\perp i} = 0)$, are the relative momentum coordinates. Thus the proton is represented as a column vector of states ψ_{uud}, ψ_{uuds}, ψ_{uudg} .... In the light-cone gauge, $A^+ = A^0 + A^3 = 0$, only the minimal "valence" Fock state needs to be considered at large momentum transfer since any additional quark or gluon forced to absorb large momentum transfer yields a power-law suppressed contribution to the hadronic amplitude. For example at large Q^2, the baryon form factor can be systematically computed by iterating the valence Fock state wavefunction equation of motion wherever large relative momentum occurs. To leading order the kernel is effectively one-gluon exchange. The sum of the hard gluon exchange contributions is the gauge invariant amplitude T_H. The residual factor from the wavefunction is the distribution amplitude ϕ_B which plays the role of the wavefunction at the origin in the analogous non-relativistic

calculation. Thus we obtain the form: [See Fig. 2(a)]

$$F_B(Q^2) = \int_0^1 [dy] \int_0^1 [dx]\ \phi_B^\dagger(y_j, Q) T_H(x_i, y_j, Q) \phi_B(x_i, Q) \quad , \tag{3.3}$$

where to leading order in $\alpha_s(Q^2)$, T_H is computed from $3q + \gamma^* \to 3q$ tree graph amplitudes: [Fig. 2(b)]

$$T_H = \left[\frac{\alpha_s(Q^2)}{Q^2}\right]^2 f(x_i, y_j) \tag{3.4}$$

and

$$\phi_B(x_i, Q) = \int [d^2 k_\perp]\ \psi_V(x_i, \vec{k}_{\perp i}) \theta(k_{\perp i}^2 < Q^2) \tag{3.5}$$

is the valence three-quark wavefunction [Fig. 2(c)] evaluated at quark impact separation $b_\perp \sim O(Q^{-1})$. Since ϕ_B only depends logarithmically on Q^2 in QCD, the main dynamical dependence of $F_B(Q^2)$ is the power behavior $(Q^2)^{-2}$ derived from scaling of the elementary propagators in T_H. Thus, modulo logarithmic factors, one obtains a dimensional counting rule[2] for any hadronic or nuclear form factor at large Q^2 ($\lambda = \lambda' = 0$ or $1/2$)

$$F(Q^2) \sim \left(\frac{1}{Q^2}\right)^{n-1} , \tag{3.6}$$

$$F_1^N \sim \frac{1}{Q^4} , \quad F_\pi \sim \frac{1}{Q^2} , \quad F_d \sim \frac{1}{Q^{10}} , \tag{3.7}$$

where n is the minimum number of fields in the hadron. Since quark helicity is conserved in T_H and $\phi(x_i, Q)$ is the $L_z = 0$ projection of the wavefunction, total hadronic helicity is conserved at large momentum transfer for any QCD exclusive reaction.[3] The dominant nucleon form factor thus corresponds to $F_1(Q^2)$ or $G_M(Q^2)$; the Pauli form factor $F_2(Q^2)$ is suppressed by an extra power of Q^2. In the case of the deuteron, the dominant form factor has helicity $\lambda = \lambda' = 0$, corresponding to $\sqrt{A(Q^2)}$. The general form of the logarithmic dependence of $F(Q^2)$ can be derived from the operator product expansion at short distance or by solving an evolution equation for the distribution amplitude computed from gluon exchange [Fig. 2(c)], the only QCD contribution which falls sufficiently small at large transverse momentum to effect the large Q^2 dependence.

The distribution amplitude for a baryon is determined by an evolution equation which can be derived from the Bethe-Salpeter equation at large transverse momentum projected on the light-cone:[1]

$$\left(Q^2 \frac{\partial}{\partial Q^2} + \frac{3C_F}{2\beta}\right) \phi(x_i, Q) = \frac{C_B}{\beta} \int [dy]\ V(x_i, y_i)\, \phi(y_i, Q) \quad , \tag{3.8}$$

where $C_F = (n_c^2 - 1)/2n_c = 4/3$, $C_B = (n_c + 1)/2n_c = 2/3$, $\beta = 11 - (2/3)n_f$, and $V(x_i, y_i)$ is computed to leading order in α_s from the single-gluon-exchange kernel. The evolution equation

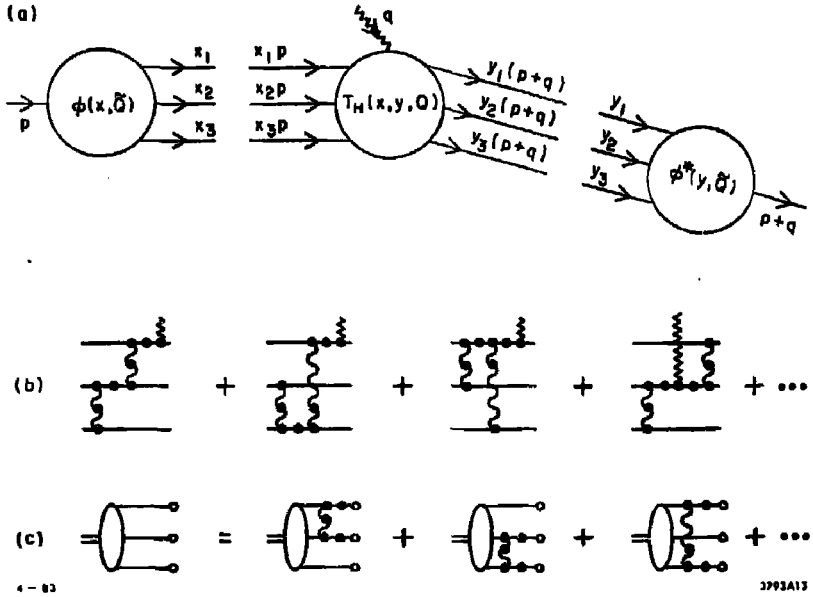

Fig. 2. (a) Factorization of the nucleon form factor at large Q^2 in QCD. The optimal scale $\tilde{Q}$ for the distribution amplitude $\phi(x,\tilde{Q})$ is discussed in Ref. 9. (b) The leading order diagrams for the hard scattering amplitude T_H. The dots indicate insertions which enter the renormalization of the coupling constant. (c) The leading order diagrams which determine the Q^2 dependence of $\phi_B(x,Q)$.

automatically sums to leading order in $\alpha_s(Q^2)$ all of the contributions from multiple gluon exchange which determine the tail of the valence wavefunction and thus the Q^2-dependence of the distribution amplitude. The general solution of this equation is

$$\phi(x_i,Q) = x_1x_2x_3 \sum_{n=0}^{\infty} a_n \left(\ell n \frac{Q^2}{\Lambda^2}\right)^{-\gamma_n} \check{\phi}_n(x_i) \quad , \tag{3.9}$$

where the anomalous dimensions γ_n and the eigenfunctions $\check{\phi}_n(x_i)$ satisfy the characteristic equation:

$$x_1x_2x_3\left(-\gamma_n + \frac{3C_F}{2\beta}\right)\check{\phi}_n(x_i) = \frac{C_B}{\beta}\int_0^1 [dy]\, V(x_i,y_i)\,\check{\phi}_n(y_i) \quad . \tag{3.10}$$

In the large Q^2 limit, only the leading anomalous dimension γ_0 contributes to the form factor.

A useful technique for solving the evolution equations is to construct completely antisymmetric representations as a polynomial orthonomal basis for the distribution amplitude of multiquark bound states.[4] In this way one obtain a distinctive classification of nucleon (N) and delta (Δ) wave functions and the corresponding Q^2 dependence which discriminates N and Δ form factors. The antisymmetrization technique will be presented in detail in chapter 6 for nuclear systems.

The result for the large Q^2 behavior of the baryon form factor in QCD is then[1,5,6]

$$F_B(Q^2) = \frac{\alpha_s^2(Q^2)}{Q^4} \sum_{n,m} d_{nm} \left(\ell n \frac{Q^2}{\Lambda^2} \right)^{-\gamma_m - \gamma_n} \tag{3.11}$$

where the γ_n are computable anomalous dimensions of the baryon three-quark wave function at short distance and the d_{nm} are determined from the value of the distribution amplitude $\phi_B(x, Q_0^2)$ at a given point Q_0^2 and the normalization of T_H. Asymptotically, the dominant term has the minimum anomalous dimension. The dominant part of the form factor comes from the region of the x integration where each quark has a finite fraction of the light cone momentum; the end point region where the struck quark has $x \simeq 1$ and spectator quarks have $x \sim 0$ is asymptotically suppressed by quark (Sudakov) form factor gluon radiative corrections.

In Table 3.1 we give a summary of the main scaling laws and properties of large momentum transfer exclusive and inclusive cross sections which are derivable starting from the light-cone Fock space basis and the perturbative expansion for QCD.

As shown in Fig. 3 the power laws predicted by perturbative QCD are consistent with experiment.[7] The behavior $Q^4 G_M(Q^2) \sim const$ at large Q^2 [see Fig. 4] provides a direct check that the minimal Fock state in the nucleon contains three quarks and that the quark propagator and the $qq \to qq$ scattering amplitudes are approximately scale-free. More generally, the nominal power law predicted for large momentum transfer exclusive reactions is given by the dimensional counting rule $M \sim Q^{4-n_{TOT}} F(\theta_{cm})$ where n_{TOT} is the total number of elementary fields which scatter in the reaction. The predictions are apparently compatible with experiment.[8] In addition, for some scattering reactions there are contributions from multiple scattering diagrams (Landshoff contributions) which together with Sudakov effects can lead to small power-law corrections, as well as a complicated spin, and amplitude phase phenomenology.[9] As shown in Fig. 5, recent measurements of $\gamma\gamma \to \pi^+\pi^-$, K^+K^- at large invariant pair mass are also consistent with the QCD predictions.[10] In principle it should be possible to use measurements of the scaling and angular dependence of the $\gamma\gamma \to M\bar{M}$ reactions to measure the shape of the distribution amplitude $\phi_M(x, Q)$.

An actual calculation of $\phi(x, Q)$ from QCD requires non-perturbative methods such as lattice gauge theory, or more directly, the solution of the light-cone equation of motion

$$\left[M^2 - \sum_{i=1}^{n} \left(\frac{k_\perp^2 + m^2}{x} \right)_i \right] \Psi = V_{\rm QCD} \Psi \tag{3.12}$$

The explicit form for the matrix representation of $V_{\rm QCD}$ and a discussion of the infrared and ultraviolet regulation required to interpret this result is given in Ref. 1. Thus far experiment has not been sufficiently precise to measure the logarithmic modification of dimensional counting rules predicted by QCD.

Table 3.1 Comparison of Exclusive and Inclusive Cross Sections

Exclusive Amplitudes	Inclusive Cross Sections
$\mathcal{M} \sim \prod \phi(x_i, Q) \otimes T_H(x_i, Q)$	$d\sigma \sim \prod G(x_a, Q) \otimes d\hat{\sigma}(x_a, Q)$
$\phi(x, Q) = \int^Q [d^2k_\perp]\, \psi^Q_{\rm val}(x, k_\perp)$	$G(x, Q) = \sum_a \int^Q [d^2k_\perp]\, [dx]'\, \lvert\psi^Q_a(x, k_\perp)\rvert^2$
Measure ϕ in $\gamma\gamma \to M\overline{M}$	Measure G in $\ell p \to \ell X$
$\sum_{i \in H} \lambda_i = \lambda_H$	$\sum_{i \in H} \lambda_i \neq \lambda_H$
	Evolution
$\frac{\partial \phi(x, Q)}{\partial \log Q^2} = \alpha_s \int [dy]\, V(x, y)\, \phi(y)$	$\frac{\partial G(x, Q)}{\partial \log Q^2} = \alpha_s \int dy\; P(x/y)\, G(y)$
$\lim_{Q \to \infty} \phi(x, Q) = \prod_i x_i \cdot C_{\rm flavor}$	$\lim_{Q \to \infty} G(x, Q) = \delta(x)\, C$
	Power Law Behavior
$\frac{d\sigma}{dx}(A + B \to C + D) \cong \frac{1}{s^{n-2}} f(\theta_{\rm c.m.})$	$\frac{d\sigma}{d^2p/E}(AB \to CX) \cong \sum \frac{(1 - x_T)^{2n_a - 1}}{(Q^2)^{n_{act} - 2}} f(\theta_{\rm c.m.})$
$n = n_A + n_B + n_C + n_D$	$n_{act} = n_a + n_b + n_c + n_d$
T_H : expansion in $\alpha_s(Q^2)$	$d\hat{\sigma}$: expansion in $\alpha_s(Q^2)$
	Complications
End point singularties	**Multiple scales**
Pinch singularities	**Phase-space limits on evolution**
High Fock states	**Heavy quark thresholds**
	Higher twist multiparticle processes
	Initial and final state interactions

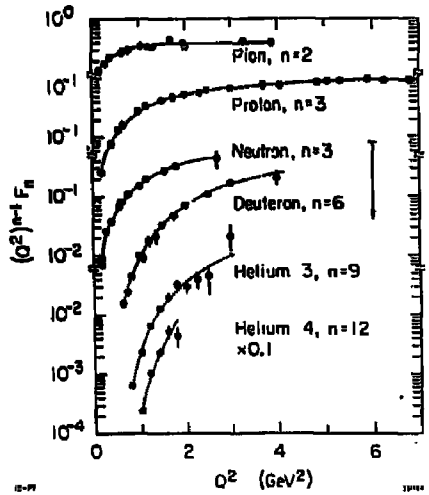

Fig. 3. Comparison of experiment with the QCD dimensional counting rule $(Q^2)^{n-1}F(Q^2) \sim const$ for form factors. The proton data extends beyond 30 GeV^2.

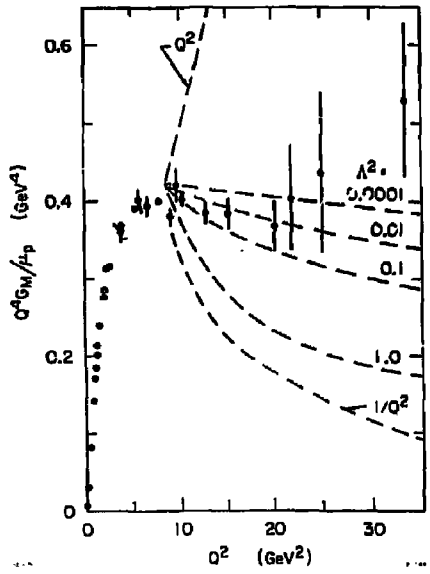

Fig. 4. Prediction for $Q^4G_M^p(Q^2)$ for various QCD scale parameters Λ^2 (in GeV^2). The data are from Ref. 25. The initial wave function is taken as $\phi(x,\lambda) \propto \delta(x_1 - \frac{1}{3})\delta(x_2 - \frac{1}{3})$ at $\lambda^2 = 2$ GeV^2. The factor $(1 + \frac{m_p^2}{Q^2})^{-2}$ is included in the prediction as a representative of mass effects; problems with the overall normalization and sign are ignored here.

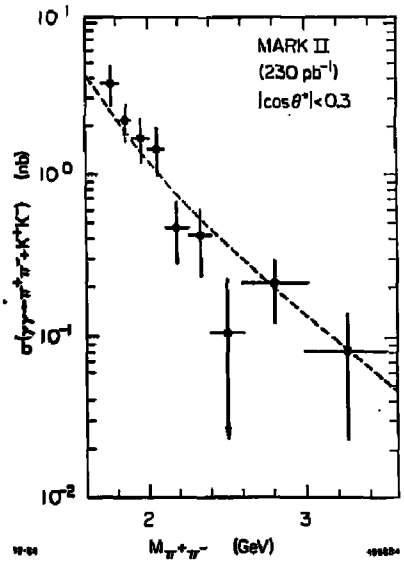

Fig. 5. Measured cross section for $\gamma\gamma \to \pi^+\pi^-$ plus $\gamma\gamma \to K^+K^-$ integrated over the angular region $|\cos\theta^*| < 0.3$. The errors contain systematic as well as statistical contributions. The curve is a perturbative QCD prediction.

Checks of the normalization of $(Q^2)^{n-1}F(Q^2)$ require independent determinations of the valence wavefunction, for example, as has been obtained through QCD sum rules. [See Section 3.1.] It has also been suggested that the relatively large normalization of $Q^4G_M^p(Q^2)$ at large Q^2 can be understood if the valence three-quark state has small transverse size, i.e., is large at the origin.[11] The physical radius of the proton measured from $F_1(Q^2)$ at low momentum transfer then reflects the contributions of the higher Fock states $qqqg$, $qqqq\bar{q}q$ (or meson cloud), etc. A small size for the proton valence wavefunction (e.g., $R^p_{qqq} \sim 0.2$ to $0.3\ fm$) can also explain the large magnitude of $\langle k_\perp^2 \rangle$ of the intrinsic quark momentum distribution needed to understand hard-scattering inclusive reactions. The necessity for small valence state Fock components can be demonstrated explicitly for the pion wavefunction, since $\psi_{q\bar{q}/\pi}$ is constrained by sum rules derived from $\pi^+ \to \ell^+\nu$, and $\pi^0 \to \gamma\gamma$. One finds a valence state radius $R^\pi_{q\bar{q}} \sim 0.4\ fm$, corresponding to a probability $P^\pi_{q\bar{q}} \sim 1/4$. The consequences of a small valence radius are discussed in Chapter 6.

3.1 QCD Sum Rule Constraints on Hadron Wavefunctions

Useful constraints[5] on the lowest moments of the distribution amplitude can be obtained using the QCD sum rule approach of the ITEP Group or by resonance saturation of vertex functions.[12] Although the numerical accuracy of these complementary methods is not known the general agreement between their predictions and overall consistency with other hadron phenomenology lends credence to their validity.

Let us first illustrate the QCD sum rule method for the case of the pion distribution amplitude. The moments $\langle x^n \rangle$ are expressible as matrix elements of gauge invariant local operators:

$$(z\cdot P)^{n+1} f_\pi \langle x^n \rangle = \langle \Omega | O_n(x) | \pi(p) \rangle \equiv \langle \Omega | \bar{d}\, \not{z}\gamma_5 (iz\cdot \overleftrightarrow{D})^n u | \pi(p) \rangle$$

$$\langle x^n \rangle = \int_{-1}^{1} dx\, x^n \phi_\pi(x)$$

where $x = x_1 - x_2$, $\langle x^0 \rangle = 1$, $f_\pi \cong 133$ MeV, p^μ is the pion four momentum, z is a light-like vector: $z^2 = 0$, $z\cdot p = p^+$, $\overleftrightarrow{D}_\mu = \overrightarrow{D}_\mu - \overleftarrow{D}_\mu$, where $\overrightarrow{D}_\mu = \overrightarrow{\partial}_\mu - igA^a_\mu \cdot \frac{\lambda^a}{2}$. This relation is simplest in the gauge $z\cdot A = A^+ = 0$. The state $|\Omega\rangle$ is the true QCD vacuum.

In order to obtain constraints on the $\langle x^n \rangle$ one considers the correlation function between two of the O_n:

$$I_{no}(z,q) = i \int d^4y\, e^{iq\cdot y} \langle \Omega | T\, O_n(y) O_o(0) | \Omega \rangle$$

$$= (z\cdot q)^{n+2}\, I_{no}(q^2)\ .$$

The "signal" between $O_0^{(0)}$ and $O_n(y)$ is carried by the pion, higher meson resonances, and the continuum. At high $q^2 \Rightarrow -\infty$, $y^2 \sim 0(1/Q^2)$ and the operator product expansion allows one to

calculate I_{no} as an expansion in power of $1/Q^2$:

$$I_{no}(q^2) = -\frac{ln(-q^2)}{4\pi^2}\frac{3}{(n+1)(n+3)} + \frac{\langle\Omega|\frac{\alpha_s}{\pi}G^2_{\mu\nu}(0)|\Omega\rangle}{12q^4}$$
$$-\frac{32\pi}{81}(11+4n)\frac{|\langle\Omega|\sqrt{\alpha_s}\,\bar{u}u|\Omega\rangle|^2}{q^6} + \sum_{k>4}\frac{\langle\bar{O}_n\rangle}{(q^2)^k}\,.$$

Operators proportional to current quark masses m_s and m_d have been neglected. The first term is the perturbative quark-pair contribution. The "condensates" $\langle G^2\rangle$ and $|\langle\bar{u}u\rangle|^2$ terms give the leading effect for quark propagation in the QCD vacuum. From other phenomenology the ITEP group have determined

$$\left\langle O\left|\frac{\alpha_s}{\pi}G^2\right|O\right\rangle = 1.2\times10^{-2}\ GeV^4,$$

$$\left\langle O\left|\sqrt{\alpha_s}\bar{u}u\right|0\right\rangle = 1.35\times10^{-2}\ GeV^{-2}\,.$$

On the other hand $I_{no}(q^2)$ can be computed from a dispersion integral over intermediate states:

$$I_{no}(q^2) = \frac{1}{\pi}\int_0^\infty Im\frac{I_{no}(s)ds}{s-q^2+ie}\,.$$

In the approach of Ref. 5 one approximates the spectral density by the form

$$\frac{1}{\pi}ImI_{no}(s) = f_\pi^2\langle x^n\rangle_\pi + f_A^2\langle x^n\rangle_{A_1} + \theta(s-s_n)\frac{3}{4\pi^2(n+1)(n+3)}$$

which takes into account the pion and A_1-meson contributions and a continuum which coincides with the contribution of free quarks. The threshold value s_n is an adjustable parameter.

The identification of the power-law and resonance contributions is a form of a duality relation. The matching of contributions is usually performed using a Borel transformation which de-emphasizes the high mass region:

$$\frac{1}{\pi M^2}\int_0^\infty ds\ e^{-s/M^2}Im\ I_{no}(s) = \frac{1}{4\pi^2}\frac{3}{(n+1)(n+3)} + \frac{\langle0|\frac{\alpha_s}{\pi}G^2|0\rangle}{12M^4}$$
$$+\frac{16}{81}\pi(11+4n)\frac{|\langle0|\sqrt{\alpha_s}\bar{u}u|0\rangle|^2}{M^6} + \sum_{k>6}C_k(n)\frac{(-1)^k}{(k-1)!}\frac{\langle0|\bar{O}_k|0\rangle}{(M^2)^k}\,.$$

For small n, M^2 can be chosen small so that the simultaneous values for the $\langle|\bar{O}_k|\rangle$ and values

for the $\langle x^n \rangle$ can be extracted. The best fit obtained in Ref. 5 are

$$\langle x^2 \rangle_\pi = 0.40, \qquad \langle x^2 \rangle_{A_1} = 0.04 - 0.07$$
$$(M^2 = 1.5 \text{ GeV}^2, \quad S_2 \cong 1.8 \text{ GeV}^2)$$
$$\langle x^4 \rangle_\pi = 0.24$$
$$(M^2 = 2.2 \text{ GeV}^2, \quad S_4 \cong 2.5 \text{ GeV}^2)$$

($\langle x^4 \rangle_{A_1}$ is small but not determined accurately.) The value of the renormalization scale is of the order of M^2 or S_n.

The relatively large values for the second and fourth moments imply that the pion distribution is quite broad. An additional constraint on the distribution amplitude is that ϕ vanishes at least as fast as ϕ_π^{asympt} at the endpoints $x \to \pm 1$. Together these constraints imply a double-humped distribution; the model proposed in Ref. 5 is

$$\phi_\pi(x, \mu) = \frac{15}{4} x^2 (1 - x^2) \, .$$

There are a number of approximations which make it difficult to assess the numerical accuracy of the results. Nevertheless the distribution amplitudes derived by Chernyak and Zhitnitshy serve as useful forms for making QCD predictions for exclusive processes.

One of the consequences of the QCD sum rule approach is a striking dependence of the shape of the ρ—meson distribution amplitude on its helicity. This can be traced to the fact that the $\langle \bar{\psi}\psi\bar{\psi}\psi \rangle$ contribution changes sign because of the helicity dependence of the gluon-exchange interaction. A simple model for the ρ which satisfy the moment constraints is:

$$\phi^\rho(x, \mu) = \phi_{asympt}(x) \begin{cases} \frac{15}{16} x_1 x_2 & \lambda = \pm 1 \\ 1 + \frac{3}{2}\left((x_1 - x_2)^2 - \frac{1}{5}\right) & \lambda = 0 \, . \end{cases}$$

In each case the evolution from $\mu = 500$ MeV can be computed by expanding in terms of two lowest order Gegenbauer polynominal eigensolution. The strong helicity dependence of the ρ distribution amplitude has interesting consequences of the angular dependence of $\gamma\gamma \to \rho\rho$ cross sections.[5,10]

The requirement that the nucleon is the $I = 1/2$, $S = 1/2$ color singlet representation of three quark fields in QCD uniquely specifies the x_i permutation symmetry of the proton distribution amplitude:[13]

$$\phi_\uparrow^p(x_i, \mu) \propto \frac{1}{\sqrt{6}} \left[d_\uparrow u_\downarrow u_\uparrow + u_\uparrow u_\downarrow d_\uparrow - 2u_\uparrow d_\downarrow u_\uparrow\right] \cdot \frac{1}{8} f_N \left[\phi_N(x_1 x_2 x_3) + \phi_N(x_3 x_2 x_1)\right]$$
$$+ \frac{1}{\sqrt{2}} \left[d_\uparrow u_\downarrow u_\uparrow - u_\uparrow u_\downarrow d_\uparrow\right] \cdot \frac{1}{8\sqrt{3}} f_N \left[\phi_N(x_3 x_2 x_1) - \phi_N(x_1 x_2 x_3)\right]$$

The neutron distribution amplitude is determined by the substitution $\phi_n = -\phi_p(u \to d)$. Mo-

ments of the nucleon distribution amplitude can be computed from the correlation function of the appropriate local quark field operators that carry the nucleon quantum numbers.

The model wavefunction proposed in Ref. 13, consistent with the derived moments, is

$$\phi_N(x_1x_2x_3) = \phi_{asympt} \cdot [11.35(x_1^2 + x_2^2) + 8.82x_3^2 - 1.68x_3 - 2.94 - 6.72(x_2^2 - x_1^2)]$$

where $\phi_{asymt} = 120\ x_1x_2x_3$. The renormalization scale is $\mu \cong 1$ GeV. The normalization of the nucleon valence wavefunction is also determined:

$$f_N(\mu = 1\ GeV) = (5.2 \pm 0.3) \times 10^{-3}\ \text{GeV}\ .$$

A striking feature of the QCD sum rule prediction is the strong asymmetry implied by the first moment: 65% of the proton momentum (at $P_z \Rightarrow \infty$) is carried by the u quark with helicity parallel to that of the proton. [See Fig. 6.] The two remaining quarks each carry ~ 15 to 20% of the total momentum. It is this feature of strong asymmetry, together with the value for f_N, which gives perturbative predictions for the proton and neutron form factors consistent in sign and magnitude with experiment. [See Fig. 7.]

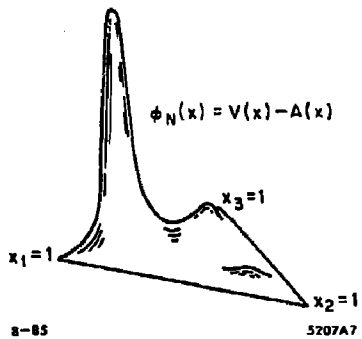

Fig. 6. QCD sum rule prediction for a proton distribution amplitude.

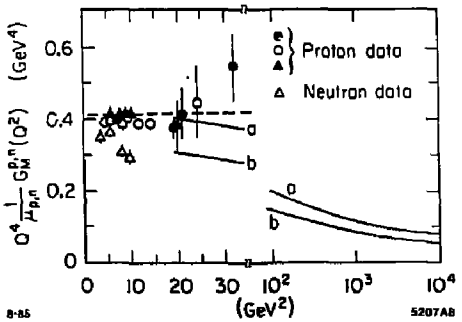

Fig. 7. Perturbative QCD predictions for the proton (curve a) and the neutron (curve b) form factors given by Ref. 13.

The distribution amplitudes based on QCD sum rules are strikingly different from the symmetric forms derived in the $Q^2 \to \infty$ limit. This is in analogy to the case of deep inelastic structure functions which only approach the formal limit of a δ-function at $x = 0$ at a momentum transfer scale very remote from the experimentally accessible range. The implication that the nucleon and pion valence wavefunctions are broad in longitudinal momentum also suggests a broad transverse momentum distribution (small radius) and indicates that quarks bound in light hadrons are highly relativistic.

3.2 Exclusive Production of Higher Generation Hadrons and Form Factor Zeros in QCD

As we have discussed in this chapter, one of the important testing grounds of the perturbative aspects of QCD is exclusive processes at moderate to large momentum transfer. By use of the factorization theorem for exclusive processes and evolution equations for distribution amplitudes, the leading scaling behavior and helicity dependence of form factors and hadron scattering amplitudes can be predicted. In some cases, notably $\gamma\gamma \to \pi^+\pi^-$ and K^+K^-, predictions for the normalization and angular behavior of the cross sections can also be made without explicit information on the nature of the bound state wavefunctions.[10] Recent measurements of the normalization and scaling behavior are, in fact, in good agreement with the QCD predictions. [See Fig. 5]. In most cases, however, detailed predictions for exclusive processes require knowledge of the nonperturbative structure of the hadrons as summarized by the valence quark distribution amplitudes $\phi_H(x_i, Q)$ of the hadrons. For example, we have discussed how, by imposing constraints from QCD sum rules, Chernyak and Zhitnitsky have constructed nucleon distribution amplitudes which account for the sign and normalization as well as the scaling behavior of the proton and neutron magnetic form factors at $-q^2 > 10\ \text{GeV}^2$.

In this section we show that exclusive pair production of heavy hadrons $|Q_1\overline{Q}_2\rangle$, $|Q_1Q_2Q_3\rangle$ consisting of higher generation quarks ($Q_i = t, b, c$, and possibly s) can be reliably predicted[14] within the framework of perturbative QCD, since the required wavefunction input is essentially determined from nonrelativistic considerations. The results can be applied to e^+e^- annihilation, $\gamma\gamma$ annihilation, and W and Z decay into higher generation pairs. The normalization, angular dependence and helicity structure can be predicted away from threshold, allowing a detailed study of the basic elements of heavy quark hadronization.

A particularly striking feature of the QCD predictions is the existence of a zero in the form factor and e^+e^- annihilation cross section for zero-helicity hadron pair production close to the specific timelike value $q^2/4M_H^2 = m_h/2m_\ell$ where m_h and m_ℓ are the heavier and lighter quark masses, respectively. This zero reflects the destructive interference between the spin-dependent and spin-independent (Coulomb exchange) couplings of the gluon in QCD. In fact, all pseudoscalar meson form factors are predicted in QCD to reverse sign from spacelike to timelike asymptotic momentum transfer because of their essentially monopole form. For $m_h > 2m_\ell$ the form factor zero occurs in the physical region.

To leading order in $1/q^2$, the production amplitude for hadron pair production is given by the factorized form

$$M_{H\overline{H}} = \int [dx_i] \int [dy_j]\, \phi_H^\dagger(x_i, \tilde{q}^2)\, \phi_{\overline{H}}^\dagger(y_j, \tilde{q}^2)\, T_H(x_i, y_j; q^2, \theta_{CM}) \tag{3.13}$$

where $[dx_i] = \delta\left(\sum_{k=1}^n x_k - 1\right) \prod_{k=1}^n dx_k$ and $n = 2, 3$ is the number of quarks in the valence

Fock state. The scale $\tilde{q}^2$ is set from higher order calculations, but it reflects the minimum momentum transfer in the process.[1] The main dynamical dependence of the form factor is controlled by the hard scattering amplitude T_H which is computed by replacing each hadron by collinear constituents $P_i^\mu = x_i P_H^\mu$. Since the collinear divergences are summed in ϕ_H, T_H can be systematically computed as a perturbation expansion in $\alpha_s(q^2)$.

The distribution amplitude

$$\phi_H(x_i, q^2) = \int^{k_\perp^2 < |q^2|} [d^2 k_{\perp i}] \psi^{(q^2)}(x_i, \vec{k}_{\perp i}) \tag{3.14}$$

with

$$[d^2 k_{\perp i}] = 2(2\pi)^3 \delta \left(\sum_{j=1}^{n} k_{\perp j} \right) \prod_{i=1}^{n} \frac{d^2 k_{\perp i}}{2(2\pi)^3}$$

is computed from the valence wavefunction of the hadron at equal time $\tau = t + z$ on the light cone and gives the probability amplitude for the constituents with light-cone momentum fraction $x_i = (k_i^0 + k_i^z)/(P_H^0 + P_H^z)$ to combine into the hadron with relative transverse momentum up to the scale Q^2. For the case of heavy quark bound states, we shall assume that the constituents are sufficiently non-relativistic that gluon emission, higher Fock states, and retardation of the effective potential can be neglected. The quark distributions are then controlled by a simple nonrelativistic wavefunction, which we take in the model form:

$$\psi_M(x_i, \vec{k}_{\perp i}) = \frac{C}{x_1^2 x_2^2 \left[M_H^2 - \frac{\vec{k}_{\perp 1}^2 + m_1^2}{x_1} - \frac{\vec{k}_{\perp 2}^2 + m_2^2}{x_2} \right]^2} \tag{3.15}$$

We choose this form since it coincides with the usual Schrödinger- Coulomb wavefunction in the nonrelativistic limit for hydrogenic atoms and has the correct large momentum behavior induced from the spin- independent gluon couplings. The wavefunction is peaked at the mass ratio $x_i = m_i/M_H$:

$$\left(x_i - \frac{m_i}{M_H} \right)^2 \sim \frac{\langle k_z^2 \rangle}{M_H^2} \tag{3.16}$$

where $\langle k_z^2 \rangle$ is evaluated in the rest frame. Normalizing the wavefunction to unit probability gives

$$C^2 = 128\pi \left(\langle v^2 \rangle \right)^{5/2} m_r^5 (m_1 + m_2) \tag{3.17}$$

where $\langle v^2 \rangle$ is the mean square relative velocity and $m_r = m_1 m_2/(m_1 + m_2)$ is the reduced mass.

The corresponding distribution amplitude is

$$\phi(x_i) = \frac{C}{16\pi^2} \frac{1}{[x_1 x_2 M_H^2 - x_2 m_1^2 - x_1 m_2^2]} \cong \frac{1}{\sqrt{2\pi}} \frac{\gamma^{3/2}}{M_H^{1/2}} \delta\left(x_1 - \frac{m_1}{m_1+m_2}\right) . \tag{3.18}$$

It is easy to see from the structure of T_H for $e^+e^- \to M\overline{M}$ that the spectator quark pair is produced with momentum transfer squared $q^2 x_s y_s \geq 4m_s^2$. Thus heavy hadron pair production is dominated by diagrams in which the primary coupling of the virtual photon is to the heavier quark pair. The perturbative predictions are thus expected to be accurate even near threshold to leading order in $\alpha_s(4m_\ell^2)$ where m_ℓ is the mass of lighter quark in the meson.

We have computed the leading order e^+e^- production helicity amplitudes for higher generation meson ($\lambda = 0, \pm 1$) and baryon ($\lambda = \pm 1/2, \pm 3/2$) pairs from Eq. (3.13) as a function of q^2 and the quark masses. The Lorentz and gauge invariant form factors for meson pair production are defined by the electromagnetic coupling of the meson as shown in Table 3.2. The analysis is simplified by using the peaked form of the distribution amplitude, Eq. (3.18). From the calculation of helicity amplitudes, we found that $V_2(q^2) = M_H T(q^2)$. Therefore, we use the following notation:

$$F_{0,0}(q^2) = S(q^2)$$

$$F_{1,1}(q^2) = V_1(q^2)$$

$$F_{0,1}(q^2) = M_H\, T(q^2) = V_2(q^2) .$$

In the case of meson pairs the (unpolarized) e^+e^- annihilation cross section has the general form

$$\begin{aligned} 4\pi \frac{d\sigma}{d\Omega}(e^+e^- \to M_\lambda \overline{M}_{\overline{\lambda}}) = \frac{3}{4}\beta \sigma_{e^+e^-\to\mu^+\mu^-} \Bigg[\frac{1}{2}\beta^2 \sin^2\theta \\ \times \Bigg[|F_{0,0}(q^2)|^2 + \frac{1}{(1-\beta^2)^2} \Big\{ (3 - 2\beta^2 + 3\beta^4)|F_{1,1}(q^2)|^2 \\ - 4(1+\beta^2)\ \mathrm{Re}\,(F_{1,1}(q^2)F_{0,1}^*(q^2)) + 4|F_{0,1}(q^2)|^2 \Big\} \Bigg] \\ + \frac{3\beta^2}{2(1-\beta^2)} (1+\cos^2\theta)|F_{0,1}(q^2)|^2 \Bigg] \end{aligned} \tag{3.19}$$

where $q^2 = s = 4M_H^2/\beta^2$ and the meson velocity is $\beta = 1 - \frac{4M_H^2}{q^2}$. The production form factors

Table 3.2. Definition of meson form factors. The dashed and solid lines represent the pseudoscalar and vector mesons respectively.

Vertex Type	$ie\Gamma_\mu$
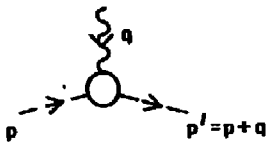	$ie\,(p_\mu + p'_\mu)\;S(q^2)$
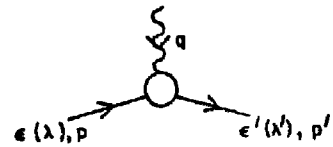	$ie\epsilon(\lambda)\cdot\epsilon^{*\prime}(\lambda')\,(p_\mu + p'_\mu)\,V_1(q^2)$ $-ie\left\{\epsilon(\lambda)\cdot p'\;\epsilon^{*\prime}_\mu(\lambda')\right.$ $\left.+\,\epsilon^{*\prime}(\lambda')\cdot p\;\epsilon_\mu(\lambda)\right\}V_2(q^2)$
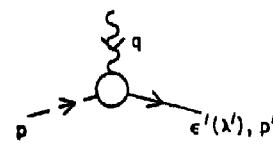	$e\,\epsilon_{\mu\nu\rho\sigma}\,p^\nu\,\epsilon^{*\rho}(\lambda')\,q^\sigma\,T(q^2)$

have the general form

$$F_{\lambda\bar{\lambda}} = \frac{\langle v^2\rangle^2}{(\bar{q}^2)^2}\,(A_{\lambda\bar{\lambda}} + \bar{q}^2 B_{\lambda\bar{\lambda}}) \tag{3.20}$$

where A and B reflect the Coulomb-like and transverse gluon couplings, respectively. The results to leading order in α_s are given in Table 3.3. In general A and B have a slow logarithmic dependence due to the q^2-evolution of the distribution amplitudes. The form factor zero for the case of pseudoscalar pair production reflects the numerator structure of the T_H amplitude.

$$\text{Numerator} \sim e_1\left(\bar{q}^2 - \frac{m_1^2}{4M_H^2}\,\frac{1}{x_2 y_1} - \frac{m_2^2}{4M_H^2}\,\frac{x_1}{x_2^2 y_2}\right) \tag{3.21}$$

For the peaked wavefunction,

$$F_{0,0}^M(q^2) \propto \frac{1}{(\bar{q}^2)^2}\left\{e_1\left(\bar{q}^2 - \frac{m_1}{2m_2}\right) + e_2\left(\bar{q}^2 - \frac{m_2}{2m_1}\right)\,\frac{m_2^2}{m_1^2}\right\} \tag{3.22}$$

If m_1 is much greater than m_2 then the e_1 is dominant and changes sign at $q^2/4M_H^2 = m_1/2m_2$.

The contribution of the e_2 term and higher order contributions are small and nearly constant in the region where the e_1 term changes sign; such contributions can displace slightly but not remove the form factor zero.

Table 3.3. The results for the meson form factors.

A and B are defined by Eq. (3.23).

	(0,0)	(0,1)	(1,1)
A	$\frac{e_1 m_1^4 + e_2 m_2^4}{(m_1+m_2)^4}$	$\frac{e_1 m_1^3 + e_2 m_2^3}{(m_1+m_2)^3}$	$\frac{e_1 m_1^4 + e_2 m_2^4}{(m_1+m_2)^4}$
B	$-\frac{2m_1 m_2 (e_1 m_1^2 + e_2 m_2^2)}{(m_1+m_2)^4}$	0	0

These results also hold in quantum electrodynamics; e.g. pair production of muonium $(\mu - e)$ atoms in e_+e_- annihilation. Gauge theory predicts a zero for paramuonium production at $\bar{q}^2 = m_{\mu}/2m_e$.

These explicit results for form factors also shows that the onset of the leading power-law scaling of a form factor is controlled by the ratio of the A and B terms in Eq. (3.20); i.e., when the transverse contributions exceed the Coulomb mass-dominated contributions. The Coulomb contribution to the form factor can also be computed directly from the convolution of the initial and final wavefunctions. Thus, contrary to the claim of Ref. 15 there are no extra factors of $\alpha_s(q^2)$ which suppress the "hard" versus nonperturbative contributions.

The form factors for the heavy hadrons are normalized by the constraint that the Coulomb contribution to the form factor equals the total hadronic charge at $q^2 = 0$. Further, by the correspondence principle, the form factor should agree with the standard non-relativistic calculation at small momentum transfer. All of these constraints are satisfied by the form

$$F^M_{0,0}(q^2) = e_1 \frac{16\gamma^4}{(q^2+\gamma^2)^2} \left(\frac{M_H^2}{m_2^2}\right)^2 \left(1 - \frac{q^2}{4M_H^2}\frac{2m_2}{m_1}\right) + 1 \leftrightarrow 2 \,. \tag{3.23}$$

At large q^2 the form factor can also be written as

$$F^M_{(0,0)} = e_1 \frac{16\pi\alpha_s f_M^2}{9q^2} \left(\frac{M_H^2}{m_2^2}\right) + (1 \leftrightarrow 2) \,, \quad \frac{f_M}{2\sqrt{3}} = \int_0^1 dx\, \phi(x,Q) \tag{3.24}$$

where $f_M = (6\gamma^3/\pi M_H)^{1/2}$ is the meson decay constant. Predictions for various heavy mesons are shown in the figures. The results for the cross sections are given in units of R using the $\mu^+\mu^-$ rate as reference. The basic unknown is $\gamma^2 = v^2 m_q^2$ which sets the scale for capture into the wavefunction in relative transverse momentum. The same probability amplitude enters the normalization of the inclusive production of heavy hadrons in heavy quark hadronization.

Although the mass of the strange quark may be too low to trust these predictions, we also give predictions for $F\overline{F}$ production [see Figs. 8 and 9] since the predicted zero appears in a domain accessible to present storage rings.

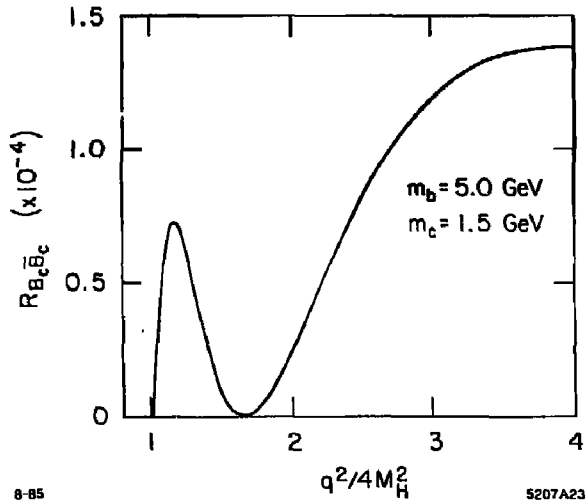

Fig. 8. Perturbative QCD prediction for $R_{B_c\overline{B}_c} = \dfrac{\sigma(e^+e^- \to B_c\overline{B}_c)}{\sigma(e^+e^- \to \mu^+\mu^-)}$.

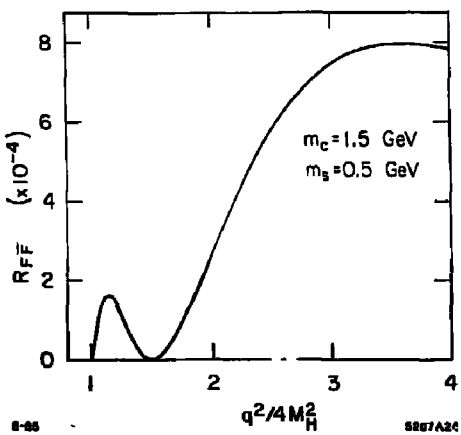

Fig. 9. Perturbative QCD prediction for $R_{F\overline{F}} = \dfrac{\sigma(e^+e^- \to F\overline{F})}{\sigma(e^+e^- \to \mu^+\mu^-)}$.

At low relative velocity of the hadron pair one also expects resonance contributions to the form factors. For these heavy systems such resonances could be related to $qq\bar{q}\bar{q}$ bound states. From Watson's theorem, one expects any resonance structure to introduce a final-state phase factor, but not destroy the zero of the underlying QCD prediction.

We have also performed analogous calculations of the baryon form factor, retaining the constituent mass structure. The numerator structure for spin 1/2 baryons has the form

$$A + B\bar{q}^2 + c\bar{q}^4 \,. \tag{3.25}$$

Thus it is possible to have two form factor zeros; e.g. at spacelike and timelike values of q^2.

Although the measurements are difficult and require large luminosity, the observation of the striking zero structure predicted by QCD would provide a unique test of the theory and its applicability to exclusive processes. As we have shown, the onset of leading power behavior is controlled simply by the mass parameters of the theory; there is no way to postpone the region of validity of the perturbative predictions. The results of this work may also be applicable to lower mass systems, but in this case the mass parameters for the light quarks are evidently replaced by vacuum condensate and other nonperturbative contributions.

REFERENCES

1. G. P. Lepage and S. J. Brodsky, Phys. Rev. D22, 2157 (1980).
2. S. J. Brodsky and G. R. Farrar, Phys. Rev. Lett. 31, 1153 (1973), and Phys. Rev. D11, 1309 (1975).
3. S. J. Brodsky and G. P. Lepage, Phys. Rev. D24, 1808 (1981).
4. S. J. Brodsky and C.-R. Ji, SLAC-PUB-3706 (1985).
5. V. L. Chernyak and I. R. Zhitnitskii, Phys. Rept. 112, 173 (1984) and references therein.
6. M. Peskin, Phys. Lett. 88B, 128 (1979); A. Duncan and A. H. Mueller, Phys. Lett. 90B, 159 (1980), and Phys. Rev. D21, 1636 (1980).
7. M. D. Mestayer, SLAC-Report 214 (1978) F. Martin, et al., Phys. Rev. Lett. 38, 1320 (1977); W. P. Schultz, et al., Phys. Rev. Lett. 38, 259 (1977); R. G. Arnold, et al., Phys. Rev. Lett. 40, 1429 (1978); SLAC-PUB-2373 (1979); B. T. Chertok, Phys. Lett. 41, 1155 (1978); D. Day, et al., Phys. Rev. Lett. 43, 1143 (1979). Summaries of the data for nucleon and nuclear form factors at large Q^2 are given in B. T. Chertok, in Progress in Particle and Nuclear Physics, Proceeding of the International School of Nuclear Physics, 5th Course, Erice (1978), and Proceedings of the XVI Rencontre de Moriond, Les Arcs, Savoie, France, 1981.
8. D. Sivers, S. Brodsky, R. Blankenbecler, Phys. Rept. 23C, 1 (1976).
9. S. S. Kanwal, Phys. Lett. 142B, 294 (1984). A. Mueller, Phys. Rept. 73, 237 (1981).
10. S. J. Brodsky and G. P. Lepage, Phys. Rev. D24, 1808 (1981). The calculation of $\gamma\gamma \to B\bar{B}$ is given by G. R. Farrar, E. Maina, and F. Neri, RU-85-08 (1985).

11. S. J. Brodsky, T. Huang, G. P. Lepage, in Particles and Fields 2, edited by A. Z. Capri, A. N. Kamal, Plenum (1983), and T. Huang, SLAC-PUB-2580 (1980), published in the Proceedings of the XXth International Conference on High Energy Physics, Madison, Wisconsin (1980).

12. M. J. Lavelle, Imperial College preprint, TP/84-84/58 (1984).

13. V. L. Chernyak and I. R. Zhitnitskii, Nucl. Phys. B246, 52 (1984).

14. S. J. Brodsky and C.-R. Ji, to be published (1985).

15. N. Isgur and C. H. Llewellyn Smith, Phys. Rev. Lett. 52, 1080 (1984). N. Isgur, Progress in Particle and Nuclear Physics, Vol. 13, "Nucleon Physics with Chromodynamics: From High Q^2 to Baryon Spectroscopy to Nuclear Physics," ed. A. Faessler.

4. NUCLEAR CHROMODYNAMICS

Nuclear chromodynamics is concerned with the application of quantum chromodynamics to nuclear physics. Its goal is to give a fundamental description of nuclear dynamics and nuclear properties in terms of quark and gluon fields at short distance, and to obtain a synthesis at long distances with the normal nucleon, isobar, and meson degrees of freedom. NCD provides an important testing ground for coherent effects in QCD and nuclear effects at the interface between perturbative and non-perturbative dynamics.[1]

Among the areas of interest:

1. The representation of the nuclear force in terms of quark and gluon subprocesses.[2] The nuclear force between nucleons can in principle be represented at a fundamental level in QCD in terms of quark interchange (equivalent at large distances to pion and other meson exchange) and multiple-gluon exchange. Although calculations from first principles are still too complicated, recent results derived from effective potential, bag, and soliton models suggest that many of the basic features of the nuclear force can be understood from the underlying QCD substructure. At a more basic level we will show directly from QCD that the nucleon-nucleon force must be repulsive at short distances. At high momentum transfer the nucleon-nucleon interactions agree with the scaling laws predicted by the simplest constituent exchange processes.

2. The composition of the nucleon and nuclear state in terms of quark and gluon quanta. The light-cone quantization formalism provides a consistent relativistic Fock state momentum space representation of multiquark and gluon color singlet bound states.

3. The propagation of quarks and gluons through nuclear matter:[3] one is interested in the interplay between multiple scattering, induced radiation, the Landau-Pomeranchuk coherence effect,[4] shadowing phenomena, and confinement.

4. Factorization theorems for inclusive and exclusive reactions: for nuclear reactions one is particularly interested in the origin of the EMC non-additivity effect[5] and other nuclear-induced effects in high transverse momentum reactions.[6]

5. Novel nuclear phenomena in QCD such as (a) color coherence effects in high momentum transfer quasi-elastic reactions in nuclei;[7] (b) the nuclear number dependence of strange and charm quarks in the sea; (c) new color singlet multiquark states.

6. The use of reduced nuclear amplitudes in order to obtain a consistent and covariant identification of the effects of nucleon compositeness in nuclear reactions.

Conversely, nuclear chromodynamics implies in some cases a breakdown of traditional nuclear physics concepts. For example, we can identify where off-shell effects modify traditional nuclear

physics formulas, such as the impulse approximation for elastic nuclear form factors. At high momentum transfer nuclear amplitudes are predicted to have a power law fall off in QCD in contrast to the Gaussian or exponential fall off usually assumed in nuclear physics. There are other areas where conventional techniques in nuclear theory, such as the use of local meson nucleon field theories break down. We discuss some of these problems in the last chapter.

In QCD, the fundamental degrees of freedom of nuclei as well as hadrons are postulated to be the spin-1/2 quark and spin-1 gluon quanta. Nuclear systems are identified as color-singlet composites of quark and gluon fields, beginning with the six-quark Fock component of the deuteron. An immediate consequence is that nuclear states are a mixture of several color representations which *cannot* be described solely in terms of the conventional nucleon, meson, and isobar degrees of freedom: there must also exist "hidden color" multiquark wavefunction components—nuclear states which are not separable at large distances into the usual color singlet nucleon clusters.

The goal of nuclear chromodynamics is thus to understand the fundamental basis of nuclear amplitudes. Solutions to QCD for bound states eventually may be obtained from lattice gauge theory or the light-cone quantization formalism. Nevertheless, even without explicit solutions, (1) we can use asymptotic freedom to calculate the underlying quark and gluon subprocess amplitudes at short distances, (2) we can derive factorization theorems for both inclusive and exclusive processes which separate the hadronic bound state physics from perturbative dynamics, and (3) we can use the apparatus of light cone quantization (i.e.: equal time $\tau = t + z/c$ wave functions) to represent bound states of composite systems in a consistent covariant manner. In some cases, we can derive exact constraints on the wave functions, or use approximation methods and sum rules to model the wave functions.[8,9] We can also derive connections with the non-relativistic wavefunctions. In the case of multiquark systems we can derive asymptotic constraints such as the form of the deuteron wavefunction.[10] Using these techniques we can analyze the role of hidden color degrees of freedom in ordinary nuclei, and understand the role of QCD relativistic effects. The introduction of reduced nuclear amplitudes then allows the direct phenomenological study of the specific role of QCD in nuclear physics. Finally, we can derive constraints on the hadronic meson nucleon vertices which are required for calculating meson and exchange currents and similar coherent phenomena.

Just as Bohr's correspondence principle played a crucial role in bridging the gap between classical and quantum mechanics, we also need a similar correspondence principle to bridge the gap between nuclear physics at large distances and QCD at short distances. Since QCD has the same natural length scale ~ 1 fm as nuclear physics it is difficult to argue that nuclear physics can be studied in isolation from QCD. Thus one of the most interesting questions in nuclear physics is the transition between conventional meson-nucleon degrees of freedom to the quark

and gluon degrees of freedom of QCD. As one probes distances shorter than $\Lambda_{QCD}^{-1} \sim 1$ fm the meson-nucleon degrees of freedom must break down, and we expect new nuclear phenomena, new physics intrinsic to composite nucleons and mesons, and new phenomena outside the range of traditional nuclear physics. One apparent signal for this is the experimental evidence from deep inelastic lepton-nucleus scattering that nuclear structure functions deviate significantly from simple nucleon additivity, much more than would have been expected for lightly bound systems.[6] Certainly for distances greater than 1 fm, i.e.: momentum transfer less than 200 MeV, non-relativistic Schroedinger equation and potential theory provide an accurate phenomenological description of nuclear matter. Similarly, in the short distance domain (distances less than 0.2 fm or momentum transfer $\geq$ 1 GeV) the quark-gluon degrees of QCD give a good representation of strong interaction dynamics.

The synthesis between nuclear physics and QCD is then the analogue to the correspondence principle. For example, the nuclear potential can now be understood in terms of quark interchange and gluon exchange amplitude at the high momentum transfer region.[11] At long distances these contributions must merge into the traditional meson and Yukawa force. The nuclear state, which can be primarily represented as meson and nucleon degrees of freedom at large distances; at short distances must give way to a description in terms of quark and gluon degrees of freedom, specifically hidden color components, at very short distances. The electromagnetic and weak interactions of the nucleus, which is traditionally described in terms of nucleon and meson currents, is replaced in QCD by interactions which couple directly to the quark currents at any momentum transfer scale. What we perceive at large distances and refer to as meson and nucleon degrees of freedom are thus coherent effects in QCD. The form factor in nuclear physics in the non-relativistic domain can be represented as a Fourier transform of a charge distribution. At relativistic energies, this is replaced by an exact QCD calculation of the probability amplitude for the nuclear system to remain intact. Asymptotic results are given in later sections of this chapter.

The joining of nuclear physics at long distances and QCD at short distances also brings a number of new general analytical tools, including (a) light cone quantization, (b) a relativistic Fock state expansion, (c) factorization theorems, (d) evolution equations which give the leading behavior of hadronic amplitudes at short distances, and (e) a system of counting rules for obtaining the leading power behavior and leading helicity behavior of nuclear reduced amplitudes.[12] In particular, one now has a completely relativistic framework for multi-particle systems applicable to nuclear systems: light cone quantization provides a Hamiltonian formulation for QCD and is an alternative to the Bethe-Salpeter formalism.

Despite its generality, in concept, and often in practice, light-cone quantization is as simple to use as Schroedinger many body theory.[8,9] Using this formalism one can readily obtain exact

results for the form of the nucleon, meson, and nuclear form factors and other exclusive nuclear amplitudes at large momentum transfer, such as the photo-disintegration of the deuteron at large θ_{CM}. One obtains rigorous constraints on the six-quark wave function of the deuteron at small relative distances as well as a value for the percentage of hidden color at short distances in the deuteron wave function. More generally, as we discuss in a later section, one can identify the degrees of freedom of multi-quark system and obtain a completely anti-symmetrized basis Fock state representation for multi-quark states.[13]

The fact that the degrees of freedom and permutation symmetries of the covariant QCD equation of motion for multiquark states on the light-cone are the same as those of the non-relativistic quark model[14] can account for the successes of the non-relativistic approach for describing the hadronic spectrum despite the dynamical failure of non-relativistic equations for describing wavefunctions and structure functions.

4.1 THE DEUTERON IN QCD

Of the five color-singlet representations of six quarks, only one corresponds to the usual system of two color singlet baryonic clusters.[13,15] Notice that the exchange of a virtual gluon in the deuteron at short distance inevitably produces Fock state components where the three-quark clusters correspond to color octet nucleons or isobars. Thus, in general, the deuteron wavefunction will have a complete spectrum of hidden-color wavefunction components, although it is likely that these states are important only at small internucleon separation.

Despite the complexity of the multi-color representations of nuclear wavefunctions, the analysis[13] of the deuteron form factor at large momentum transfer can be carried out in parallel with the nucleon case. Only the minimal six-quark Fock state needs to be considered to leading order in $1/Q^2$. The deuteron form factor can then be written as a convolution [see Fig. 10],

$$F_d(Q^2) = \int_0^1 [dx]\,[dy]\;\phi_d^\dagger(y,Q)\;T_H^{6q+\gamma^*\to 6q}(x,y,Q)\;\;\phi_d(x,Q)\;, \tag{4.1}$$

where the hard scattering amplitude scales as

$$T_H^{6q+\gamma^*\to 6q} = \left[\frac{\alpha_s(Q^2)}{Q^2}\right]^5 t(x,y)\;\;\left[1+O(\alpha_s(Q^2))\right] \tag{4.2}$$

The anomalous dimensions γ_n^d are calculated from the evolution equations for $\phi_d(x_i,Q)$ derived

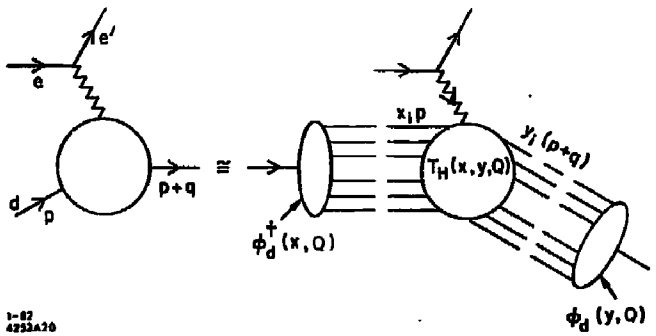

Fig. 10. Factorization of the deuteron form factor at large Q^2.

to leading order in QED from pairwise gluon-exchange interactions: ($C_F = 4/3$, $C_d = -C_F/5$)

$$\prod_{k=1}^{6} x_k \left[\frac{\partial}{\partial \xi} + \frac{3C_F}{\beta}\right] \widetilde{\Phi}(x_i, Q) = -\frac{C_d}{\beta} \int_0^1 [dy]\, V(x_i, y_i) \widetilde{\Phi}(y_i, Q) \ . \tag{4.3}$$

Here we have defined

$$\Phi(x_i, Q) = \prod_{k=1}^{6} x_k \widetilde{\Phi}(x_i, Q), \tag{4.4}$$

and the evolution is in the variable

$$\xi(Q^2) = \frac{\beta}{4\pi} \int_{Q_0^2}^{Q^2} \frac{dk^2}{k^2} \alpha_s(k^2) \sim ln\left(\frac{ln\frac{Q^2}{\Lambda^2}}{ln\frac{Q_0^2}{\Lambda^2}}\right) \ . \tag{4.5}$$

The kernel V is computed to leading order in $\alpha_s(Q^2)$ from the sum of gluon interactions between quark pairs. The general matrix representations of γ_n with bases $\left|\prod_{i=1}^{5} x_i^{m_i}\right\rangle$ will be given in Ref. 13. The effective leading anomalous dimension γ_0, corresponding to the eigenfunction $\widetilde{\Phi}(x_i) = 1$, is $\gamma_0 = (6/5)(C_F/\beta)$ (see the next section).

In order to make more detailed and experimentally accessible predictions, we will define the "reduced" nuclear form factor in order to remove the effects of nucleon compositeness:[16]

$$f_d(Q^2) \cong \frac{F_d(Q^2)}{F_N^2(Q^2/4)} \ . \tag{4.6}$$

The arguments for each of the nucleon form factors (F_N) is $Q^2/4$ since in the limit of zero binding energy each nucleon must change its momentum from $\sim p/2$ to $(p+q)/2$. Since the leading

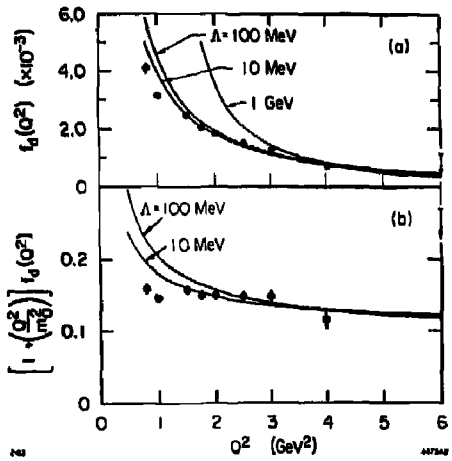

Fig. 11. (a) Comparison of the asymptotic QCD prediction (18) and (19) with experiment using $F_N(Q^2) = [1 + (Q^2/0.71\,\mathrm{GeV}^2)]^{-2}$. The normalization is fit at $Q^2 = 4$ GeV^2. (b) Comparison of the prediction $[1 + (Q^2/m_0^2)]f_d(Q^2) \propto (\ell n\, Q^2)^{-1-(2/5)(C_F/\beta)}$ with data. The value $m_0^2 = 0.28$ GeV^2 is used.

anomalous dimensions of the nucleon distribution amplitude is $C_F/2\beta$, the QCD prediction for the asymptotic Q^2-behavior of $f_d(Q^2)$ is

$$f_d(Q^2) \sim \frac{\alpha_s(Q^2)}{Q^2}\left(ln\frac{Q^2}{\Lambda^2}\right)^{-\frac{1}{2}\frac{C_F}{\beta}}, \tag{4.7}$$

where $-(2/5)(C_F/\beta) = -8/145$ for $n_f = 2$.

Although this QCD prediction is for asymptotic momentum transfer, it is interesting to compare it directly with the available high Q^2 data[17] [see Fig. 11]. In general one would expect corrections from higher twist effects (e.g., mass and $k_\perp$ smearing), higher particle number Fock states, higher order contributions in $\alpha_s(Q^2)$, as well as non-leading anomalous dimensions. However, the agreement of the data with simple $Q^2 f_d(Q^2) \sim const$ behavior for $Q^2 > 1/2$ GeV^2 implies that, unless there is a fortuitous cancellation, all of the scale-breaking effects are small, and the present QCD perturbative calculations are viable and applicable even in the nuclear physics domain. The lack of deviation from the QCD parameterization also suggests that the parameter A is small. A comparison with a standard definition such as $\Lambda_{\overline{MS}}$ would require a calculation of next to leading effects. A more definitive check of QCD can be made by calculating the normalization of $f_d(Q^2)$ from T_H and the evolution of the deuteron wave function to short

distances. It is also important to confirm experimentally that the helicity $\lambda = \lambda' = 0$ form factor is indeed dominant.

The calculation of the normalization $T_H^{6q+\gamma^* \to 6q}$ to leading order in $\alpha_s(Q^2)$ will require the evaluation of over 300,000 Feynman diagrams involving five exchanged gluons. Fortunately this appears possible using the algebraic computer methods introduced by Farrar and Neri.[18] The method of setting the appropriate scale $\hat{Q}$ of $\alpha_s^5(\hat{Q}^2)$ in T_H is given in Ref. 19.

We note that the deuteron wave function which contributes to the asymptotic limit of the form factor is the totally antisymmetric wave function corresponding to the orbital Young symmetry given by [6] and isospin (T)+ spin (S) Young symmetry given by {33}. The deuteron state with this symmetry is related to the NN, $\Delta\Delta$, and hidden color (CC) physical bases, for both the $(TS) = (01)$ and (10) cases, by the formula[20]

$$\psi_{[6]\{33\}} = \sqrt{\frac{1}{9}}\,\psi_{NN} + \sqrt{\frac{4}{45}}\,\psi_{\Delta\Delta} + \sqrt{\frac{4}{5}}\,\psi_{CC} \quad . \tag{4.8}$$

Thus the physical deuteron state, which is mostly ψ_{NN} at large distance, must evolve to the $\psi_{[6]\{33\}}$ state when the six quark transverse separations $b_\perp^i \leq O(1/Q) \to 0$. Since this state is 80% hidden color, the deuteron wave function cannot be described by the meson-nucleon isobar degrees of freedom in this domain. The fact that the six-quark color singlet state inevitably evolves in QCD to a dominantly hidden-color configuration at small transverse separation also has implications for the form of the nucleon-nucleon $(S_z = 0)$ potential, which can be considered as one interaction component in a coupled scattering channel system. As the two nucleons approach each other, the system must do work in order to change the six-quark state to a dominantly hidden color configuration; i.e., QCD requires that the nucleon-nucleon potential must be repulsive at short distances [see Fig. 12].[21] The evolution equation for the six-quark system suggests that the distance where this change occurs is in the domain where $\alpha_s(Q^2)$ most strongly varies. The general solutions of the evolution equation for multiquark systems is discussed in Chapter 5. Some of the solutions are orthogonal to the usual nuclear configurations which correspond to separated nucleons or isobars at large distances.

4.2 REDUCED NUCLEAR AMPLITUDES

One of the basic problems in the analysis of nuclear scattering amplitudes is how to consistently account for the effects of the underlying quark/gluon component structure of nucleons. Traditional methods based on the use of an effective nucleon/meson local Lagrangian field theory are not really applicable, giving the wrong dynamical dependence in virtually every kinematic variable for composite hadrons. The inclusion of *ad hoc* vertex form factors is unsatisfactory since one must understand the off-shell dependence in each leg while retaining gauge invariance; such

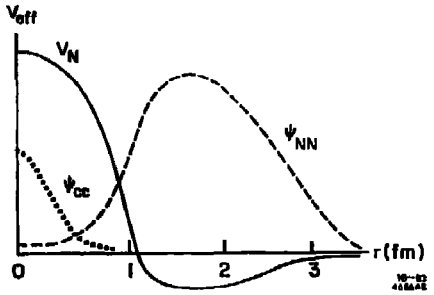

Fig. 12. Schematic representation of the deuteron wave function in QCD indicating the presence of hidden color six-quark components at short distances.

methods have little predictive power. On the other hand, the explicit evaluation of the multiquark hard-scattering amplitudes needed to predict the normalization and angular dependence for a nuclear process, even at leading order in α_s requires the consideration of millions of Feynman diagrams. Beyond leading order one must include contributions of non-valence Fock states wavefunctions, and a rapidly expanding number of radiative corrections and loop diagrams.

The reduced amplitude method,[16] although not an exact replacement for a full QCD calculation, provides a simple method for identifying the dynamical effects of nuclear substructure, consistent with covariance, QCD scaling laws and gauge invariance. The basic idea has already been introduced for the reduced deuteron form factor. More generally if we neglect nuclear binding, then the light-cone nuclear wavefunction can be written as a cluster decomposition of collinear nucleons: $\psi_{q/A} = \psi_{N/A} \prod_N \Psi_{q/N}$ where each nucleon has $1/A$ of the nuclear momentum. A large momentum transfer nucleon amplitude then contains as a factor the probability amplitude for each nucleon to remain intact after absorbing $1/A$ of the respective nuclear momentum transfer. We can identify each probability amplitude with the respective nucleon form factor $F\left(\hat{t}_i = \frac{1}{A^2}\, t_A\right)$. Thus for any exclusive nuclear scattering process, we define the reduced nuclear amplitude

$$m = \frac{M}{\prod_{i=1}^{A} F_N(\hat{t}_i)} \tag{4.9}$$

The QCD scaling law for the reduced nuclear amplitude m is then identical to that of nuclei with point-like nuclear components: e.g., the reduced nuclear form factors obey

$$f_A(Q^2) \equiv \frac{F_A(Q^2)}{\left[F_N(Q^2/A^2)\right]^A} \sim \left[\frac{1}{Q^2}\right]^{A-1} . \tag{4.10}$$

Comparisons with experiment and predictions for leading logarithmic corrections to this result

are given in Ref. 16. In the case of photo- (or electro-) disintegration of the deuteron one has

$$m_{\gamma d\to np} = \frac{M_{\gamma d\to np}}{F_n(t_n)F_p(t_p)} \sim \frac{1}{p_T}\, f(\theta_{cm}) \tag{4.11}$$

i.e., the same elementary scaling behavior as for $M_{\gamma M\to qq}$. Comparison with experiment is encouraging [see Fig. 13], showing that as was the case for $Q^2 f_d(Q^2)$, the perturbative QCD scaling regime begins at $Q^2 \gtrsim 1$ GeV^2. Detailed comparisons and a model for the angular dependence and the virtual photon-mass dependence of deuteron electrodisintegration are discussed in Ref. 16. Other potentially useful checks of QCD scaling of reduced amplitudes are

$$\begin{aligned} m_{pp\to d\pi^+} &\sim p_T^{-2}\, f(t/s) \\ m_{pd\to H^3\pi^+} &\sim p_T^{-4}\, f(t/s) \\ m_{\pi d\to \pi d} &\sim p_T^{-4}\, f(t/s)\ . \end{aligned} \tag{4.12}$$

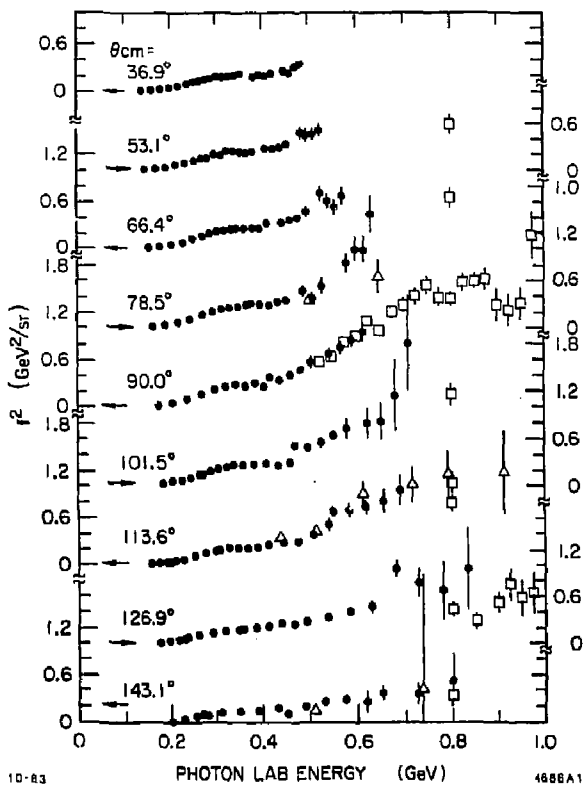

Fig. 13. Comparison of deuteron photo-disintegration data with the scaling prediction which requires $f^2(\theta_{c.m.})$ to be independent of energy at large momentum transfer. The data are from H. Myers *et al.*, Phys. Rev. 121, 630 (1961); R. Ching and C. Schaerf, Phys. Rev. 141, 1320 (1966); P. Dougan *et al.*, Z. Phys. A 276, 55 (1976).

It is also possible to use these QCD scaling laws for the reduced amplitude as a parametrization for the background for detecting possible new dibaryon resonance states.

REFERENCES

1. For additional discussion of applications of QCD to nuclear physics and references, see S. J. Brodsky, published in the proceedings of the conference "New Horizons in Electromagnetic Physics", University of Virginia, April 1982; S. J. Brodsky, T. Huang and G. P. Lepage, SLAC-PUB-2868 (1982) published in Springer Tracts in Modern Physics, Vol. 100, "Quarks and Nuclear Forces", ed. D. Fries and B. Zeitnitz (1982); S. J. Brodsky and G. P. Lepage, in the proceedings of the Eugene Few Body Conference 1980: 247C (Nucl. Phys. A363, 1981) and S. J. Brodsky, in the proceedings of the NATO Pacific Summer Institute Progress in Nuclear Dynamics, Vancouver Island (1982).

2. For a recent discussion of progress in the derivation of nuclear forces from QCD-based models, see K. Maltman and N. Isgur, Phys. Rev. Lett. 50, 1827 (1983), E. L. Lomon, MIT preprint CTP No. 1116 (1983); and references therein. The quark interchange mechanism for $N-N$ scattering is discussed in J. F. Gunion, S. J. Brodsky, and R. Blankenbecler, Phys. Rev. D8, 287 (1973). Qualitative QCD-based arguments for the repulsive $N-N$ potential at short distances are given in C. Detar, HU-TFT-82-6 (1982); M. Harvey, Nucl. Phys. A352, 301 (1981); A352, 326 (1981); R. L. Jaffe, Phys. Rev. Lett. 24, 228 (1983); and G. E. Brown, in Erice 1981, Proceedings, Quarks and the Nucleus. The possibility that the deuteron form factor is dominated at large momentum transfer by hidden color components is discussed in V. A. Matveev and P. Sorba, Nuovo Cimento 45A, 257 (1978); Nuovo Cimento 20, 435 (1977).

3. The eikonal scattering of quarks in hard scattering processes such as massive lepton pair production, including $k_\perp$ smearing and induced radiation is discussed by G. Bodwin, S. J. Brodsky, and G. P. Lepage, SLAC-PUB-2927 (1982) and S. J. Brodsky, SLAC-PUB-3263 (1984), to be published in Acta Physica Polonica. Other uses of the Drell-Yan process for studying quark and gluon distributions and shadowing processes in nuclei are discussed by L. L. Frankfurt and M. I. Strikman, Leningrad preprint 838 (1983).

4. L. Landau and I. Pomeranchuk, Dok. Akademii Nauk SSSR 92, 535 (1953), and 92, 735 (1953); L. Stodolsky, MPI-PAE/TH 23/75 (1981); I. M. Dremin, Lebedev preprint 250 (1981). The Landau-Pomeranchuk effect, which is an essential component of factorization theorems for inclusive reactions, predicts that there is no induced hard radiation within a nucleus for incident constituents of energy large compared to the nucleon length. This leads to new conditions for the validity of QCD factorization for the Drell-Yan process, etc.

5. R. T. Aubert, et al., Phys. Lett. 105B, 315, 322 (1981); Phys. Lett. 123B, 123, 275 (1983). A. Bodek, et al., Phys. Rev. Lett. 50, 1431; 51, 524 (1983). For recent theoretical discussions and references to the EMC effect see e.g., M. Chemtob and R. Peschanski, Saclay preprint SPh.T/83/116 (1983) and E. L. Berger, ANL preprint (1985). Various models are discussed in H. J. Pirner and J. P. Vary, Phys. Rev. Lett. 46, 1376 (1981); R. Jaffe, Phys. Rev. Lett. 50, 228 (1983). L. S. Celenza and C. Shakin, Brooklyn College preprint BCINT-82/111/117 (1982). M. Staszel, J. Roznek, G. Wilk, Warsaw preprint IFT19/83 (1983). F. E. Close, R. B. Robert, G. G. Ross, Rutherford preprint RL-83-051 (1983). O. Nachtmann and J. H. Pirner, Heidelberg preprint HD-THE-8-83-8 (1983). The experimental situation is reviewed in E. Gabathuler, Progress in Particle and Nuclear Physics, Vol. 13, "Deep Inelastic Scattering Off Nucleons and Nuclei Including the EMC Effect," ed. A. Faessler.

6. There are many possible origins of non-additive effects in nuclear structure functions including rearrangements of meson, nucleon, and isobar degrees of freedom, increasing size of a nucleon inside a nucleus (C. Shakin, Brooklyn College preprints; C. Wilk, A. Faessler), color conductivity and quark flow between nucleons which are related to meson exchange effects. In addition the effect of QCD radiative corrections can be modified by the nucleus at low momentum transfer (see Pirner and Nachtman). [It should be emphasized the nuclear state is not itself changed (in leading twist) by the momentum transfer of the probe.] Strange quarks in the nucleus would be non-additive if the origin of heavy quarks is due to higher dimension operators (S. Brodsky and M. Soldate, unpublished). Theories of the EMC effect also have to account for the indicated absence of deviation from additivity for low x_{bj} in deep inelastic neutrino reactions and the low energy American University/SLAC data. See R. G. Arnold et al., SLAC-PUB-3320 (1984). Actually the small value of binding energy per nucleon is not a reliable guide to the magnitude of non-additivity effects, as witnessed by the strikingly large nuclear effects ($O(20\%)$) observed for the g_ℓ magnetic moment of the nucleons in high orbital states. See T. Yamagishi, in Mesons and Nuclei, Vol. II, (North-Holland, Amsterdam), edited by M. Rho and D. Wilkinson (1979), and T. Yamagishi, this volume.

7. Because of color cancellations, QCD predicts no initial or final state corrections to quasi-elastic high momentum transfer reactions such as $\pi A \to \pi N(A-1)$. See A. H. Mueller, to be published in Proceedings of the Moriond Conference (1982). Applications to elastic hadron-nucleus amplitudes are given in S. J. Brodsky and B. T. Chertok, Phys. Rev. Lett. 37, 269 (1976). Color singlet cancellations for valence states interacting inclusively in nuclei are discussed in G. Bertsch, S. J. Brodsky, A. S. Goldhaber and J. F. Gunion, Phys. Rev. Lett. 47, 297 (1981). Further discussion may be found in S. J. Brodsky, SLAC-PUB-2970 (1982), published in the Proceedings of the XIIIth International Symposium on Multiparticle Dynamics, Volendam, The Netherlands (1982). The generalization of y-scaling to such reactions appears to be successful phenomenologically. [S. Gurvitz, private communication.]

8. V. L. Chernyak and I. R. Zhitnitskii, Nucl. Phys. B246, 52 (1984).

9. For lattice gauge theory constraints see S. Gottlieb and A. S. Kronfeld, CLNS-85/646 (June 1985).

10. S. J. Brodsky, C.-R. Ji and G. P. Lepage, Phys. Rev. Lett. 51, 83 (1983).

11. For a recent discussion of progress in the derivation of nuclear forces from QCD-based models, see K. Maltman and N. Isgur, Phys. Rev. Lett. 50, 1827 (1983), E. L. Lomon, MIT preprint CTP No. 1116 (1983); and references therein. The quark interchange mechanism for $N-N$ scattering is discussed in J. F. Gunion, S. J. Brodsky, and R. Blankenbecler, Phys. Rev. D8, 287 (1973). Qualitative QCD-based arguments for the repulsive $N-N$ potential at short distances are given in C. Detar, HU-TFT-82-6 (1982); M. Harvey, Nucl. Phys. A352, 301 (1981); A352, 326 (1981); R. L. Jaffe, Phys. Rev. Lett. 24, 228 (1983); and G. E. Brown, in Erice 1981, Proceedings, Quarks and the Nucleus. The possibility that the deuteron form factor is dominated at large momentum transfer by hidden color components is discussed in V. A. Matveev and P. Sorba, Nuovo Cimento 45A, 257 (1978); Nuovo Cimento 20, 435 (1977).

12. S. J. Brodsky and J. R. Hiller, Phys. Rev. C28, 475 (1983). Fig. 7 is corrected for a phase-space factor $\sqrt{s/(s-m_d^2)}$. S. J. Brodsky and B. T. Chertok, Phys. Rev. Lett. 37, 269 (1976); Phys. Rev. D14, 3003 (1976). S. J. Brodsky, in Proceedings of the International Conference on Few Body Problems in Nuclear and Particle Physics, Laval University, Quebec (1974).

13. A detailed discussion will be given in C.-R. Ji and S. J. Brodsky, SLAC-PUB-3148 (1985).

14. G. Karl, Progress in Particle and Nuclear Physics, Vol. 13, "Elements of Baryon Spectroscopy," ed. A. Faessler.

15. See, e.g., V. Matveev and P. Sorba, Nuovo Cimento Lett. 20, 435 (1977).

16. S. J. Brodsky and J. R. Hiller, Phys. Rev. C28, 4115 (1983). Figure 7 is corrected for a phase-space factor $\sqrt{s/(s-m_d^2)}$. S. J. Brodsky and B. T. Chertok, Phys. Rev. Lett. 37, 269 (1976); Phys. Rev. D14, 3003 (1976). S. J. Brodsky, in Proceedings of the International Conference on Few Body Problems in Nuclear and Particle Physics, Laval University, Quebec (1974).

17. M. D. Mestayer, SLAC-Report 214 (1978); F. Martin *et al.*, Phys. Rev. Lett. 38, 1320 (1977); W. P. Schultz *et al.*, Phys. Rev. Lett. 38, 259 (1977); R. G. Arnold *et al.*, Phys. Rev. Lett. 40, 1429 (1978); SLAC-PUB-2373 (1979); B. T. Chertok, Phys. Lett. 41, 1155 (1978); D. Day *et al.*, Phys. Rev. Lett. 43, 1143 (1979). Summaries of the data for nucleon and nuclear form factors at large Q^2 are given in B. T. Chertok, in Progress in Particle and Nuclear Physics, Proceeding of the International School of Nuclear Physics, 5th Course, Erice (1978), and Proceedings of the XVI Rencontre de Moriond, Les Arcs, Savoie, France, 1981.

18. G. R. Farrar and F. Neri, Phys. Lett. 130B, 109 (1983).

19. S. J. Brodsky, G. P. Lepage, P. B. Mackenzie, Phys. Rev. D28, 228 (1983).

20. M. Harvey, Nucl. Phys. A352, 301 (1981); A352, 326 (1981).

21. Similar considerations for nonrelativistic system are given in A. Faessler *et al.*, Nucl. Phys. A402, 555 (1983); S. Furui and A. Faessler Nucl. Phys. A397, 413 (1983).

5. EVOLUTION OF MULTIQUARK STATES

The short-distance behavior of multiquark wavefunctions can be systematically computed in perturbative QCD. In this paper we analyze the wavefunction of a four-quark color-singlet bound state in $SU(2)_C$ as an analogue to the six-quark problem in QCD. We first solve the QCD evolution equation for the multi-quark distribution amplitude at short distances in the basis of completely antisymmetrized quark representations. The eigensolutions of the evolution kernel correspond to a spectrum of candidate states of the relativistic multi-quark system. We then connect the four-quark antisymmetric representations and the eigensolutions to the physical two-cluster basis of $SU(2)_C$ dibaryon (NN, $N\Delta$, $\Delta\Delta$) and hidden color (CC) components and derive constraints on the effective nuclear potential between two clusters. We also find anomalous states in the spectrum which cannot exist without substantial hidden-color degrees of freedom.

Among the most important goals in the application of quantum chromodynamics (QCD) to nuclear physics are to predict the bound-state spectrum of relativistic multi-quark color-singlet systems and to identify the role of non-nucleonic degrees of freedom in a nucleus. In Appendix C we have given a general method for solving the QCD evolution equations for distribution amplitudes, the equations which determine the behavior of hadron wavefunctions at short distances. An important simplification of the analysis is to choose as a basis of the evolution kernel the set of antisymmetrized multi-quark representations. Since the evolution equation is relativistic and obeys all the conservation laws and symmetries of the full QCD Lagranglan, its set of eigensolutions should correspond closely to the structure of the true spectrum. Applications of the method to the baryon system have been presented in Ref. 1.

In this chapter, we analyze the structure of the spectrum and the short-distance behavior of the four-quark system in $SU(2)_C$ as a first attempt in analyzing actual multiquark color-singlet bound states in QCD. Even though this is a toy model, the results have a number of interesting implications for the realistic dibaryon system.

An outline of the method is as follows: we first construct the set of completely antisymmetric four-quark representations as a basis for diagonalizing the QCD evolution kernel. After diagonalizing the mixing matrices, we find the eigenvalues and the eigensolutions of the four-quark evolution equation. The eigenvalues are the anomalous dimensions of the distribution amplitudes which describe the short distance behavior of the system. The eigensolutions correspond to candidate four-quark states for the spectrum of the full $SU(2)_C$ Hamiltonian.

A relativistic color-singlet bound state in QCD has a consistent Fock representation at equal time on the light cone in A^+ gauge. The lowest Fock amplitude is referred to as the valence wavefunction. In the evolution equation formalism,[2] the valence wavefunction is represented by the distribution amplitude $\phi(x_i, Q)$, the amplitude for the valence quanta to each carry light-cone

longitudinal momentum fraction

$$x_i = \frac{k_i^+}{\sum_{i=1}^4 k_i^+} = \frac{k_i^0 + k_i^3}{\sum_{i=1}^4 (k_i^0 + k_i^3)},$$

collinear in relative transverse momenta up to the scale Q. Physically, $\phi(x_i, Q)$ at large Q^2 probes the short-distance behavior of the quark system, in the regime where all the constituents are within a transverse distance $1/Q$ of each other. In general, the logarithmic Q^2 dependence for $\phi(x_i, Q)$ is predicted by QCD from the anomalous dimensions (eigenvalues) of the evolution equation.

The four-quark eigensolutions can be expanded on the physical basis of effective clusters, the analogs of the NN, $\Delta\Delta$, $N\Delta$, and CC states in QCD. By analyzing the behavior of $\phi(x_i, Q)$ at large Q^2, we can predict the effective potential between two clusters. For example, we find that one of the hidden color states has a large projection on the eigensolution with leading anomalous dimension (dominant at short distances), whereas the states analogous to NN and $\Delta\Delta$ in QCD have an almost negligible leading component. This implies that the effective potential tends to be repulsive between color-singlet clusters and attractive between colored clusters at short distance.

We also find two other types of four-quark states in $SU(2)$ color which cannot be identified with dibaryon degrees of freedom. One of these states has equal NN, $\Delta\Delta$ and CC components. The other state is an anomalous hidden-color two-cluster system orthogonal to the usual hidden-color state which has the unusual feature that it has very small projection on the eigensolutions which dominate at short distance; i.e. the effective potential between the colorful clusters of the anomalous hidden color state tends to be repulsive. We speculate that the analogous anomalous states in QCD could be quasi-stable non-nucleonic nuclear systems, possibly related to the anomalous phenomena apparently observed in nuclear collisions.[3,4] These results also give some support to the conjecture that multiquark hidden color components exist in ordinary nuclei.[4]

In Ref. 1 we presented a general method for constructing antisymmetric representations of relativistic many-fermion systems at equal time on the light-cone and used it to solve the evolution equation in QCD for the three quark system.[2] Essentially, we use the following procedure:.

1. Construct the irreducible representations in each quantum space, color (C), isospin (T), spin (S) and orbital (O) in terms of the irreducible representations of the permutation group by using the Young diagram technique.[5] For the orbital representations, we use the index-power space which is constructed from the powers n_i of the longitudinal momentum fractions x_i. The orbital representations for the ℓ quark system are the polynomials $\prod_{i=1}^{\ell} x_i^{n_i}$ with the orthonormalization condition,

$$\int [dx]\, \omega(x_i)\, \phi_m^*(x_i)\, \phi_n(x_i) = \delta_{mn}, \tag{5.1}$$

where ϕ_n and ϕ_m are the orbital representations constructed by the same Young diagram

with the index-power n and m, and $\omega(x_i) = \prod_{i=1}^{\ell} x_i$.

2. Construct completely antisymmetric representations in the entire $CTSO$ space from the inner product of Young diagrams, using the Clebsch-Gordan coefficients of the S_ℓ permutation group.

The color singlet state of the four-quark system in $SU(2)_C$ is given by the Young diagram $\begin{array}{|c|c|}\hline \ & \ \\ \hline \ & \ \\ \hline \end{array}$. There are two orthogonal representations given by

$$\begin{array}{|c|c|}\hline b & b \\ \hline w & w \\ \hline \end{array} = \begin{cases} \begin{array}{|c|c|}\hline 1 & 3 \\ \hline 2 & 4 \\ \hline \end{array} = \dfrac{1}{\sqrt{2}}\,(\varsigma_1 - \varsigma_2) \\ \begin{array}{|c|c|}\hline 1 & 2 \\ \hline 3 & 4 \\ \hline \end{array} = -\dfrac{1}{\sqrt{6}}\,(\varsigma_1 + \varsigma_2 - 2\varsigma_3), \end{cases} \tag{5.2}$$

where

$$\varsigma_1 = \frac{1}{\sqrt{2}}(bwbw + wbwb)$$
$$\varsigma_2 = \frac{1}{\sqrt{2}}(wbbw + bwwb)$$

and

$$\varsigma_3 = \frac{1}{\sqrt{2}}(bbww + wwbb) \quad . \tag{5.3}$$

Note that unlike the three quark system in QCD which has a unique antisymmetric color representation, the $SU(2)_C$ multiquark system has mixed color symmetry; i.e., several orthogonal representations.

The notation used in Eq. (5.3) can be repeated for isospin and spin. We denote these representations by T_1, T_2, and T_3 (S_1, S_2, and S_3) for $T = 0$ ($S = 0$) with the substitution of (b, w) by (u, d) $((\uparrow, \downarrow))$. Also we use the conjugate notation $\overline{T}_1$, $\overline{T}_2$, and $\overline{T}_3$ ($\overline{S}_1$, $\overline{S}_2$ and $\overline{S}_3$) with the "–" sign instead of "+" sign between the two terms in the respective representations for the $(T,\ T_Z) = (1,0)$ $((S,\ S_Z) = (1,0))$ states. In this analysis, we consider the $T = 0$ case, the analogue to the actual deuteron system.

The results of the four-quark antisymmetric representations are summarized in Table I. For convenience, we present only effective representations which are sufficient to show the operation of the evolution kernel. In the $S_Z = 0$ case, the S_1T_2 and $\overline{S}_1T_2$ terms are presented for $S = 0$ and 1 representations, respectively. In the $S_Z = 1$ and 2 cases the $(\uparrow\uparrow\uparrow\downarrow)T_1$ and $(\uparrow\uparrow\uparrow\uparrow)T_1$ terms are presented, respectively. Also, we denote in parentheses in Table I the spin-orbit Young diagrams for the cases in which several spin-orbit total symmetries are allowed from the inner product of spin and orbit representations.

TABLE I

A set of antisymmetric representations for $T = 0$ four-quark distribution amplitude (i) $S_Z = 0$ (ii) $S_Z = 1$ (iii) $S_Z = 2$ case. The normalisation factors are given in (iv). For simplicity we present the effective representations which are a part of completely antisymmetric representations such as S_1T_2 or $\overline{S}_1T_2$ terms for (i), $(\uparrow\uparrow\uparrow\downarrow)$ T_1 terms for (ii), and $(\uparrow\uparrow\uparrow\uparrow)$ T_1 terms for (iii).

(i) $S_Z = 0$: S_1T_2 or $\overline{S}_1T_2$ terms

Spin × Orbital (SO)	Effective Representations
$\boxed{\uparrow}\boxed{\uparrow}\boxed{\downarrow}\boxed{\downarrow} \times \boxed{0}\boxed{0}\boxed{0}\boxed{0}$	$\frac{1}{\sqrt{2}}(\varsigma_2 - \varsigma_1)$
$\begin{array}{|c|c|}\hline\uparrow&\uparrow\\\hline\downarrow&\downarrow\\\hline\end{array} \times \boxed{0}\boxed{0}\boxed{0}\boxed{0}$	$\frac{1}{\sqrt{2}}(\varsigma_1 - \varsigma_2)$
$\begin{array}{|c|c|c|}\hline\uparrow&\uparrow&\downarrow\\\hline\downarrow\\\cline{1-1}\end{array} \times \begin{array}{|c|c|c|}\hline0&0&0\\\hline1\\\cline{1-1}\end{array} \; (\square\square\square\square)$	$\frac{1}{2\sqrt{2}}(\varsigma_2 - \varsigma_1)(x_1 - x_2 + x_3 - x_4)$
$\begin{array}{|c|c|c|}\hline\uparrow&\uparrow&\downarrow\\\hline\downarrow\\\cline{1-1}\end{array} \times \begin{array}{|c|c|c|}\hline0&0&0\\\hline1\\\cline{1-1}\end{array} \; \left(\begin{array}{|c|c|}\hline\;&\;\\\hline\;&\;\\\hline\end{array}\right)$	$\frac{1}{2\sqrt{2}}(\varsigma_1 - \varsigma_2)(x_1 - x_2 + x_3 - x_4)$
$\boxed{\uparrow}\boxed{\uparrow}\boxed{\downarrow}\boxed{\downarrow} \times \boxed{0}\boxed{0}\boxed{1}\boxed{1}$	$\frac{1}{2\sqrt{3}}(\varsigma_2 - \varsigma_1)\left(x_1x_2 + x_1x_3 + x_1x_4 + x_2x_3 + x_2x_4 + x_3x_4 - \frac{1}{3}\right)$
$\begin{array}{|c|c|}\hline\uparrow&\uparrow\\\hline\downarrow&\downarrow\\\hline\end{array} \times \boxed{0}\boxed{0}\boxed{1}\boxed{1}$	$\frac{1}{2\sqrt{3}}(\varsigma_1 - \varsigma_2)\left(x_1x_2 + x_1x_3 + x_1x_4 + x_2x_3 + x_2x_4 + x_3x_4 - \frac{1}{3}\right)$
$\begin{array}{|c|c|c|}\hline\uparrow&\uparrow&\downarrow\\\hline\downarrow\\\cline{1-1}\end{array} \times \begin{array}{|c|c|c|}\hline0&0&1\\\hline1\\\cline{1-1}\end{array} \; (\square\square\square\square)$	$\frac{1}{2}(\varsigma_2 - \varsigma_1)\left\{x_2x_4 - x_1x_3 + \frac{1}{5}(x_1 - x_2 + x_3 - x_4)\right\}$
$\begin{array}{|c|c|c|}\hline\uparrow&\uparrow&\downarrow\\\hline\downarrow\\\cline{1-1}\end{array} \times \begin{array}{|c|c|c|}\hline0&0&1\\\hline1\\\cline{1-1}\end{array} \; \left(\begin{array}{|c|c|}\hline\;&\;\\\hline\;&\;\\\hline\end{array}\right)$	$\frac{1}{2}(\varsigma_1 - \varsigma_2)\left\{x_2x_4 - x_1x_3 + \frac{1}{5}(x_1 - x_2 + x_3 - x_4)\right\}$
$\begin{array}{|c|c|}\hline\uparrow&\uparrow\\\hline\downarrow&\downarrow\\\hline\end{array} \times \begin{array}{|c|c|}\hline0&0\\\hline1&1\\\hline\end{array} \; (\square\square\square\square)$	$\frac{1}{2\sqrt{6}}(\varsigma_2 - \varsigma_1)\{-x_1x_2 - x_3x_4 - x_1x_4 - x_2x_3 + 2(x_1x_3 + x_2x_4)\}$
$\boxed{\uparrow}\boxed{\uparrow}\boxed{\downarrow}\boxed{\downarrow} \times \begin{array}{|c|c|}\hline0&0\\\hline1&1\\\hline\end{array}$	$\frac{1}{2\sqrt{3}}\{\varsigma_1(x_1 - x_2)(x_3 - x_4) + \varsigma_2(x_1 - x_4)(x_2 - x_3) + \varsigma_3(x_1 - x_3)(x_4 - x_2)\}$
$\begin{array}{|c|c|}\hline\uparrow&\uparrow\\\hline\downarrow&\downarrow\\\hline\end{array} \times \begin{array}{|c|c|}\hline0&0\\\hline1&1\\\hline\end{array} \; \left(\begin{array}{|c|c|}\hline\;&\;\\\hline\;&\;\\\hline\end{array}\right)$	$\frac{1}{2\sqrt{3}}\{\varsigma_1(x_1 - x_4)(x_3 - x_2) + \varsigma_2(x_1 - x_2)(x_4 - x_3) + \varsigma_3(x_1 - x_3)(x_2 - x_4)\}$
$\begin{array}{|c|c|}\hline\uparrow&\uparrow\\\hline\downarrow&\downarrow\\\hline\end{array} \times \begin{array}{|c|c|}\hline0&0\\\hline1&1\\\hline\end{array} \; \left(\begin{array}{|c|}\hline\;\\\hline\;\\\hline\;\\\hline\;\\\hline\end{array}\right)$	$\frac{1}{2\sqrt{6}}(-\varsigma_1 + 2\varsigma_2 - \varsigma_3)(x_1 - x_3)(x_2 - x_4)$

(ii) $S_z = 1$: ($\uparrow\uparrow\uparrow\downarrow$) T_1 terms

Spin × Orbital (SO)	Effective Representations
$\boxed{\uparrow}\boxed{\uparrow}\boxed{\uparrow}\boxed{\downarrow} \times \boxed{0}\boxed{0}\boxed{0}\boxed{0}$	$\frac{1}{\sqrt{2}}(\varsigma_2 - \varsigma_3)$
$\begin{array}{|c|c|c|}\hline\uparrow&\uparrow&\uparrow\\\hline\downarrow\\\cline{1-1}\end{array} \times \begin{array}{|c|c|c|}\hline 0&0&0\\\hline 1\\\cline{1-1}\end{array} \left(\begin{array}{|c|c|c|c|}\hline&&&\\\hline\end{array}\right)$	$\frac{1}{2\sqrt{6}}(\varsigma_2 - \varsigma_3)(-x_1 - x_2 - x_3 + 3x_4)$
$\begin{array}{|c|c|c|}\hline\uparrow&\uparrow&\uparrow\\\hline\downarrow\\\cline{1-1}\end{array} \times \begin{array}{|c|c|c|}\hline 0&0&0\\\hline 1\\\cline{1-1}\end{array} \left(\begin{array}{|c|c|}\hline&\\\hline&\\\hline\end{array}\right)$	$\frac{1}{\sqrt{6}}\{\varsigma_1(x_1 - x_3) + \varsigma_2(x_2 - x_1) + \varsigma_3(x_3 - x_2)\}$
$\boxed{\uparrow}\boxed{\uparrow}\boxed{\uparrow}\boxed{\downarrow} \times \boxed{0}\boxed{0}\boxed{1}\boxed{1}$	$\frac{1}{2\sqrt{3}}(\varsigma_2 - \varsigma_3)\left(x_1x_2 + x_1x_3 + x_1x_4 + x_2x_3 + x_2x_4 + x_3x_4 - \frac{1}{3}\right)$
$\begin{array}{|c|c|c|}\hline\uparrow&\uparrow&\uparrow\\\hline\downarrow\\\cline{1-1}\end{array} \times \begin{array}{|c|c|c|}\hline 0&0&1\\\hline 1\\\cline{1-1}\end{array} \left(\begin{array}{|c|c|c|c|}\hline&&&\\\hline\end{array}\right)$	$\frac{1}{2\sqrt{3}}(\varsigma_2 - \varsigma_3)\left\{x_1x_2 + x_1x_3 - x_1x_4 + x_2x_3 - x_2x_4 - x_3x_4 + \frac{1}{5}(-x_1 - x_2 - x_3 + 3x_4)\right\}$
$\begin{array}{|c|c|c|}\hline\uparrow&\uparrow&\uparrow\\\hline\downarrow\\\cline{1-1}\end{array} \times \begin{array}{|c|c|c|}\hline 0&0&1\\\hline 1\\\cline{1-1}\end{array} \left(\begin{array}{|c|c|}\hline&\\\hline&\\\hline\end{array}\right)$	$\frac{1}{2\sqrt{3}}\left[\varsigma_1\left\{-x_1x_2 + x_3x_4 - x_1x_4 + x_2x_3 + \frac{2}{5}(x_1 - x_3)\right\} + \varsigma_2\left\{-x_2x_4 + x_1x_3 + x_1x_4 - x_2x_3 + \frac{2}{5}(-x_1 + x_2)\right\} + \varsigma_3\left\{x_1x_2 - x_3x_4 + x_2x_4 - x_1x_3 + \frac{2}{5}(-x_2 + x_3)\right\}\right]$
$\boxed{\uparrow}\boxed{\uparrow}\boxed{\uparrow}\boxed{\downarrow} \times \begin{array}{|c|c|}\hline 0&0\\\hline 1&1\\\hline\end{array}$	$\frac{1}{2\sqrt{3}}\{\varsigma_1(x_1 - x_3)(x_4 - x_2) + \varsigma_2(x_1 - x_2)(x_3 - x_4) + \varsigma_3(x_1 - x_4)(x_2 - x_3)\}$

(iii) $S_z = 2$: ($\uparrow\uparrow\uparrow\uparrow$) T_1 terms

Spin × Orbital	Effective Representations
$\boxed{\uparrow}\boxed{\uparrow}\boxed{\uparrow}\boxed{\uparrow} \times \boxed{0}\boxed{0}\boxed{0}\boxed{0}$	$\frac{1}{\sqrt{2}}(\xi_2 - \xi_3)$
$\boxed{\uparrow}\boxed{\uparrow}\boxed{\uparrow}\boxed{\uparrow} \times \boxed{0}\boxed{0}\boxed{1}\boxed{1}$	$\frac{1}{2\sqrt{3}}(\xi_2 - \xi_3)\left(x_1x_2 + x_1x_3 + x_1x_4 + x_2x_3 + x_2x_4 + x_3x_4 - \frac{1}{3}\right)$
$\boxed{\uparrow}\boxed{\uparrow}\boxed{\uparrow}\boxed{\uparrow} \times \begin{array}{|c|c|}\hline 0&0\\\hline 1&1\\\hline\end{array}$	$\frac{1}{2\sqrt{3}}(\xi_1(x_1 - x_3)(x_4 - x_2) + \xi_2(x_1 - x_2)(x_3 - x_4) + \xi_3(x_1 - x_4)(x_2 - x_3))$

(iv) Normalisation Factors: For every representations, the following normalisation constants must be multiplied according to their orbital representations.

Orbital	Normalisation
$\boxed{0}\boxed{0}\boxed{0}\boxed{0}$	$\sqrt{71}$
$\begin{array}{|c|c|c|}\hline 0&0&0\\\hline 1\\\cline{1-1}\end{array}$	$6\sqrt{71}$
$\boxed{0}\boxed{0}\boxed{1}\boxed{1}$	$6\sqrt{165} \times \sqrt{71}$
$\begin{array}{|c|c|c|}\hline 0&0&1\\\hline 1\\\cline{1-1}\end{array}$	$10\sqrt{33} \times \sqrt{71}$
$\begin{array}{|c|c|}\hline 0&0\\\hline 1&1\\\hline\end{array}$	$6\sqrt{55} \times \sqrt{71}$

5.1 EVOLUTION OF THE FOUR-QUARK SYSTEM

The distribution amplitude $\phi(x_i, Q)$ is the valence Fock State wave function at equal time on the light cone integrated over transverse momenta $\vec{k}_{\perp i}^2 \lesssim Q^2$:

$$\phi(x_i, Q) = \int^Q \left(\prod_{i=1}^4 \frac{d^2\vec{k}_{\perp i}}{16\pi^3} \right) 16\,\pi^3 \delta^2 \left(\sum_i \vec{k}_{\perp i} \right) \psi^Q(x_i, \vec{k}_{\perp i}) \,. \tag{5.4}$$

The wavefunction $\psi^Q(x_i, \vec{k}_{\perp i})$ satisfies a Bethe-Salpeter type bound state wave equation. One can derive an evolution equation for the four-quark color-singlet state which expresses the variation of $\phi(x_i, Q)$ as Q^2 is increased:

$$\left(\frac{\partial}{\partial \xi} + \frac{2C_F}{\beta} \right) \widetilde{\phi}(x_i, Q) = -\frac{2}{\beta} \int [dy] V(x_i, y_i) \widetilde{\phi}(y_i, Q) \,, \tag{5.5}$$

where

$$\xi(Q^2) = \frac{\beta}{4\pi} \int_{Q_0^2}^{Q^2} \frac{dk_\perp^2}{k_\perp^2} \alpha_s(k_\perp^2) \,, \tag{5.6}$$

$$\phi(x_i, Q) = x_1 x_2 x_3 x_4 \, \widetilde{\phi}(x_i, Q), \tag{5.7}$$

and $\beta = 11 - \frac{2}{3} n_f$ (n_f is the number of flavors) and $C_F = (n_c^2 - 1)/2n_c$ (=3/4 in $SU(2)_C$). The term $\frac{2C_F}{\beta}$ in Eq. (5.5) is derived from the wavefunction renormalization of the quark propagators. To leading order in $\alpha_s(Q^2)$, $V(x_i, y_i)$ is computed from the single-gluon exchange kernel and is given by

$$\begin{aligned} V(x_i, y_i) = & \sum_{i \neq j} \left(\frac{\vec{\tau}_i}{2} \cdot \frac{\vec{\tau}_j}{2} \right) \theta(y_i - x_i) \prod_{k \neq i,j} \delta(x_k - y_k) \\ & \times \frac{y_j}{x_j} \left(\frac{\delta_{h_i \bar{h}_j}}{x_i + x_j} + \frac{\Delta}{y_i - x_i} \right) \\ & = V(y_i, x_i) \,, \end{aligned} \tag{5.8}$$

where $\vec{\tau} = (\tau_1, \tau_2, \tau_3)$ are the $SU(2)_C$ Pauli matrices and $\delta_{h_i \bar{h}_j} = 1(0)$ when the constituents $\{i, j\}$ have antiparallel (parallel) helicities. The infrared singularity in the kernel at $x_i = y_i$ cancels for color singlet bound states: $\Delta\widetilde{\phi}(y_i, Q) = \widetilde{\phi}(y_i, Q) - \widetilde{\phi}(x_i, Q)$.

The general solution of Eq. (5.5) can be written in the form

$$\widetilde{\phi}(x_i, Q) = \sum_{n=0}^{\infty} a_n \, \widetilde{\phi}_n(x_i) e^{-\gamma_n \xi(Q^2)} \, , \tag{5.9}$$

where γ_n and $\widetilde{\phi}_n$ are the eigenvalues and eigensolutions of the following characteristic equation:

$$\left(\frac{2C_F}{\beta} - \gamma_n\right) \widetilde{\phi}_n(x_i) = -\frac{2}{\beta} \int_0^1 [dy] \, V(x_i, y_i) \widetilde{\phi}_n(y_i) \, . \tag{5.10}$$

The $\widetilde{\phi}_n$ basis is given in Table I, as explained in the last section. The remaining task is to find the anomalous dimensions γ_n which determine the short-distance behavior of the four-quark wave function by computing the matrix of the evolution kernel in this basis and diagonalizing it. Note that when a gluon is exchanged between the first and second quarks then the basis vectors ζ_1 and ζ_2 can be interchanged while ζ_3 preserves itself. Thus the calculation of the color factors is not as simple as the three-quark QCD case and requires a complete matrix analysis.

The mixing between different spin and orbital multiplets is similar to the three-quark case. For example, the mixing matrix for the orbital power $n = 2$ has dimension 4×4 for the $S_Z = 1$ case and dimension 6×6 for the $S_Z = 0$. After diagonalizing the mixing matrices, we find the eigenvalues γ_n and the eigensolutions $\widetilde{\phi}_n$. The results are summarized in Table II.

5.2 TWO-CLUSTER DECOMPOSITION

In this section, we will connect the eigensolutions of the four-quark evolution equation to the physical two-cluster basis and derive constraints on the effective nuclear potential between the clusters.

The four-quark antisymmetric representations can always be decomposed into a sum of products of pairs of two-quark representations. The two-quark antisymmetric representation is called a cluster which is classified according to its quantum numbers under $G = SU(2)_C \times SU(2)_T \times SU(2)_S$. In $SU(2)_C$ a four-quark color singlet can be constructed not only from a pair of two-quark color singlet, but also from the product of two-quark color triplets (C). These correspond to dibaryon and hidden color states, respectively. The dibaryon states are classified by their isospin quantum numbers : N and Δ correspond to $T = 0$ and 1, in analogy to the $T = 1/2$ and $3/2$ states in QCD.

A given four-quark antisymmetric representation (A) can be decomposed onto two clusters $(A_1 \otimes A_2)$ using the following steps:

1. Represent the four-quark antisymmetric representation as an inner product form $A = C \times T \times S \times O$.

TABLE II

Eigenvalues and eigensolutions for $T = 0$ four-quark system up to total orbital power $n = 2$. Every eigensolution is a linear combination of completely antisymmetric representations given by Table I. For convenience, we represent eigensolutions as Young diagrams of spin and orbital spaces since the color and isospin Young diagram is fixed by $\begin{array}{|c|c|}\hline b & b \\ \hline u & u \\ \hline \end{array} \times \begin{array}{|c|c|}\hline u & u \\ \hline d & d \\ \hline \end{array}$.

	$b_n[\gamma_n = (2+b_n)C_F/\beta]$	Spin × Orbit (SO)
$S_z = 0$	$-\frac{8}{3}$	$\frac{1}{\sqrt{2}}\left(\begin{array}{|c|c|c|c|}\hline \uparrow & \uparrow & \downarrow & \downarrow \\ \hline \end{array} - \begin{array}{|c|c|}\hline \uparrow & \uparrow \\ \hline \downarrow & \downarrow \\ \hline \end{array}\right) \times \begin{array}{|c|c|c|c|}\hline 0 & 0 & 0 & 0 \\ \hline \end{array}$
	-2.13	$0.56\left(\begin{array}{|c|c|c|c|}\hline \uparrow & \uparrow & \downarrow & \downarrow \\ \hline \end{array} - \begin{array}{|c|c|}\hline \uparrow & \uparrow \\ \hline \downarrow & \downarrow \\ \hline \end{array}\right) \times \begin{array}{|c|c|c|c|}\hline 0 & 0 & 1 & 1 \\ \hline \end{array} - 0.43 \begin{array}{|c|c|c|c|}\hline \uparrow & \uparrow & \downarrow & \downarrow \\ \hline \end{array} \times \begin{array}{|c|c|}\hline 0 & 0 \\ \hline 1 & 1 \\ \hline \end{array}$
		$+ \begin{array}{|c|c|}\hline \uparrow & \uparrow \\ \hline \downarrow & \downarrow \\ \hline \end{array} \times \begin{array}{|c|c|}\hline 0 & 0 \\ \hline 1 & 1 \\ \hline \end{array} \left(0.32 \begin{array}{|c|c|c|}\hline & & \\ \hline \end{array} - 0.03 \begin{array}{|c|c|}\hline & \\ \hline & \\ \hline \end{array} - 0.28 \begin{array}{|c|}\hline \\ \hline \\ \hline \\ \hline \end{array}\right)$
	-1.94	$-0.22\left(\begin{array}{|c|c|c|c|}\hline \uparrow & \uparrow & \downarrow & \downarrow \\ \hline \end{array} + \begin{array}{|c|c|}\hline \uparrow & \uparrow \\ \hline \downarrow & \downarrow \\ \hline \end{array}\right) \times \begin{array}{|c|c|c|c|}\hline 0 & 0 & 1 & 1 \\ \hline \end{array} + 0.28 \begin{array}{|c|c|c|c|}\hline \uparrow & \uparrow & \downarrow & \downarrow \\ \hline \end{array} \times \begin{array}{|c|c|}\hline 0 & 0 \\ \hline 1 & 1 \\ \hline \end{array}$
		$+ \begin{array}{|c|c|}\hline \uparrow & \uparrow \\ \hline \downarrow & \downarrow \\ \hline \end{array} \times \begin{array}{|c|c|}\hline 0 & 0 \\ \hline 1 & 1 \\ \hline \end{array} \left(-0.24 \begin{array}{|c|c|c|}\hline & & \\ \hline \end{array} - 0.61 \begin{array}{|c|c|}\hline & \\ \hline & \\ \hline \end{array} - 0.63 \begin{array}{|c|}\hline \\ \hline \\ \hline \\ \hline \end{array}\right)$
	$-\frac{2}{9}$	$\begin{array}{|c|c|c|}\hline \uparrow & \uparrow & \downarrow \\ \hline \downarrow \\ \cline{1-1} \end{array} \times \begin{array}{|c|c|c|}\hline 0 & 0 & 1 \\ \hline 1 \\ \cline{1-1} \end{array} \left(\frac{1}{\sqrt{2}} \begin{array}{|c|c|c|}\hline & & \\ \hline \end{array} - \frac{1}{\sqrt{2}} \begin{array}{|c|c|}\hline & \\ \hline & \\ \hline \end{array}\right)$
	0	$\frac{1}{\sqrt{2}}\left(\begin{array}{|c|c|c|c|}\hline \uparrow & \uparrow & \downarrow & \downarrow \\ \hline \end{array} + \begin{array}{|c|c|}\hline \uparrow & \uparrow \\ \hline \downarrow & \downarrow \\ \hline \end{array}\right) \times \begin{array}{|c|c|c|c|}\hline 0 & 0 & 0 & 0 \\ \hline \end{array}$
	0	$\begin{array}{|c|c|c|}\hline \uparrow & \uparrow & \downarrow \\ \hline \downarrow \\ \cline{1-1} \end{array} \times \begin{array}{|c|c|c|}\hline 0 & 0 & 0 \\ \hline 1 \\ \cline{1-1} \end{array} \left(\frac{1}{\sqrt{2}} \begin{array}{|c|c|c|}\hline & & \\ \hline \end{array} + \frac{1}{\sqrt{2}} \begin{array}{|c|c|}\hline & \\ \hline & \\ \hline \end{array}\right)$

	$b_n[\gamma_n = (2+b_n)C_F/\beta]$	Spin × Orbit (SO)
$S_z = 0$	0.006	$-0.47\left(\boxed{\uparrow}\boxed{\uparrow}\boxed{\downarrow}\boxed{\downarrow} + \begin{array}{|c|c|}\hline\uparrow&\uparrow\\\hline\downarrow&\downarrow\\\hline\end{array}\right) \times \boxed{0}\boxed{0}\boxed{1}\boxed{1} + 0.40\,\boxed{\uparrow}\boxed{\uparrow}\boxed{\downarrow}\boxed{\downarrow} \times \begin{array}{|c|c|}\hline0&0\\\hline1&1\\\hline\end{array}$ $+ \begin{array}{|c|c|}\hline\uparrow&\uparrow\\\hline\downarrow&\downarrow\\\hline\end{array} \times \begin{array}{|c|c|}\hline0&0\\\hline1&1\\\hline\end{array}\left(0.53\,\square\square\square\square + 0.35\,\begin{array}{|c|c|}\hline&\\\hline&\\\hline\end{array} - 0.03\,\begin{array}{|c|}\hline\\\hline\\\hline\\\hline\end{array}\right)$
	$\frac{8}{9}$	$\begin{array}{|c|c|c|}\hline\uparrow&\uparrow&\downarrow\\\hline\downarrow\\\cline{1-1}\end{array} \times \begin{array}{|c|c|c|}\hline0&0&0\\\hline1\\\cline{1-1}\end{array}\left(-\frac{1}{\sqrt{2}}\,\square\square\square\square + \frac{1}{\sqrt{2}}\,\begin{array}{|c|c|}\hline&\\\hline&\\\hline\end{array}\right)$
	$\frac{10}{3}$	$\begin{array}{|c|c|c|}\hline\uparrow&\uparrow&\downarrow\\\hline\downarrow\\\cline{1-1}\end{array} \times \begin{array}{|c|c|c|}\hline0&0&1\\\hline1\\\cline{1-1}\end{array}\left(\frac{1}{\sqrt{2}}\,\square\square\square\square + \frac{1}{\sqrt{2}}\,\begin{array}{|c|c|}\hline&\\\hline&\\\hline\end{array}\right)$
	3.5	$-0.42\left(\boxed{\uparrow}\boxed{\uparrow}\boxed{\downarrow}\boxed{\downarrow} - \begin{array}{|c|c|}\hline\uparrow&\uparrow\\\hline\downarrow&\downarrow\\\hline\end{array}\right) \times \boxed{0}\boxed{0}\boxed{1}\boxed{1} - 0.53\,\boxed{\uparrow}\boxed{\uparrow}\boxed{\downarrow}\boxed{\downarrow} \times \begin{array}{|c|c|}\hline0&0\\\hline1&1\\\hline\end{array}$ $+ \begin{array}{|c|c|}\hline\uparrow&\uparrow\\\hline\downarrow&\downarrow\\\hline\end{array} \times \begin{array}{|c|c|}\hline0&0\\\hline1&1\\\hline\end{array}\left(0.52\,\square\square\square\square - 0.21\,\begin{array}{|c|c|}\hline&\\\hline&\\\hline\end{array} - 0.23\,\begin{array}{|c|}\hline\\\hline\\\hline\\\hline\end{array}\right)$
	4.75	$-0.48\left(\boxed{\uparrow}\boxed{\uparrow}\boxed{\downarrow}\boxed{\downarrow} + \begin{array}{|c|c|}\hline\uparrow&\uparrow\\\hline\downarrow&\downarrow\\\hline\end{array}\right) \times \boxed{0}\boxed{0}\boxed{1}\boxed{1} - 0.52\,\boxed{\uparrow}\boxed{\uparrow}\boxed{\downarrow}\boxed{\downarrow} \times \begin{array}{|c|c|}\hline0&0\\\hline1&1\\\hline\end{array}$ $+ \begin{array}{|c|c|}\hline\uparrow&\uparrow\\\hline\downarrow&\downarrow\\\hline\end{array} \times \begin{array}{|c|c|}\hline0&0\\\hline1&1\\\hline\end{array}\left(-0.40\,\square\square\square\square - 0.06\,\begin{array}{|c|c|}\hline&\\\hline&\\\hline\end{array} + 0.32\,\begin{array}{|c|}\hline\\\hline\\\hline\\\hline\end{array}\right)$
	5.40	$0.11\left(\boxed{\uparrow}\boxed{\uparrow}\boxed{\downarrow}\boxed{\downarrow} - \begin{array}{|c|c|}\hline\uparrow&\uparrow\\\hline\downarrow&\downarrow\\\hline\end{array}\right) \times \boxed{0}\boxed{0}\boxed{1}\boxed{1} + 0.18\,\boxed{\uparrow}\boxed{\uparrow}\boxed{\downarrow}\boxed{\downarrow} \times \begin{array}{|c|c|}\hline0&0\\\hline1&1\\\hline\end{array}$ $+ \begin{array}{|c|c|}\hline\uparrow&\uparrow\\\hline\downarrow&\downarrow\\\hline\end{array} \times \begin{array}{|c|c|}\hline0&0\\\hline1&1\\\hline\end{array}\left(0.35\,\square\square\square\square - 0.67\,\begin{array}{|c|c|}\hline&\\\hline&\\\hline\end{array} + 0.61\,\begin{array}{|c|}\hline\\\hline\\\hline\\\hline\end{array}\right)$

	$b_n[\gamma_n = (2+b_n)C_F/\beta]$	Spin × Orbit (SO)
$S_q = 1$	$\frac{11-\sqrt{1033}}{18}$	$\begin{array}{|c|}\hline\uparrow\\\hline\downarrow\\\hline\end{array}\times\begin{array}{|c|}\hline 0\\\hline 1\\\hline\end{array}\left(a\,\square\!\square\!\square\!\square+b\begin{array}{|c|c|}\hline\ &\ \\\hline\ &\ \\\hline\end{array}\right)\left(\frac{a}{b}=\frac{32}{3+\sqrt{1033}}\right)$
	-1	$\begin{array}{|c|}\hline\uparrow\\\hline\uparrow\\\hline\uparrow\\\hline\downarrow\\\hline\end{array}\times\begin{array}{|c|}\hline 0\\\hline 0\\\hline 0\\\hline 0\\\hline\end{array}$
	-0.98	$0.64\begin{array}{|c|}\hline\uparrow\\\hline\uparrow\\\hline\uparrow\\\hline\downarrow\\\hline\end{array}\times\begin{array}{|c|}\hline 0\\\hline 0\\\hline 1\\\hline 1\\\hline\end{array}+0.74\begin{array}{|c|}\hline\uparrow\\\hline\uparrow\\\hline\uparrow\\\hline\downarrow\\\hline\end{array}\times\begin{array}{|c|c|}\hline 0&0\\\hline 1&1\\\hline\end{array}$
		$+\begin{array}{|c|}\hline\uparrow\\\hline\uparrow\\\hline\downarrow\\\hline\end{array}\times\begin{array}{|c|}\hline 0\\\hline 0\\\hline 1\\\hline\end{array}\left(-0.17\,\square\!\square\!\square-0.16\begin{array}{|c|c|}\hline\ &\ \\\hline\ &\ \\\hline\end{array}\right)$
	1.13	$-0.12\begin{array}{|c|}\hline\uparrow\\\hline\uparrow\\\hline\uparrow\\\hline\downarrow\\\hline\end{array}\times\begin{array}{|c|}\hline 0\\\hline 0\\\hline 1\\\hline 1\\\hline\end{array}-0.20\begin{array}{|c|}\hline\uparrow\\\hline\uparrow\\\hline\uparrow\\\hline\downarrow\\\hline\end{array}\times\begin{array}{|c|c|}\hline 0&0\\\hline 1&1\\\hline\end{array}$
		$+\begin{array}{|c|}\hline\uparrow\\\hline\uparrow\\\hline\downarrow\\\hline\end{array}\times\begin{array}{|c|}\hline 0\\\hline 0\\\hline 1\\\hline\end{array}\left(-0.77\,\square\!\square\!\square-0.60\begin{array}{|c|c|}\hline\ &\ \\\hline\ &\ \\\hline\end{array}\right)$
	$\frac{11+\sqrt{1033}}{18}$	$\begin{array}{|c|}\hline\uparrow\\\hline\uparrow\\\hline\downarrow\\\hline\end{array}\times\begin{array}{|c|}\hline 0\\\hline 0\\\hline 1\\\hline\end{array}\left(-b\,\square\!\square\!\square+a\begin{array}{|c|c|}\hline\ &\ \\\hline\ &\ \\\hline\end{array}\right)$
	2.51	$0.04\begin{array}{|c|}\hline\uparrow\\\hline\uparrow\\\hline\uparrow\\\hline\downarrow\\\hline\end{array}\times\begin{array}{|c|}\hline 0\\\hline 0\\\hline 1\\\hline 1\\\hline\end{array}-0.07\begin{array}{|c|}\hline\uparrow\\\hline\uparrow\\\hline\uparrow\\\hline\downarrow\\\hline\end{array}\times\begin{array}{|c|c|}\hline 0&0\\\hline 1&1\\\hline\end{array}$
		$+\begin{array}{|c|}\hline\uparrow\\\hline\uparrow\\\hline\downarrow\\\hline\end{array}\times\begin{array}{|c|}\hline 0\\\hline 0\\\hline 1\\\hline\end{array}\left(0.62\,\square\!\square\!\square-0.78\begin{array}{|c|c|}\hline\ &\ \\\hline\ &\ \\\hline\end{array}\right)$
	4.4	$0.76\begin{array}{|c|}\hline\uparrow\\\hline\uparrow\\\hline\uparrow\\\hline\downarrow\\\hline\end{array}\times\begin{array}{|c|}\hline 0\\\hline 0\\\hline 1\\\hline 1\\\hline\end{array}-0.64\begin{array}{|c|}\hline\uparrow\\\hline\uparrow\\\hline\uparrow\\\hline\downarrow\\\hline\end{array}\times\begin{array}{|c|c|}\hline 0&0\\\hline 1&1\\\hline\end{array}$
		$+\begin{array}{|c|}\hline\uparrow\\\hline\uparrow\\\hline\downarrow\\\hline\end{array}\times\begin{array}{|c|}\hline 0\\\hline 0\\\hline 1\\\hline\end{array}\left(-0.02\,\square\!\square\!\square+0.09\begin{array}{|c|c|}\hline\ &\ \\\hline\ &\ \\\hline\end{array}\right)$
$S_q = 2$	0	$\begin{array}{|c|}\hline\uparrow\\\hline\uparrow\\\hline\uparrow\\\hline\uparrow\\\hline\end{array}\times\begin{array}{|c|}\hline 0\\\hline 0\\\hline 0\\\hline 0\\\hline\end{array}$
	0	$\begin{array}{|c|}\hline\uparrow\\\hline\uparrow\\\hline\uparrow\\\hline\uparrow\\\hline\end{array}\times\left(\sqrt{\frac{4}{7}}\begin{array}{|c|}\hline 0\\\hline 0\\\hline 1\\\hline 1\\\hline\end{array}-\sqrt{\frac{3}{7}}\begin{array}{|c|c|}\hline 0&0\\\hline 1&1\\\hline\end{array}\right)$
	$\frac{14}{3}$	$\begin{array}{|c|}\hline\uparrow\\\hline\uparrow\\\hline\uparrow\\\hline\uparrow\\\hline\end{array}\times\left(\sqrt{\frac{3}{7}}\begin{array}{|c|}\hline 0\\\hline 0\\\hline 1\\\hline 1\\\hline\end{array}+\sqrt{\frac{4}{7}}\begin{array}{|c|c|}\hline 0&0\\\hline 1&1\\\hline\end{array}\right)$

2. Decompose each four-quark representations C, T, S and O as an outer product of two two-quark representations using fractional parentage coefficients,[6] e.g. $C = C_1 \otimes C_2$.

3. Recombine the representations as an inner product: $A = (C_1 \otimes C_2) \times (T_1 \otimes T_2) \times (S_1 \otimes S_2) \times (O_1 \otimes O_2)$.

4. Commute the order of inner product and outer product, gathering together representations of the same cluster: $A = (C_1 \times T_1 \times S_1 \times O_1) \otimes (C_2 \times T_2 \times S_2 \times O_2) \equiv A_1 \otimes A_2$.

5. It is sufficient to consider only the coefficient of the symmetric orbitals O_1 and O_2 to classify the clusters such as NN, $N\Delta$, $\Delta\Delta$ and CC.

Using these steps, we can determine the relation between antisymmetrized four-quark antisymmetric representations and the effective two-cluster representations. For the $T = S = 0$ case, we obtain the transition table given in Table III which relates the two kinds of representations. M. Harvey[7] has already obtained the analogous transformation matrices between the physical basis and the symmetry basis for six-quark systems. His definitions of the physical and symmetry bases are essentially the same as the two-cluster representations and the completely antisymmetric representations used here.

TABLE III

Transition between four-quark antisymmetric representations and effective two-cluster representations. Square and curly brackets represent the orbital (O) and spin-isospin (TS) symmetries respectively.

	$[4]\{22\}$	$[22]\{22\}$	$[22]\{4\}$	$[22]\{1111\}$
NN	$-1/2$	$-1/2$	$1/\sqrt{2}$	0
$\Delta\Delta$	$1/2$	$1/2$	$1/\sqrt{2}$	0
$(CC)_1$	$1/\sqrt{2}$	$-1/\sqrt{2}$	0	0
$(CC)_2$	0	0	0	1

From Table III, we can relate the two-cluster distribution amplitudes with the completely antisymmetric quark distribution amplitudes. For example, the dinucleon distribution amplitude is given by

$$\phi_{NN}(x_i, Q) = -\frac{1}{2}\,\phi_{[4]\{22\}}(x_i, Q) + \frac{1}{2}\,\phi_{[22]\{22\}}(x_i, Q) - \frac{1}{\sqrt{2}}\,\phi_{[22]\{4\}}(x_i, Q)\,, \tag{5.11}$$

where the orbital and the spin-isospin symmetries are represented inside the square and the

curly brackets. Since the eigensolutions are linear combinations of completely antisymmetric representations, we can relate the right-hand side of Eq. (5.11) with the eigensolutions given by Table II. The eigensolutions $\phi_{\gamma_n}(x_i, Q)$ have the following form:

$$\phi_{\gamma_n}(x_i, Q) = e^{-\gamma_n \xi(Q^2)}\, \phi_{\gamma_n}(x_i) \ . \tag{5.12}$$

Consequently, we can expand each two-cluster distribution amplitudes in terms of the orbital index power representations $\phi_{\gamma_n}(x_i)$. To probe the high Q^2 behavior of the two-cluster distribution amplitudes, it is sufficient to consider only the leading terms which have the lowest anomalous dimensions γ_n because of the damping factor of Eq. (5.12). The lowest orbital power with representations which provide well-defined two-cluster distribution amplitudes is $n = 2$. We will discuss the special properties of the $n = 0$ representation in the next section.

The $n = 2$ two-cluster distribution amplitudes can be expanded in terms of the orbital representations $\phi_{\gamma_2}(x_i) \equiv \phi_{\gamma_2}$:

$$\begin{aligned}\phi_{NN}(x_i, Q) = {} & 0.07\, e^{0.13\widetilde{\xi}}\, \phi_{0.13} - 0.64\, e^{-0.06\widetilde{\xi}} \phi_{-0.06} \\ & + 0.39\, e^{-2.01\widetilde{\xi}}\, \phi_{-2.01} - 0.47\, e^{-5.50\widetilde{\xi}} \phi_{-5.50} \\ & + 0.44\, e^{-6.75\widetilde{\xi}}\, \phi_{-6.75} + 0.15\, e^{-7.40\widetilde{\xi}} \phi_{-7.40} \ ,\end{aligned} \tag{5.13a}$$

$$\begin{aligned}\phi_{\Delta\Delta}(x_i, Q) = {} & -0.07\, e^{0.13\widetilde{\xi}}\, \phi_{0.13} - 0.59\, e^{-0.06\widetilde{\xi}} \phi_{-0.06} \\ & + 0.32\, e^{-2.01\widetilde{\xi}}\, \phi_{-2.01} + 0.47\, e^{-5.50\widetilde{\xi}} \phi_{-5.50} \\ & - 0.55\, e^{-6.75\widetilde{\xi}}\, \phi_{-6.75} - 0.15\, e^{-7.40\widetilde{\xi}} \phi_{-7.40} \ ,\end{aligned} \tag{5.13b}$$

and

$$\begin{aligned}\phi_{(CC)_1} = {} & -0.70\, e^{0.13\widetilde{\xi}}\, \phi_{0.13} - 0.35\, e^{-0.06\widetilde{\xi}} \phi_{-0.06} \\ & - 0.61\, e^{-2.01\widetilde{\xi}}\, \phi_{-2.01} - 0.08\, e^{-5.50\widetilde{\xi}} \phi_{-5.50} \\ & + 0.02\, e^{-6.75\widetilde{\xi}}\, \phi_{-6.75} + 0.05\, e^{-7.40\widetilde{\xi}} \phi_{-7.40} \ ,\end{aligned} \tag{5.13c}$$

where $\widetilde{\xi} = \frac{Q}{\beta}\xi(Q^2)$. We will discuss the second hidden-color state $\phi_{(CC)_2}$ in the next section.

As seen from Eq. (5.13), each distribution amplitude has a distinct high Q^2 behavior which depends on whether it is composed of colorless or colorful clusters. The prototypes of the dibaryon system have a negligible coefficient for the most leading term at high Q^2 and relatively large coefficients for the next-to-leading terms, whereas the hidden color state $(CC)_1$ has a large coefficient for the leading term.

One can imagine constructing a state at the scale Q_0 which only has the NN component of Eq. (5.13a) and then studying its evolution as Q increases. The high Q^2 behavior of $\phi(x_i, Q)$ gives the probability amplitude that all the quarks have impact separation less than $1/Q$. Thus the colorful clusters tend to coexist at short distances; i.e., the colorful clusters tend to attract each other and the colorless clusters tend to repel each other at short distances. Although these results are strictly only applicable in the limit of vanishing interparticle separation, they do provide rigorous constraints on the effective nuclear potential at short distances.

5.3 ANOMALOUS STATES

In the last section, we expanded the effective two-cluster representations in terms of the eigensolutions of the evolution equation and derived constraints on the effective nuclear potential at short distances. A state which at large distances corresponds to two colorless clusters (such as NN and $\Delta\Delta$) acts as if there is a short-distance repulsive potential between them. On the other hand, a state which consists of two colorful clusters at large distance ($(CC)_1$) sees an attractive potential at short distances. These results show that the leading contribution of QCD to the multiquark wavefunction at short distances has a behavior consistent with the repulsive core nucleon-nucleon potential of conventional nuclear physics.[8] However, we also find that the theory predicts the existence of anomalous states which differ from the normal nuclear degree of freedoms.

As shown in Table III, if the total power n of orbital representation is zero, then only the completely symmetric orbital is possible. Thus, we can read Table III vertically but not horizontally. Since this state cannot exist without including hidden color components with 50% probability,[9] we cannot interpret this state with normal nucleonic degrees of freedom. If such states exist in physical nuclei then they can provide non-additive nuclear phenomena, such as that observed in the EMC effect[4] in deep inelastic lepton-nucleus structure functions.

The $(CC)_2$ state in the orthonormal cluster basis also has anomalous properties. If we expand the $n = 2$ component in terms of eigensolutions, then

$$\begin{aligned}\phi_{(CC)_2}(x_i, Q) = &- 0.04e^{0.13\tilde{\xi}}\,\phi_{0.13} - 0.30e^{-5.50\tilde{\xi}}\,\phi_{-5.50} \\ &- 0.95e^{-7.40\tilde{\xi}}\phi_{-7.40}\,.\end{aligned} \tag{5.14}$$

Since this state has negligible coefficients for the leading terms and very large coefficient for the strongly damped non-leading terms, the $(CC)_2$ state acts as if there is a repulsive potential between two colorful clusters at short distances. This behavior contrasts with the more conventional behavior of $(CC)_1$.

If such a nuclear state were quasi-stable it could have unusual interaction properties. Since it consists of separated triplets (octets in $SU(3)_C$) the state has a large color-dipole moment, producing large hadronic cross sections and short mean free paths. It is amusing to speculate whether the states in QCD analogous to the $(CC)_2$ cluster configurations have any connection with the anomalous phenomena apparently observed in heavy ion collisions.[3,10]

5.4 Implications of Hidden Color States

The results discussed in this chapter represent a first attempt to extract exact results for the composition and interactions of multiquark nuclear systems at short distances. For simplicity, we have analyzed four-quark bound states in $SU(2)_C$, but we expect that many of the derived properties extend to six-quark states in QCD.[11] In particular, since the leading eigensolution at high momentum transfer has 80% hidden color probability,[9] we expect a transition of the ordinary nuclear state to non-nucleonic degrees of freedom as one evolves from long to short distances.

The set of eigensolutions of the evolution equation represent all the possible degrees of freedom of the multiquark bound state system since its kernel has the same invariances and symmetries of the full QCD Hamiltonian. We thus expect that the eigensolutions of the evolution kernel which are dominantly hidden-color to correspond to actual states and excitations of ordinary nuclei. A careful experimental search for these exotic resonances should be made. Possible channels where signals for such states may be observed include Compton and pion photoproduction on a deuteron target at large angles.

REFERENCES

1. S. J. Brodsky and Chueng-Ryong Ji, SLAC-PUB-3076(1985).
2. G. P. Lepage and S. J. Brodsky, Phys. Rev. D 22, 2157 (1980). S. J. Brodsky, SLAC-PUB-3191, published in *Short-distance Phenomena in Nuclear Physics*, D. H. Boal and R. M. Woloshyn eds. Plenum (1983).
3. B. Judek, Can. J. Phys. 46, 343 (1968); 50, 2082 (1972); I. Otterlund, Sixth High Energy Heavy Ion Study and Second Workshop on Anomaly, held at LBL, June 28 to July 1 (1983); E.M.Friedlander et. al., Phys. Rev.Lett. 45, 1084(1980).
4. R. Jaffe, Nature, 296, 305 (1982); E. Gabathuler, Progress in Particle and Nuclear Physics, Vol. 13, Chapter 12, edited by A. Faessler (1985).
5. M. Hammermesh, *Group Theory* (Addison-Wesley, Reading, Mass. 1962).
6. M. Harvey, lectures given at TRIUMF, 20-24 October 1980; H. A. Jahn and H. Van Wieringen, Proc. Roy. Soc. A209, 502 (1951); J. P. Elliott, J. Hope and H. A. Jahn, Phil. Trans. Roy. Soc. 246, 241 (1953).
7. M. Harvey, Nucl. Phys. A352, 301 (1981); A352, 326 (1981).

8. C. Detar, Harvard University Report No. HU-TFT-82-6, 1982 (unpublished); M. Harvey, Ref. 7; R. L. Jaffe, Phys. Rev. Lett. 50, 228 (1983); G. E. Brown, Progress in Particle Nuclear Physics, Vol. 8, Chapter 5, edited by D. Wilkinson (1982); A. Faessler, Progress in Particle and Nuclear Physics, Vol. 13, Chapter 9, edited by A. Faessler (1985).

9. The realistic six-quark state has 80% hidden color state. See S. J. Brodsky, C.-R. Ji and G. P. Lepage, Phys. Rev. Lett. 51, 83 (1983).

10. P. J. S. Watson, Phys. Lett. 126B, 289 (1983); W. J. Romo and P. J. S. Watson, Phys. Lett. 88B, 354 (1979).

11. The six-quark evolution formalism is developed and the leading anomalous dimension of a realistic deuteron are given in Chueng-Ryong Ji and S. J. Brodsky, SLAC-PUB-3148.

6. LIMITATIONS OF TRADITIONAL NUCLEAR PHYSICS

The fact that the QCD prediction for the reduced form factor $Q^2 f_d(Q^2) \sim const$ [see Chapter 4] appears to be an excellent agreement with experiment for $Q^2 > 1$ GeV^2 provides an excellent check on the six-quark description of the deuteron at short-distance as well as the scale-invariance of the $qq \to qq$ scattering amplitude. On the other hand, as we show in Appendix C, the standard "impulse approximation" used in standard nuclear physics calculations[1]

$$F_d(Q^2) = F_N(Q^2) \times F_{\text{Body}}(Q^2) \tag{6.1}$$

is invalid in QCD at large Q^2 since off-shell nucleon form factors enter [see Fig. 14(a)]. The usual treatment of nuclear form factors also overestimates the contribution of meson exchange currents [Fig. 14(b)] and $N\bar{N}$ contributions [Fig. 14(c)] since they are strongly suppressed by vertex form factors as we shall show in this section.

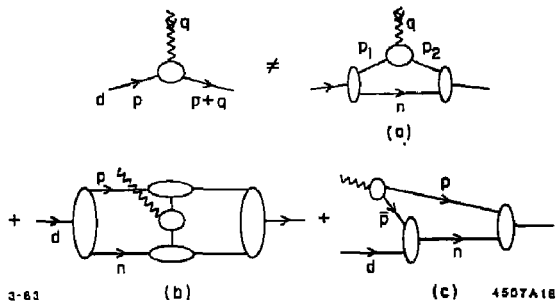

Fig. 14. Critique of the standard nuclear physics approach to the deuteron form factor at large Q^2. (a) The effective nucleon form factor has one or both legs off-shell: $|p_1^2 - p_2^2| \sim q^2/2$. (b) Meson exchange currents are suppressed in QCD because of off-shell form factors. (c) The nucleon pair contribution is suppressed because of nucleon compositeness. Contact terms appear only at the quark level.

At long distances and small, non-relativistic momenta, the traditional description of nuclear forces and nuclear dynamics based on nucleon, isobar, and meson degrees of freedom appears to give a viable phenomenology of nuclear reactions and spectroscopy. It is natural to try to extend the predictions of these models to the relativistic domain, e.g., by utilising local meson-nucleon field theories to represent the basic nuclear dynamics, and to use an effective Dirac equation to describe the propagation of nucleons in nuclear matter. An interesting question is whether such approaches can be derived as a "correspondence" limit of QCD, at least in the low momentum transfer ($Q^2 R_p^2 \ll 1$) and low excitation energy domain ($M\nu \ll M'^2 - M^2$).

The existence of hidden-color Fock state components in the nuclear state in principle precludes an exact treatment of nuclear properties based on meson-nucleon-isobar degrees of freedom since these hadronic degrees of freedom do not form a complete basis on QCD. Since the deuteron form factor is dominated by hidden color states at large momentum transfer, it cannot be described by np, $\Delta\Delta$ wavefunction components on meson exchange currents alone. It is likely that the hidden color states give less than a few percent correction to the global properties of nuclei; nevertheless, since extra degrees of freedom lower the energy of a system it is even conceivable that the deuteron would be unbound were it not for its hidden color components.

Independent of hidden color effects, we can still ask whether it is possible—in principle—to represent composite systems such as mesons and baryons as local fields in a Lagrangian field theory, at least for sufficiently long wavelengths such that internal structure of the hadrons cannot be discerned. Here we will outline a method to construct an effective Lagrangian of this sort. First, consider the ultraviolet-regulated QCD Lagrangian density $\mathcal{L}^{\kappa}_{\rm QCD}$ defined such that all internal loops in the perturbative expansion are cut off below a given momentum scale κ. Normally κ is chosen to be much larger than all relevant physical scale. Because QCD is renormalizable, $\mathcal{L}^{\kappa}_{\rm QCD}$ is form-invariant under changes of κ provided that the coupling constant $\alpha_s(\kappa^2)$ and quark mass parameter $m(\kappa^2)$ are appropriately defined. However, if we insist on choosing the cutoff κ to be as small as hadronic scales then extra ("higher twist") contributions will be generated in the effective Lagrangian density:

$$\mathcal{L}^{\kappa} = \mathcal{L}^{\kappa}_0 + \frac{e m(\kappa)}{\kappa^2}\,\bar\psi_N \sigma_{\mu\nu}\partial^\mu \psi_N A^\nu_{\rm em} + e\,\frac{f_\pi^2}{\kappa^2}\,\phi_\pi^\dagger \partial_\mu \phi_\pi A^\mu_{\rm em} + e\,\frac{f_p^2}{\kappa^2}\,\bar\psi_N \gamma_\nu \psi_N A^\nu_{\rm em} + \frac{f_p^2 f_\pi}{\kappa^6}\,\partial_\nu \bar\psi_N \gamma_5 \gamma^\nu \psi_N \phi_\pi + \cdots \tag{6.2}$$

where $\mathcal{L}^{\kappa}_0$ is the standard Lagrangian and the "higher twist" terms of order κ^{-2}, κ^{-4}, ... are schematic representations of the quark Pauli form factor, the pion and nucleon Dirac form factors, and the pion nucleon-antinucleon coupling. The pion and nucleon fields ϕ_π and ψ_N represent composite operators constructed and normalized from the valence Fock amplitudes and the leading interpolating quark operators. One can use the above equation to estimate the effective asymptotic power law behaviors of the couplings, e.g., $F^{\rm quark}_{\rm Pauli} \sim 1/Q^2$, $F_\pi \sim f_\pi^2/Q^2$, $G_M \sim f_p^2/Q^4$ and the effective $\pi \bar N \gamma_5 N F_{\pi N\bar N}$ coupling: $F_{\pi N\bar N}(Q^2) \sim M_N f_p^2 f_\pi/Q^6$. The net pion exchange amplitude for $NN-NN$ scatterings thus falls off very rapidly at large momentum transfer $M^{\pi}_{NN\to NN} \sim (Q^2)^{-7}$ much faster than the leading quark interchange amplitude $M^{q}_{NN\to NN} \sim (Q^2)^{-4}$. Similarly, the vector exchange contributions give contributions $M^{\rho}_{NN\to NN} \sim (Q^2)^{-6}$. Thus meson exchange amplitudes and currents, even summed over their excited spectra, do not contribute to the leading asymptotic behavior of the nucleon-nucleon scattering amplitudes or deuteron form factors once proper account is taken of the off-shell form factors which control the meson-nucleon-nucleon vertices.

Aside from such estimates, an effective Lagrangian only has utility as a rough tree graph approximation; in higher order the hadronic field terms give loop integrals highly sensitive to the ultraviolet cutoff because of their non-renormalizable character. Thus an effective meson-nucleon Lagrangian serves to organize and catalog low energy constraints and effective couplings, but it is not very predictive for obtaining the actual dynamical and off-shell behavior of hadronic amplitudes due to the internal quark and gluon structure.

Local Lagrangian field theories for systems which are intrinsically composite are however misleading in another respect.[2] Consider the low-energy theorem for the forward Compton amplitude on a (spin-average) nucleon target

$$\lim_{\nu \to 0} \mathcal{M}_{\gamma p \to \gamma' p}(\nu, t = 0) = -2\hat{\epsilon} \cdot \hat{\epsilon}' \, \frac{e^2}{M_p} \, . \tag{6.3}$$

One can directly derive this result from the underlying quark currents as indicated in Fig. 15(b).[3] However, if one assumes the nucleon is a local field, then the entire contribution to the Compton amplitude at $\nu = 0$ would arise from the nucleon pair s-graph amplitude, as indicated in Fig. 15(a). Since each calculation is Lorentz and gauge invariant, both give the desired result. However, in actuality, the nucleon is composite and the $N\bar{N}$ pair term is strongly suppressed: each $\gamma p\bar{p}$ vertex is proportional to

$$\langle 0 | J^{\mu}(0) | p\bar{p} \rangle \;\; \propto \;\; F_p(Q^2 = 4M_p^2) \;\; ; \tag{6.4}$$

i.e., the timelike form factor as determined from $e^+e^- \to p\bar{p}$ near threshold. Thus, as would be expected physically, the $N\bar{N}$ pair contribution is highly suppressed for a composite system (even for real photons). Clearly a Lagrangian based on local nucleon fields gives an inaccurate description of the actual dynamics and cannot be trusted away from the forward scattering, low energy limit.

We can see from the above discussion that a necessary condition for utilizing a local Lagrangian field theory as a dynamical approximation to a given composite system H is that its timelike form factor at the Compton scale must be close to 1:

$$F_H(Q^2 \simeq 4M^2) \simeq 1 \, . \tag{6.5}$$

For example, even if it turns out that the electron is a composite system at very short distances, the QED Lagrangian will still be a highly accurate tool. The above condition on the timelike form factor of threshold fails for all hadrons, save the pion. This result does suggest that effective chiral field theories which couple point-like pions to quarks could be a viable approximation to QCD.

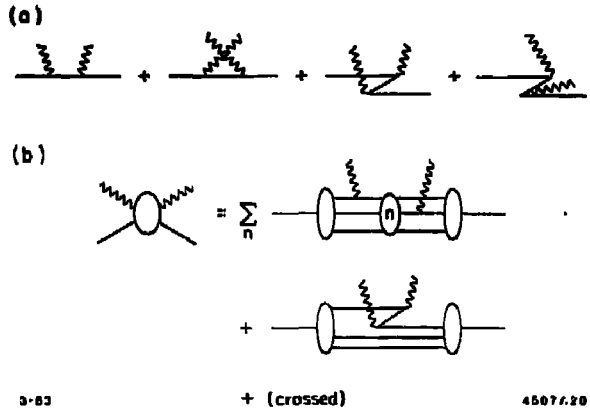

Fig. 15. Time-ordered contributions to (a) The Compton amplitudes in a local Lagrangian theory such as QED. Only the Z-graphs contribute in the forward low energy limit. (b) Calculation of the Compton amplitude for composite systems.

More generally, one should be critical of any use of point-like couplings for nucleon-antinucleon pair production, e.g., in calculations of deuteron form factors, photo- and electro-disintegration since such contributions are always suppressed by the timelike nucleon form factor. Notice that $\gamma N\bar{N}$ point-like couplings are not needed for gauge invariance, once all quark current contributions including pointlike $q\bar{q}$ pair terms are taken into account.

We also note that a relativistic composite fermionic system, whether it is a nucleon or nucleus, does not obey the usual Dirac equation—with a momentum-independent potential—beyond first Born approximation. Again, the difficulty concerns intermediate states containing $N\bar{N}$ pair terms: the validity of the Dirac equation requires that $\langle p|V_{\rm ext}|p'\rangle$ and $\langle 0|V_{\rm ext}|p'\bar{p}\rangle$ be related by simple crossing, as for leptons in QED. For composite systems the pair production terms are again suppressed by the timelike form factor. It is however possible that one can write an effective, approximate relativistic equation for a nucleon in an external potential of the form

$$(\vec{\alpha}\cdot\vec{p}+\beta m_N+\Lambda_+V_{\rm eff}\Lambda_+)\Psi_N=E\Psi_N \tag{6.6}$$

where the projection operator Λ_+ removes the $N\bar{N}$ pair terms, and $V^{\rm eff}$ includes the local (seagull) contributions from $q\bar{q}$-pair intermediate states, as well as contributions from nucleon excitation.

An essential property of a predictive theory is its renormalizability, the fact that physics at a very high momentum scale $k^2>\kappa^2$ has no effect on the dynamics other than to define the effective coupling constant $\alpha(\kappa^2)$ and mass terms $m(\kappa^2)$. Renormalizability also implies that fixed angle unitarity is satisfied at the tree-graph (no-loop) level. In addition, it has recently been shown that the tree graph amplitude for photon emission for any renormalizable gauge theory has the same

amplitude zero structure as classical electrodynamics. Specifically, the tree graph amplitude for photon emission caused by the scattering of charged particles *vanishes* (independent of spin) in the kinematic region where the ratios $Q_i/p_i\cdot k$ for all the external charged lines are identical.[4] This "null zone" of zero radiation is not restricted to soft photon momentum, although it is identical to the kinematic domain for the complete destructive interference of the radiation associated with classical electromagnetic currents of the external charged particles. Thus the tree graph structure of gauge theories, in which each elementary charged field has zero anomalous moment ($g = 2$) is properly consistent with the classical ($\hbar = 0$) limit. On the other hand, local field theories which couple particles with non-zero anomalous moments violate fixed angle unitarity and the above classical correspondence limit at the tree graph level. The anomalous moment of the nucleon is clearly a property of its internal quantum structure; by itself, this precludes the representation of the nucleon as a local field.

The essential conflict between quark and meson-nucleon field theory is thus at a very basic level: because of Lorentz invariance a conserved charge must be carried by a local (point-like) current; there is no consistent relativistic theory where fundamental constituent nucleon fields have an extended charge structure.

6.1 When is Perturbative QCD Applicable?

An important phenomenological question for the application of QCD to nuclear physics is the momentum transfer scale μ where perturbative predictions become reliable. Ignoring heavy quark thresholds, the natural scale parameters of QCD are $\Lambda_{\overline{MS}}$ ($\sim 100 \pm 50$ MeV), the mass scale of the light hadrons ($\lesssim 1$ GeV), and the constituent transverse momenta $\langle k_\perp^2\rangle^{1/2} \sim 300$ MeV. Thus *a priori* we expect the nominal power-law behavior predicted by QCD hard subprocesses to be reliable for $Q^2 \gg \mu^2$; i.e., Q^2 beyond a few GeV^2. In fact, for the explicit calculations of form factors for heavy hadrons [See Chapter 2] we find that non-leading contributions are controlled by the mass of the heavy quarks.

In the case of deep inelastic lepton-nucleon scattering, Bjorken scaling, which reflects the scale-invariant behavior of incoherent lepton quark scattering becomes evident for $Q^2 > 1$ GeV^2, $W > 1.8$ GeV. Coherent contributions, which occur when, e.g., two different struck quarks interfere become relevant for $Q^2 \lesssim O\langle k_\perp^2\rangle$ such that there is significant overlap in the final state. In the case of exclusive processes, the leading QCD power law dominates when the nucleon valence $|qqq\rangle$ or meson valence $|q\bar{q}\rangle$ Fock state contributions overtake the faster falling contributions from higher Fock states. Phenomenologically, the onset of the leading power law occurs at $Q^2 \sim$ few GeV^2. In the case of the deuteron form factor, $(Q^2)^5 F_d(Q^2)$ cannot be expected to approach constant behavior until considerably larger Q^2 since the virtual photon's momentum in the underlying hard subprocess is divided six ways: i.e. one requires $(Q/6)^2 \gg \langle k_\perp^2\rangle$. (Detailed numerical estimates

are given in Ref. 5.) On the other hand, reduced nuclear amplitudes such as the reduced deuteron form factor can be expected to approach scaling law $Q^2 f_d(Q^2) \to const$ quickly since the relevant hard propagators route to large momentum transfer $\sim 5/6\,Q$. All other sources of scale breaking by definition divide out via the nucleon form factors.

The scaling behavior of the form factors shown in Fig. 3 bear out these expectations. Other QCD predictions for the leading power behavior, including $pp \to pp$, $\pi p \to \pi p$, $\gamma p \to \pi^+ n$, etc. are consistent with the predicted nominal scaling law at momentum transfer $p_T^2 \gtrsim 3$ GeV^2. Recent measurements[6] of the basic QCD process $\gamma\gamma \to \pi^+\pi^-$ at large angles agree with the QCD predicted scaling behavior for invariant mass $W > 1.8$ GeV.

An essential question is whether QCD also correctly accounts for the normalization as well as the scaling behavior of high momentum transfer form factors and other exclusive process data. The $\gamma\gamma \to \pi^+\pi^-$, K^+K^- agree very well with the absolutely normalized QCD predictions. Meson form factor predictions for $Q^2 F_M(Q^2)$ are within a factor or two of the QCD prediction using the most naive form of the meson distribution amplitude, i.e.: $\phi(x) = Cx(1-x)$. Since this distribution is relevant only at asymptotic momentum scales (where the leading anomalous dimension dominates), there is no conflict with existing data.

As we have discussed in Chapter 2, the possibility of significant asymmetry in the x-distribution of the valence wavefunction of the nucleon has been investigated by Chernyak and Zhitnitsky using the constraints of the ITEP sum rules. The result is the prediction that the u-quark with spin parallel to the proton carries $\sim 2/3$ of the nucleon momentum, leaving $1/6$ each for the other two quarks. The predicted normalization for $Q^4 G_M^p$ and $\psi \to p\bar{p}$ is again in good agreement with the data, even using normal a valence state radius. The corresponding calculations for the pion form factor also are in excellent agreement with the available data.

In the case of the nucleon form factor, the normalization of the QCD prediction $Q^4 G_M(Q^2) \sim$ const is sensitive to three effects:

1. The average interquark separation d_v of the valence wavefunction: it should be emphasized that $G_M(Q^2)$ is proportional to the fourth inverse power of d_v.
2. The shape of the nucleon distribution amplitude $\phi_N(x_i)$ especially near $x_i \sim 1$.
3. The use of the running coupling constant $\alpha_s(Q^2)$ at the correct scale in the $3q + \gamma^* \to 3q$ hard scattering amplitudes. This removes an "accidental" cancellation in $G_M^p(Q^2)$ when the asymptotic distribution amplitude $\phi_N(x) = Cx_1x_2x_3$ is assumed.

If one uses fixed coupling constant, together with a naive non-relativistic wavefunction with symmetric quark distributions and the standard rms radius $\sim 0.8\ fm$, then the predicted normalization of $Q^4 G_M^p(Q^2)$ is two orders of magnitude below experiment. However, by taking into

account the above three effects it is straightforward to fit the experimental normalization of G_M as well as νW_2^P at $x \to 1$ and the decay rate for $\psi \to p\bar{p}$.[7]

In our work we have noted that the valance wavefunction of the nucleon is likely to be much more compact than indicated by the physical proton radius as derived from an average over all Fock states. More precisely, we define the QCD Fock state expansion for the proton wavefunction at equal $\tau = t + z$ on the light-cone and $A^+ = 0$ gauge, at a given renormalization scale κ.

$$|p\rangle = \begin{pmatrix} \psi^{\kappa}_{qqq}(x_i, k_{\perp i})\,|\,qqq\rangle \\ \psi^{\kappa}_{qqqg}(x_i, k_{\perp i})\,|\,qqqg\rangle \\ \cdot \\ \cdot \\ \cdot \end{pmatrix}$$

At small Q^2 where the proton rms radius is determined (from $6\frac{d}{dQ^2}F_1(Q^2)|_{Q^2=0}$) all Fock states contribute. At large Q^2 where $Q^4 G_M^p(Q^2)$ becomes nearly constant, the valence Fock state $\psi_{qqq}(x_i, k_{\perp i})$ is dominant. Since the higher Fock states are analogous to states containing a meson cloud, it is reasonable that the valence state radius $\langle k_\perp^2 \rangle_{3q}^{-1/2}$ is smaller than the total radius. In fact in the case of the pion, this statement can be demonstrated explicitly. Using normalization constraints from the decay amplitudes $\pi^- \to \mu^- \nu$ and $\pi^0 \to \gamma\gamma$ we can determine the valence state probability and radius ($P_{q\bar{q}/\pi} \sim \frac{1}{4}$, $\langle r^2 \rangle_{q\bar{q}/\pi}^{1/2} \sim 0.42\ f_m$). This suggests that the nucleon form factors be parametrized with at least two components, one soft, falling at least as fast as $(Q^2)^{-3}$ and the other with a large > 1 GeV^2 mass scale falling as $(Q^2)^{-2}$ asymptotically. It is in fact easy to find parametrizations of this type which fit the standard dipole form.[8]

The correct QCD explanation may well involve a combination of the above effects. A final resolution to the problem will require more Eventually, lattice gauge theory and other non-pertubative tools can provide constraints and actual solutions to the nucleon bound state wavefunction in QCD. Certainly at this point there is no evidence of any difficulty or conflict with the predictions of perturbative QCD for either the scaling behavior or the normalization of exclusive processes in the few GeV^2 momentum transfer region.

6.2 Future Directions

QCD can be regarded as the underlying theory of nuclear phenomena in the same sense that QED is the basis for atomic and molecular physics. At this point we are only at the beginning of quantitative calculations, and further progress will require the development of new theoretical techniques for solving strong coupling theories, boundary condition models, etc. We will also need new experimental input, especially in the transition region between coherent and incoherent quark processes. At this point, theoretical progress is being made in the following areas:

1. One can now find approximate analytic solutions to the light-cone equation of motion in the valence quark sector, thus allowing model computations of hadronic and nuclear wavefunctions, distribution amplitudes, and structure functions. Recently, together with M. Sawicki,[9] we have developed fixed particle number equations analogous to the non-retardation approximation in atomic physics. Because this approach consistently restricts the equation to fixed particle number, non-analytic "cusps" of the type derived by Karmonov[10] are avoided.

2. Discretized light-cone quantization [see Appendix A] provides a complimentary method to lattice gauge theory for actually solving field theories, determining both the spectrum and wavefunctions. Lattice gauge theory is now also providing constraints on the valence wavefuntions and a check on predictions from QCD sum rules. We have also emphasized the importance of two photon exclusive channels as a measure of the shape of distribution amplitudes.

3. The normalization of the deuteron form factor at large Q^2 is a formidable though feasible task. The calculation of $T_H(6q + \gamma^* \to 6q)$ should be feasible using the methods of Farrar, Maina, and Neri.[11] The normalization of $\phi_d(x_i, Q)$ requires a careful study of the six-quark evolution equation and matching to the non-relativistic regime.

4. The above study also allows estimates of corrections to the reduced amplitude formalism and the effects of hidden color states. In Appendix C we examine the transition from reduced form factors to the low momentum transfer regime ($Q^2 \lesssim 2M\epsilon_{BE}$) where the impulse approximation form becomes valid. More generally the reduced amplitude formalism can be used to redefine the nuclear potential in such a way that nucleon structure is consistently removed.

5. A systematic analysis of all sources of non-additivity in inelastic lepton-nucleus scattering, lepton pair production, and their effects on specific final states is needed before we have a clear understanding of the EMC effect. For example, one possible origin of anomalous A-dependence is non-additivity of strange and other sea quarks in the nucleus, which will be apparent in the A-dependence of K^- electroproduction. The decrease of the mean value of x with increasing nucleon number implies by rotational symmetry a corresponding decrease of $\langle k_\perp^2 \rangle^{1/2}$. The decrease of the intrinsic transverse momentum should then lead to a contribution to the average transverse momentum of lepton pairs produced in hadron-nucleus collisions decreasing with A.[12] There is also the possibility of non-additive coherent contributions at low x which leave the nucleus intact.[13] Non-additive radiative corrections must also be carefully considered.[14]

6. The role of intrinsic charm and other heavy virtual particle pairs in the hadron wavefunctions can be important for heavy hadron production. The status of this phenomenology is

discussed in Ref. 15.

ACKNOWLEDGEMENTS

We wish to thank the organizers of this meeting Professors C. A. Engelbrecht and F. Hahne for arranging this stimulating school. We also wish to thank J. P. de Vries for his excellent assistance as notetaker. Appendix A was written in colloboration with Hans C. Pauli. Appendix B is based on lectures prepared in collaboration with G. P. Lepage. Chapters 4 and 6 overlap with lectures given at the 1984 Erice International School of Nuclear Physics.

REFERENCES

1. See, e.g., S. A. Gurvitz, Phys. Rev. C22, 1650 (1980). The derivations in this paper require that hadronic interactions have Gaussian fall off.
2. S. J. Brodsky, in "New Horizons in Electromagnetic Physics," Charlottesville, Virginia (1982). Related difficulties with Dirac-equation applications have also been noted by D. A. Adams and M. Bleszynski, Los Alamos preprint LA-UR-83-2749 (1983).
3. A general analysis of Compton scattering on composite systems, including the essential effects of Lorentz boosts, is given by S. J. Brodsky and J. R. Primack, Ann. Phys. 52, 315 (1969). See also D. Drechsel, in Progress in Particle and Nuclear Physics, ed. A. Faessler, Erice 1984.
4. S. J. Brodsky, R. W. Brown and K. L. Kowalski, Phys. Rev. D28, 624 (1983), and references therein.
5. S. J. Brodsky and J. R. Hiller, Phys. Rev. C28, 475 (1983). Fig. 7 is corrected for a phase-space factor $\sqrt{s/(s-m_d^2)}$. S. J. Brodsky and B. T. Chertok, Phys. Rev. Lett. 37, 269 (1976); Phys. Rev. D14, 3003 (1976). S. J. Brodsky, in Proceedings of the International Conference on Few Body Problems in Nuclear and Particle Physics, Laval University, Quebec (1974).
6. J. R. Smith *et al.*, SLAC-PUB-3205 (1983).
7. S. J. Brodsky, T. Huang and G. P. Lepage, SLAC-PUB-2868 (1982), published in Springer Tracts in Modern Physics, Vol. 100, "Quarks and Nuclear Forces," ed. D. Fries and B. Zeitnitz (1982).
8. M. Gari and K. Rumpf, SLAC-PUB-3398 (1984).
9. S. J. Brodsky, C.-R. Ji and M. Sawicki, SLAC-PUB-3382 (1984), to be published in Phys. Rev. D.
10. V. A. Karmonov, Nucl. Phys. A362, 331 (1981), B166, 378 (1980).
11. G. R. Farrar, E. Maina and F. Neri, Rutgers preprint RU-84-13 (1984).
12. G. Bodwin, S. J. Brodsky, and G. P. Lepage, to be published.
13. S. J. Brodsky, to be published.
14. S. J. Brodsky and M. Soldate, to be published.
15. S. J. Brodsky, H. Haber and J. Gunion, SLAC-PUB-3300, published in SSC/DPF Workshop (1984).

APPENDIX A

QUANTIZATION ON THE LIGHT CONE

(This appendix was written in collaboration with H.-C. Pauli[1])

In this section we develop in detail light-cone quantization as a tool to actually solve for the spectrum and bound state wavefunctions of a quantum field theory. As a simple, but non-trivial, example we apply the method to the Yukawa theory in one-space one-time dimensions.

As we shall discuss, the problem of finding solutions to a field theory becomes enormously easier if the fields are quantized at equal light cone time $t + x/c$ rather than at equal usual time t.[2] Light cone quantization was proposed originally by Dirac,[3] and rediscovered by Weinberg[4] in the context of covariant formulation of time-ordered perturbation theory. Sometimes called the infinite momentum frame approach,[2,5-8] it continues to be an important tool for many applications.[2] The formalism was thoroughly investigated and reviewed by Chang et al.[9] In Appendix B. we quantize QCD and construct the Fock state basis and perturbation rules.

The Lagrangian density for interacting fermion and scalar boson fields, ψ and φ, respectively, is given by[10,11]

$$\mathcal{L} = \frac{1}{2}\,\partial^\mu\varphi\partial_\mu\varphi + \frac{1}{2}\,m_B^2\varphi^2 + \frac{i}{2}\,\overline{\psi}\gamma^\mu\partial_\mu\psi - \frac{i}{2}\,\partial_\mu\overline{\psi}\gamma^\mu\psi - (m_F + \lambda\varphi)\overline{\psi}\psi\ . \tag{A1}$$

m_F and m_B are the bare masses for the fermions and the bosons, respectively, to be determined below, and the bare coupling constant λ is considered a free parameter. The Lagrangian density is manifestly hermitean, although only the total Lagrangian $\int dr\mathcal{L}$ has to be so by physical reasons. The volume element dr denotes integration over all covariant coordinates x^μ.

The metric tensors $g^{\mu\nu}$ and $g_{\mu\nu}$ are defined as the raising and lowering operators, $x^\mu = g^{\mu\nu}x_\nu$ and $x_\mu = g_{\mu\nu}x^\nu$, respectively, such that the scalar product $x^\mu x_\mu \equiv g^{\mu\nu}x_\nu x_\mu$ remains an invariant under Lorentz transformations. This implies, that they are inverse to each other, i.e. $g^{\mu\nu}g_{\nu\kappa} = \delta^\mu_\kappa$. As long as one does not write out the sums explicitly, the Lagrangian in four is the same as in two dimensions. Henceforth we shall restrict ourselves to the latter case. In the usual parameterization with $x^0 = ct$ being the time and $x^1 = x$ being the space coordinate, $g^{\mu\nu}$ has the nonvanishing elements $g^{11} = -g^{00} = 1$.

There is no compelling reason why the fields must be treated always as functions of the usual time and space coordinates. Any invertible parameterization of space and time is admissible as well. For example, one can consider them as functions like $\varphi(x^-, x^+) = \varphi(x - ct, x + ct)$. If one

transforms the coordinates to a rotated frame, the metric tensor becomes ($g^{ij} = \partial x^i / \partial x_j$)

$$g^{\mu\nu} = \begin{pmatrix} g^{++} & g^{+-} \\ g^{-+} & g^{--} \end{pmatrix} = \begin{pmatrix} 0 & 2 \\ 2 & 0 \end{pmatrix}. \tag{A2}$$

Scalar products become, for example

$$k_\mu x^\mu \equiv k_+ x^+ + k_- x^- = \frac{1}{2}(k^- x^+ + k^+ x^-) = 2(k_- x_+ + k_+ x_-), \tag{A3}$$

or even simpler, $k_\mu k^\mu = k^+ k^- = 4k_- k_+$. As shown in Fig. 16, the above transformation corresponds to a *real* rotation in phase space by $-45°$, combined with an irrelevant stretching of scale. Upon rotation, time and space lose their meaning. Nevertheless, in line with familiar phrasing,[2,9] one refers to $x^+ = x^0 + x^1$ as the *light cone time*, and correspondingly, to $x^- = x^0 - x^1$ as the *light cone position*. It is somewhat unfortunate that this way of parameterization has also been described as the *infinite momentum frame approach*. In fact, the light cone formulation is frame-independent, the momentum is always finite, and it is not really correct to think of the above rotation as a Lorentz transformation which boosts the system to high momenta. Dirac's original formulation seems to be more adequate.[3]

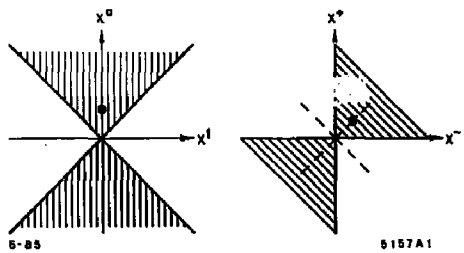

Fig. 16. The light cone in space-time (left) and in light-cone (right) representation.

In a quantized theory, the Lagrangian does not completely specify the problem, one has to know the commutation properties of the operators φ and ψ. But before one can formulate these, one must be clear about which of the field components may be considered as independent variables.[9] This can be investigated through the equations of motion, as obtained by the canonical variation[10] of the Lagrangian, i.e.

$$\partial^\mu \partial_\mu \varphi + m_B^2 \varphi + \lambda \overline{\psi}\psi = 0\,, \tag{A4}$$

and

$$i\partial_\mu\bar{\psi}\gamma^\mu + m\bar{\psi} = 0, \quad i\gamma^\mu\partial_\mu\psi - m\psi = 0 \quad , \qquad \text{with} \quad m(x) \equiv \quad m_F + \lambda\varphi(x), \tag{A5}$$

When transforming the frame, the differential equations change their structure, as we shall demonstrate now for the Dirac equation (A5). The Dirac matrices γ^μ obey the relation $\gamma^\mu\gamma^\nu + \gamma^\nu\gamma^\mu = 2g^{\mu\nu}$. In 1+1 dimensions they are 2 by 2 matrices,[12] i.e.

$$\gamma^0 = \begin{pmatrix} 1 & 0 \\ 0 & -1 \end{pmatrix} \quad \text{and} \quad \gamma^1 = \begin{pmatrix} 0 & 1 \\ -1 & 0 \end{pmatrix}. \tag{A6}$$

and transform like coordinates $\gamma^+ = \gamma^0 + \gamma^1$ and $\gamma^- = \gamma^0 - \gamma^1$. Written out, the commutation relations become $\gamma^+\gamma^+ = 0$, $\gamma^-\gamma^- = 0$, and $\gamma^+\gamma^- + \gamma^-\gamma^+ = 4$. Thus, the two operators

$$\Lambda^{(+)} = \frac{1}{4}\gamma^-\gamma^+ \quad \text{and} \quad \Lambda^{(-)} = \frac{1}{4}\gamma^+\gamma^- \tag{A7}$$

have the property of projectors with $\Lambda^{(+)} + \Lambda^{(-)} = 1$; i.e.

$$\Lambda^{(+)} = \frac{1}{2}\begin{pmatrix} 1 & 1 \\ 1 & 1 \end{pmatrix} \quad \text{and} \quad \Lambda^{(-)} = \frac{1}{2}\begin{pmatrix} 1 & -1 \\ -1 & 1 \end{pmatrix}. \tag{A8}$$

Acting from the left with $\Lambda^{(+)}$ and $\Lambda^{(-)}$, Eq. (A5) separates into a set of two coupled equations

$$\partial_-\psi^{(-)} = \frac{1}{2i}\gamma^0 m\psi^{(+)} \qquad \text{and} \tag{A9}$$

$$\partial_+\psi^{(+)} = \frac{1}{2i}\gamma^0 m\psi^{(-)}, \tag{A10}$$

where $\psi^{(+)} \equiv \Lambda^{(+)}\psi$, $\psi^{(-)} \equiv \Lambda^{(-)}\psi$, $\partial_+ \equiv \partial/\partial x^+$, and $\partial_- \equiv \partial/\partial x^-$. Suppose, one has arbitrarily fixed both the fermion component $\psi^{(+)}$ and the boson field φ at some particular light cone time $x^+ = x_0^+$ on the interval $x^- \in (-L, L)$. Then, one can integrate Eq. (A9),

$$\psi^{(-)}(x^-, x_0^+) = F(x_0^+) + \frac{i}{4}\gamma^0 \int_{-L}^{+L} dy^-\, \epsilon(x^- - y^-) m(y^-, x_0^+)\psi^{(+)}(y^-, x_0^+), \tag{A11}$$

with ϵ being the antisymmetric step function; i.e. $\epsilon'(x) = -2\delta(x)$. The function F depends only on x_0^+, but is otherwise arbitrary. A consistent boundary condition is[9]

$$F(x_0^+) = 0. \tag{A12}$$

Inserting Eqs. (A11) and (A12) into the second couple, Eq. (A10), one obtains the time derivative

as a functional of $\psi^{(+)}$ alone, i.e.

$$\partial_+\psi^{(+)}(x^-,x^+) = \frac{1}{8}m(x^-,x^+)\int_{-L}^{+L} dy^-\epsilon(x^- - y^-)m(y^-,x^+)\psi^{(+)}(y^-,x^+). \qquad \text{(A13)}$$

A similar analysis can be given for the boson field. With φ and $\psi^{(+)}$ being fixed, and therefore also $\rho = \overline{\psi}\psi$, the equation of motion (A4), i.e. $4\partial_+\partial_-\varphi + \lambda\rho + m_B^2\varphi = 0$, can be integrated

$$\partial_+\varphi(x^-,x^+) = -\frac{1}{8}\int_{-L}^{+L} dy^-\epsilon(y^- - x^-)(\lambda\rho(y^-,x^+) + m_B^2\varphi(y^-,x^+)). \qquad \text{(A14)}$$

In other words, only $\psi^{(+)}$ and φ are independent variables. Neither $\psi^{(-)}$ or its derivatives nor the light cone time derivatives $\partial_+\psi^{(+)}$ or $\partial_+\varphi$ are independent; they must satisfy Eqs. (A13) and (A14) everywhere. These constraints are a consequence of first order partial differential equations, in sharp contrast with the second order equation in the usual space-time parameterization.

The dependent components having been found, one can determine the canonical commutation relations. By means of Schwinger's action principle,[13] one obtains[9]

$$i[\varphi(x^-,x^+),\varphi(x^{-'},x^+)] = \frac{1}{4}\epsilon(x^- - x^{-'}), \qquad \text{and} \qquad \text{(A15)}$$

$$\{\psi_\alpha^{(+)}(x^-,x^+),\psi_\beta^{(+)\dagger}(x^{-'},x^+)\} = \Lambda_{\alpha\beta}^{(+)}\delta(x^- - x^{-'}) \quad . \qquad \text{(A16)}$$

All other (anti-) commutators vanish. A more thorough discussion can be found in the literature.[9] As an alternative, one can proceed canonically.[10,14,15] Taking x^+ as the time-like coordinate, one defines the momentum conjugate to the field φ as $\Pi^+ \equiv \frac{\partial\mathcal{L}}{\partial\partial_+\varphi} = \partial^+\varphi = 2\partial_-\varphi$. The canonical procedure at equal time-like coordinate gives thus

$$[\partial_-\varphi(x^-,x^+),\varphi(x^{-'},x^+)] = \frac{i}{2}\delta(x^- - x^{-'}),$$

which is identical to the space derivative of Eq. (A15). The fermion fields behave in the same manner.

A1 The Free Field Solutions and the Fock Space

At some initial time $x^+ = x_0^+ = 0$, the independent fields $\psi^{(+)}$ and φ can be chosen arbitrarily, as long as they satisfy the commutation relations and Lorentz covariance. The former is easy to arrange, and the latter is enforced by letting them be solutions of the equations of motion with vanishing coupling constant, i.e.

$$\psi^{(+)}(x^-,0) = \psi^{(+)}_{\rm free}(x^-,0) \quad \text{and} \quad \varphi(x^-,0) = \varphi_{\rm free}(x^-,0) \tag{A17}$$

The free fields can be constructed easily, and in turn define the Hilbert space in which $\psi^{(+)}$ and φ act as operators, the so-called Fock space.

The free fields obey

$$(\partial^\mu\partial_\mu + m_B^2)\varphi_{\rm free} = 0 \quad \text{and} \quad (\partial^\mu\partial_\mu + m_F^2)\,\psi^{(+)}_{\rm free} = 0\,. \tag{A18}$$

Although $\varphi_{\rm free}$ is a real scalar and $\psi^{(+)}_{\rm free}$ a complex spinor, they obey the same equation. A particular solution to the latter is $\psi^{(+)} \sim e^{ik_\mu x^\mu}$, provided one satisfies

$$k_\mu k^\mu - m_{F,B}^2 = 0 \quad \text{or} \quad k^+k^- = m_{F,B}^2\,. \tag{A19}$$

The relation between (k^+,k^-) and (k^0,k^1) is the same as for the covariant coordinates, and displayed in the Fig. 17. Because of the rotation, the usual meaning of energy and momentum gets lost, but it is justified to speak of a *single particle light cone momentum* $k^+ \equiv k^0 + k^1$ and a *single particle light cone energy* $k^- \equiv k^0 - k^1$. But there is a distinct difference. For a fixed momentum k^1 one has both a particle-state with energy $(k^0)_p = +\sqrt{m^2 + (k^1)^2}$ and a hole-state with energy $(k^0)_h = -\sqrt{m^2 + (k^1)^2}$. But in light cone parametrization, one has only one value of the single particle energy, i.e.

$$k^- = \frac{m_F^2}{k^+} \tag{A20}$$

for a fixed single particle momentum. Moreover, particles have only positive and holes only negative values of k^+ and k^-. In line with field theoretic conventions,[10] one counts energies and momenta relative to a reference state, the Fock space vacuum. After a renormalization, particles and antiparticles have both positive momenta and energies. The positive-definite momenta are responsible for the great simplicity of the present approach.

The single particle energy, Eq. (A20), seems to have a singularity at $k^+ = 0$. But a free massive particle will actually never have a vanishing light cone momentum. Its (space-time) energy can become arbitrarily close, but is never identical, to its (space-time) momentum, no

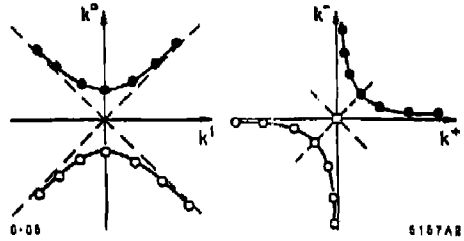

Fig. 17. Particle and hole energies in space-time (left) and in light-cone (right) representation.

matter how large its momentum is, simply because $(k^0)^2 - (k^1)^2 = m^2 \neq 0$ [see also Fig. 17 for an illustration of this fact]. The construction

$$k^+ \to k_n^+ = \frac{2\pi}{L} n \,, \quad n = 1, 2, 3, \ldots, \Lambda, \tag{A21}$$

accounts for this aspect. For the lowest possible value $n = 1$, L regulates the vicinity of $k^+ = 0$, while Λ determines the highest possible value of k^+ for each fixed L. A glance at Fig. 17 reveals, that the left running states ($k^1 < 0, k^+$ small) have a different cut-off in space-time momentum than the right runners, as opposed to space-time where they are treated symmetrically.[12]

In their most general form the free field solutions can hence be written as

$$\varphi_{\text{free}}(x^-, x^+) = \frac{1}{\sqrt{4\pi}} \sum_{n=1}^{\Lambda} \frac{1}{\sqrt{n}} \left(a_n e^{-ik_\mu^{(n)} x^\mu} + a_n^\dagger e^{+ik_\mu x^\mu} \right) \,, \quad \text{and} \tag{A22}$$

$$\psi_{\text{free}}^{(+)}(x^-, x^+) = \frac{1}{\sqrt{2L}} u \sum_{n=1}^{\Lambda} \left(b_n e^{-ik_\mu^{(n)} x^\mu} + d_n^\dagger e^{+ik_\mu^{(n)} x^\mu} \right) \,. \tag{A23}$$

The spinor u is normalized to unity, $u = \frac{1}{\sqrt{2}} \begin{pmatrix} 1 \\ 1 \end{pmatrix}$, and is independent of the momenta. Fermions and antifermions are created by the operators $b_n^\dagger$ and $d_n^\dagger$, respectively, subject to the anti-commutators

$$\{b_n, b_m^\dagger\} = \delta_{n,m} \quad \text{and} \quad \{d_n, d_m^\dagger\} = \delta_{n,m} \,. \tag{A24}$$

The boson creation and destruction operators obey the commutator

$$[a_n, a_m^\dagger] = \delta_{n,m} \,. \tag{A25}$$

Boson and fermion operators commute. The quantization rules , Eq. (A16) and (A15), are

satisfied by means of the completeness relation for Fourier series, i.e.

$$\lim_{\Lambda,L\to\infty}\left[\frac{1}{2L}+\frac{1}{2L}\sum_{n=1}^{\Lambda}\left(e^{i\frac{n\pi}{L}(x-x')}+e^{i\frac{n\pi}{L}(x'-x)}\right)\right]=\delta(x-x')\,. \tag{A26}$$

Choosing the fields according to Eq. (A17), i.e.

$$\begin{aligned}\psi^{(+)}(x^-,0)&\equiv\frac{n}{\sqrt{2L}}\,\Psi\left(\frac{\pi x^-}{L}\right)\,,\quad\text{and}\\ \varphi(x^-,0)&\equiv\frac{1}{\sqrt{4\pi}}\,\Phi\left(\frac{\pi x^-}{L}\right)\,,\end{aligned} \tag{A27}$$

one can express the fields in terms of the scalar and dimensionless operator functions

$$\begin{aligned}\Psi(\xi)&=\sum_{n=1}^{\Lambda}b_n\,e^{-in\xi}+d_n^\dagger e^{+in\xi}\,,\quad\text{and}\\ \Phi(\xi)&=\sum_{n=1}^{\Lambda}c_n\,e^{-in\xi}+c_n^\dagger e^{+in\xi},\quad\text{with}\quad c_n=\frac{1}{\sqrt{n}}\,a_n.\end{aligned} \tag{A28}$$

Because of the discretized momenta, Eq. (A21), the operators Ψ and Φ , and therefore also the fields ψ and φ are periodic functions with period $2L$ in the light cone position x^-. We define them on the interval $x^-\in(-L,+L)$. On this interval, the plane wave states are orthonormal and complete, and the series, Eq. (A27) and (A28) can be understood as the special case of an expansion into a denumerable and complete set $\langle x|n\rangle$.

The operator part of this expansion, the creation and destruction operators act in Fock space, i.e. in the representation which diagonalizes simultaneously the number operators $a_n^\dagger a_n, b_n^\dagger b_n$ and $d_n^\dagger d_n$. Since one has to specify exactly which momentum states are occupied and which are empty (c.f. also Refs. 2 and 16), denumerability seems compulsory, rather than only a formal trick.

All these advantages have the price of introducing into the formalism two at first non-physical, mathematical parameters, the *cut-off* Λ and the *length* L. Since they are redundant, one must be able to show at the end that the physical results do not depend on either of them.

A2 · The Constants of Motion

The Lagrangian, Eq. (A1), has two kinds of conserved currents, $\partial_\mu j^\mu = 0$ and $\partial_\mu J^{\mu\nu}=0$. The first arises since $\mathcal{L}$ does not depend explictly on the phase of ψ and is $j^\mu=\overline{\psi}\gamma^\mu\psi$. The

second, the energy momentum stress tensor, is a consequence of coordinate invariance and has the form

$$J^{\mu\nu} = \partial^\mu\varphi\partial^\nu\varphi + \frac{i}{2}\left(\overline{\psi}\gamma^\mu\partial^\nu\psi - \partial^\nu\overline{\psi}\gamma^\mu\psi\right) + \frac{1}{2}\,g^{\mu\nu}(m_B^2\varphi^2 - \partial_\kappa\varphi\partial^\kappa\varphi)\ . \tag{A29}$$

Integrating the currents over a closed hypersurface $\int d\sigma_a$ conjugate to the time-like coordinate x^a, i.e. $d\tau = dx^a d\sigma_a$, one generates conserved charges

$$Q = \int d\sigma_a j^a \quad \text{and} \quad P^\mu = \int d\sigma_a J^{\mu a}\ . \tag{A30}$$

They are independent of x^a. In a quantized theory, the total charge Q and the components of the energy-momentum vector P^μ are operators, as well as the contraction of the latter, the Lorentz scalar $M^2 = P_\mu P^\mu$. In space-time quantization, P^1 is the operator for the total momentum, P^0 for the total energy , and M^2 is the operator for the square of the invariant mass, i.e. $M^2 = (P^0)^2 - (P^1)^2$. They mutually commute.[10] In light cone quantization, P^+ is the operator for the *total light cone momentum*, P^- for the *total light cone energy*, and M^2 again the operator for the *invariant mass squared*,

$$P^+ = P^0 + P^1, \quad P^- = P^0 - P^1 \quad \text{and} \quad M^2 = P^+P^-. \tag{A31}$$

The notation implies that M^2 is a positive operator, i.e. one which has only positive eigenvalues. We shall come back to this question below. Chang et al.[9] have shown that Q, P^+ and P^- mutually commute if the fields satisfy the commutation relations, Eqs. (A15) and (A16) . Thus, they can be diagonalized simultaneously, for example in Fock space representation, which is equivalent to solving the equations of motion.[10]

Written out in light cone metric, the operators are

$$Q = \frac{1}{2}\int_{-L}^{+L} dx^- 2[\psi^{(+)}]^\dagger\psi^{(+)}, \tag{A32}$$

$$P^+ = \frac{1}{2}\int_{-L}^{+L} dx^- \left[4\partial_-\varphi\partial_-\varphi + 2i([\psi^{(+)}]^\dagger\partial_-\psi^{(+)} - [\partial_-\psi^{(+)}]^\dagger\psi^{(+)})\right]\ , \tag{A33}$$

$$P^- = \frac{1}{2}\int_{-L}^{+L} dx^- \left[m_B^2\varphi\varphi + 2i([\psi^{(+)}]^\dagger\partial_+\psi^{(+)} - [\partial_+\psi^{(+)}]^\dagger\psi^{(+)})\right]\ . \tag{A34}$$

The factor $\frac{1}{2}$ arises from the Jacobian $dx^0dx^1 = \frac{1}{2}dx^+dx^-$. The momentum P^+ and the charge Q are independent of the coupling constant $\lambda \equiv g\sqrt{4\pi}$, but P^- depends on λ through $\partial_+\psi^{(+)}$. By

means of the dimensionless operators as defined above, one can extract the dependence on the box size L,

$$P^+ = \frac{2\pi}{L} K \quad \text{and} \quad P^- = \frac{L}{2\pi} H \,. \tag{A35}$$

After some algebraic manipulations, one obtains with $\xi = \frac{\pi x^-}{L}$

$$Q = \frac{1}{2\pi} \int_{-\pi}^{+\pi} d\xi \; \Psi^\dagger \Psi \quad \text{and} \quad K = \frac{1}{4\pi} \int_{-\pi}^{+\pi} d\xi \left[\frac{\partial \Phi}{\partial \xi} \frac{\partial \Phi}{\partial \xi} + 2i \Psi^\dagger \frac{\partial \Psi}{\partial \xi} \right] . \tag{A36}$$

The modified momentum operator K is dimensionless, while the modified energy operator H carries the dimension of a mass squared,

$$\begin{aligned} H = &+i \frac{m_F^2}{4\pi} \int_{-\pi}^{+\pi} d\xi \int_{-\pi}^{+\pi} d\xi' \epsilon(\xi - \xi') \, \Psi^\dagger(\xi) \Psi(\xi') + \frac{m_B^2}{4\pi} \int_{-\pi}^{+\pi} d\xi \, \Phi(\xi) \Phi(\xi) \\ &+i \frac{m_F g}{4\pi} \int_{-\pi}^{+\pi} d\xi \int_{-\pi}^{+\pi} d\xi' \epsilon(\xi - \xi') \, \Psi^\dagger(\xi) \Phi(\xi) \Psi(\xi') \\ &+i \frac{g^2}{4\pi} \int_{-\pi}^{+\pi} d\xi \int_{-\pi}^{+\pi} d\xi' \epsilon(\xi - \xi') \, \Psi^\dagger(\xi) \Phi(\xi) \Psi(\xi') \Phi(\xi') \,. \end{aligned} \tag{A37}$$

The appearance of a term quadratic in the coupling constant reflects the instantaneous, Coulomb-like interaction, which is not propagated by the exchange of bosons.[2]

The integrals over ξ can be carried out in closed form. With the identity $\frac{1}{2\pi} \int_{-\pi}^{+\pi} d\xi \, e^{im\xi} = \delta_{m,0}$, the normal ordered operators Q and K become

$$Q = \sum_n b_n^\dagger b_n - d_n^\dagger d_n \quad \text{and} \quad K = \sum_n n (a_n^\dagger a_n + b_n^\dagger b_n + d_n^\dagger d_n) \,. \tag{A38}$$

Some of the most important conclusions can be drawn even without knowing the Fock space structure of H, the reader not interested in these details may skip the remainder. The terms quadratic in g with an *even* number of creation operators become most directly

$$
\begin{aligned}
g^2 \sum_{k,l,m,n} \Big[& b_k^\dagger c_l^\dagger d_m^\dagger c_n^\dagger \{+k+l|+m+n\} + b_k^\dagger c_l^\dagger b_m c_n \{+k+l|-m-n\} \\
& + b_k^\dagger c_l d_m^\dagger c_n \{+k-l|+m-n\} + b_k^\dagger c_l b_m c_n^\dagger \{+k-l|-m+n\} \\
& + d_k c_l^\dagger d_m^\dagger c_n \{-k+l|+m-n\} + d_k c_l^\dagger b_m c_n^\dagger \{-k+l|-m+n\} \\
& + d_k c_l d_m^\dagger c_n^\dagger \{-k-l|+m+n\} + d_k c_l b_m c_n \{-k-l|-m-n\} \Big] .
\end{aligned}
\tag{A39}
$$

The matrix elements

$$
\{n|m\} = \frac{i}{4\pi} \int_{-\pi}^{+\pi} d\xi \int_{-\pi}^{+\pi} d\xi' \epsilon(\xi - \xi') e^{i(n\xi + m\xi')}
\tag{A40}
$$

take upon calculation the values

$$
\{n|m\} = \begin{cases} 0 & \text{if } n = 0 \text{ and } m = 0, \\ \frac{1}{n}\delta_{m,-n} & \text{if } n \neq 0 \text{ and } m \neq 0. \end{cases}
\tag{A41}
$$

With the symmetry properties $\{n|m\} = -\{m|n\} = \{-m|-n\} = -\{-n|-m\}$, the normal ordered product can be cast into the *seagull part H_S of the Hamiltonian*

$$
\begin{aligned}
H_S = g^2 \sum_{k,l,m,n} & b_k^\dagger b_m c_l^\dagger c_n \left[\{k-n|l-m\} + \{k+l|-m-n\} \right] \\
& + d_k^\dagger d_m c_l^\dagger c_n \left[\{k-n|l-m\} + \{k+l|-m-n\} \right] \\
& + (d_k b_m c_l^\dagger c_n^\dagger + b_m^\dagger d_k^\dagger c_n c_l) \{l-k|n-m\} \quad .
\end{aligned}
\tag{A42}
$$

The nomenclature[2] has its origin in the structure of the graphs of Fig. 18. The terms corresponding to a simultaneous creation of bosons and fermion-antifermion pairs do not contribute. They are kinematically suppressed in light cone quantization,[2] because $\{+k+l|+m+n\}$ vanishes for positive values of the momenta. However, the time and the normal ordered product, Eqs. (A39) and (A42), respectively, are not the same! Consider for example the fourth term in Eq. (A39), i.e. $\sum_{k,l,m,n} b_k^\dagger c_l b_m c_n^\dagger \{+k-l|-m+n\}$. Using the commutation relations to generate the normal ordered product $b_k^\dagger b_m c_n^\dagger c_l$, leaves one with $\sum_{m,n} \frac{1}{n} b_m^\dagger b_m \{+m-n|-m+n\}$. Contrary to a c-number,this operator can not be omitted. It represents *instantaneous, self-induced inertias*, which so far have apparently not been mentioned in the literature. These inertias are naturally combined with the mass terms of Eq. (A37) to yield the *massive part H_M of the Hamiltionian*. i.e.

$$H_M = \sum_n \frac{1}{n}\left[a_n^\dagger a_n\left(m_B^2 + g^2\alpha_n\right) + b_n^\dagger b_n\left(m_B^2 + g^2\beta_n\right) + d_n^\dagger d_n\left(m_B^2 + g^2\gamma_n\right)\right], \tag{A43}$$

with the coefficients α, β and γ given by

$$\begin{aligned} \alpha_n &= \sum_{m=1}^{A} \{n-m|m-n\} - \{n+m|-m-n\}, \\ \beta_n &= \sum_{m=1}^{A} \frac{n}{m}\{n-m|m-n\} \quad \text{and} \quad \gamma_n = \sum_{m=1}^{A} \frac{n}{m}\{n+m|-m-n\}. \end{aligned} \tag{A44}$$

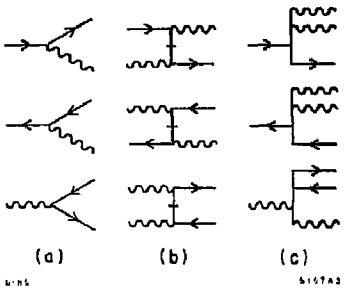

Fig. 18. Diagrams: (a) Vertices, (b) Seagulls and, (c) Forks.

The terms quadratic in g with an *odd* number of creation operators are computed in the same manner. The normal ordering does *not* induce new terms and one can cast them into the *fork part H_F of the Hamiltonian*, i.e.

$$\begin{aligned} H_F = g^2 \sum_{k,l,m,n} & \left(b_k^\dagger b_m c_l^\dagger c_n^\dagger + b_m^\dagger b_k c_n c_l\right)\{k+l|n-m\} \\ & + \left(d_k^\dagger d_m c_l^\dagger c_n^\dagger + d_m^\dagger d_k c_n c_l\right)\{k+l|n-m\} \\ & + b_k^\dagger d_m^\dagger c_l^\dagger c_n \left[\{k-n|m+l\} + \{k+l|m-n\}\right] \\ & + d_m b_k c_n^\dagger c_l \left[\{k-n|m+l\} + \{k+l|m-n\}\right], \end{aligned} \tag{A45}$$

Graphical representations of H_F and H_V are given in Fig. 18. The *vertex part H_V of the Hamil-*

tonian includes all terms linear in the coupling constant, i.e.

$$H_V = gm_F \sum_{k,l,m} (b_k^\dagger b_m c_l^\dagger + b_m^\dagger b_k c_l) \left[\{k+l|-m\} + \{k|+l-m\} \right]$$
$$+ (d_k^\dagger d_m c_l^\dagger + d_m^\dagger d_k c_l) \left[\{k+l|-m\} + \{k|+l-m\} \right] \qquad \text{(A46)}$$
$$+ (b_k d_m c_l^\dagger + d_m^\dagger b_k^\dagger c_l) \left[\{k-l|+m\} + \{k|-l+m\} \right] .$$

For the same reason as above, the terms with *only* creation or *only* destruction operators vanish by the selection rules of the matrix elements. Collecting all terms, the Hamiltonian $H = H_M + H_V + H_S + H_F$ is the sum of four parts defined above.

The self-induced inertias are the only parts of the Hamiltonian, which depend on the cut-off A [see Eq. (A44)]. Approximating sums by integrals, this dependence can be worked out explicitly.[16] For vanishing 1/A, the fermion and the antifermion inertias become independent of the cut-off, while the boson inertias diverge logarithmically; however, such that the divergence cancels in the differences $\alpha_n - \alpha_m$. In this limit, the eigenvalues and eigenfunctions of the Hamiltonian become strictly independent of the cut-off in the limit of vanishing 1/A, as can be shown numerically, and for some of the cases, even analytically.

A3 Conclusions: Finite Dimensional Representations, Labelled by the Harmonic Resolution

The discretization of the momentum eigenvalues k^+ allows one to denumerate the momentum eigenstates. The price one has to pay is the appearance of two additional, formal parameters in the theory, the length L and the cut-off A. One must be able to show that the physical results do not depend on either of the these, at least not in the limit $L \to \infty$ and $A \to \infty$.

In light cone quantization, discretization has rather unexpected consequences, which seem not to have been noticed so far.

First, and perhaps most remarkably, the length cancels in the only Lorentz scalar of the theory, the invariant mass squared, i.e. $M^2 = P^+P^- = KH$. The eigenvalues of I are *independent* of L for *any* value of L.

The eigenvalues and eigenfunctions of the Hamiltonian H, or of the invariant mass squared M^2, are also independent of the cut-off A and positive definite. This is shown in an accompanying paper in the context of mass renormalization. For sufficiently simple cases, i.e. for small g^2 or for $K = 1$ and $K = 2$, it can be done analytically.

Second, the number operators of Fock space representation are diagonal and have positive or zero eigenvalues. Therefore, both the operators for charge and momentum are diagonal, with eigenvalues Q and K. The single particle momenta are positive by definition, and consequently

K has only positive or zero eigenvalues. But, by the same reason, only a *finite* number of Fock states can have the same eigenvalue K. Since Q, K and H commute, the latter can be arranged in block diagonal form. Each block is labelled by the eigenvalues K and Q and has a *finite dimension: Since diagonalization is a closed operation, the eigenvalue problem on the light cone can be solved exactly in 1+1 dimension.* This aspect of light cone quantization is profoundly different from space-time quantization. There, too, charge and total momentum are diagonal, but the momentum operator has infinite degeneracy. The energy matrix must be truncated by brute force,[13] in order to become numerically tractable.

Third, K is a dynamical quantum number. Its value characterizes a wave function as much as the charge Q. What is its physical meaning? Suppose one has diagonalized H for some charge, for a given value of K, and for some value of the coupling constant λ, the bare fermion mass m_F and the bare boson mass m_B. Suppose, the lowest eigenvalue KH is identical with M^2, the invariant mass squared of a physical particle. Can one go back to space-time representation and calculate the momentum P and the energy E of this particle? In a way one can, since $E = \frac{1}{2}(P^+ + P^-)$ and $P = \frac{1}{2}(P^+ - P^-)$. But actually one has to know the length L, since

$$P^+ = \frac{2\pi}{L} K \quad \text{and} \quad P^- = \frac{L}{2\pi} \frac{M^2}{K}.$$

However, one can fix L by the requirement of vanishing center of mass momentum, $P = 0$, which implies $P^+ = P^-$. This in turn requires

$$2\pi K/L = M^2 L/(2\pi K) \quad ,$$

or upon restoring the correct units

$$K = \frac{L}{\lambda_C} \qquad \text{with} \quad \lambda_C = \frac{2\pi\hbar}{Mc}.$$

Thus in the rest frame the *dynamical quantum number, the 'harmonic resolution' K becomes the ratio of the length L to the Compton wavelength of the particle.* The larger one chooses the period of the wavefunction in phase space, the larger K becomes and therefore the dimension of the Hamiltonian matrix. Thus, K plays the role of a resolving power. Increasing K allows the observation of a more detailed and more complex structure of the eigenfunction in terms of Fock states. One must conclude that the wavefunction of a particle in one space and one time dimension depends on the resolution, on the accuracy one imposes by the choice of L or, more precisely, by the value of the harmonic resolution K.

The length L thus has apparently two aspects. On the one hand, for a particle a rest, it has to be a multiple of the Compton wave length. On the other hand, for a particle in motion, it can take any value required for the continuum limit $K \to \infty$ and $L \to \infty$.

Last but not least, these conclusions do not depend on the detailed structure of the Hamiltonian. They hold as well for other field theories.

REFERENCES

1. H. C. Pauli, *Z. Phys.* **A319** (1984) 303.
2. S. J. Brodsky, R. Roskies and R. Suaya, *Phys. Rev.* **D8** (1973) 4574.
3. P.A.M. Dirac, *Rev. Mod. Phys.* **21** (1949) 392.
4. S. Weinberg, *Phys. Rev.* **150** (1966) 1313.
5. L. Susskind, *Phys. Rev.* **165** (1968) 1535.
6. K. Bardakci and M. B. Halpern, *Phys. Rev.* **176** (1968) 1686.
7. J. B. Kogut and D. E. Soper, *Phys. Rev.* **D1** (1970) 2901.
8. J. D. Bjørken, J. B. Kogut and D. E. Soper, *Phys. Rev.* **D3** (1971) 1382.
9. S. J. Chang, R. G. Root, and T. M. Yan, *Phys. Rev.* **D7** (1973) 1133.
10. J. D. Bjørken and S. D. Drell, *Relativistic Quantum Fields* (McGraw-Hill, New York, 1965).
11. B. D. Serot, S. E. Koonin and J. W. Negele, *Phys. Rev.* **C28** (1983) 1679.
12. E. D. Brooks and S. C. Frautschi, *Z. Phys.* **23** (1984) 263.
13. J. Schwinger, *Phys. Rev.* **127** (1962) 324.
14. G. P. Lepage and S. J. Brodsky, *Phys. Rev.* **D22** (1980) 2157.
15. G. P. Lepage, S. J. Brodsky, T. Huang, and P. Mackenzie in *Banff 1981, Particle and Fields 2*; S. J. Brodsky, in *Short-Distance Phenomena in Nuclear Physics* (Plenum Publishing Corporation, 1983), p.141-217.
16. H. C. Pauli and S. J. Brodsky, SLAC-PUB-3714, to be published.

APPENDIX B

LIGHT CONE QUANTIZATION AND PERTURBATION THEORY

In this Appendix, we outline the canonical quantization of QCD in $A^+ = 0$ gauge.[1] This proceeds in several steps. First we identify the independent dynamical degrees of freedom in the Lagrangian. The theory is quantized by defining commutation relations for these dynamical fields at a given light-cone time $\tau = t + z$ (we choose $\tau = 0$). These commutation relations lead immediately to the definition of the Fock state basis. Expressing dependent fields in terms of the independent fields, we then derive a light-cone Hamiltonian, which determines the evolution of the state space with changing τ. Finally we derive the rules for τ-ordered perturbation theory.

The major purpose of this exercise is to illustrate the origins and nature of the Fock state expansion, and of light-cone perturbation theory. We will ignore subtleties due to the large scale structure of non-Abelian gauge fields (e.g. 'instantons'), chiral symmetry breaking, and the like. Although these have a profound effect on the structure of the vacuum, the theory can still be described with a Fock state basis and some sort of effective Hamiltonian. Furthermore, the short distance interactions of the theory are unaffected by this structure, or at least this is the central ansatz of perturbative QCD.

Quantization

The Lagrangian (density) for QCD can be written

$$\mathcal{L} = -\frac{1}{2}\,\mathrm{Tr}\,(F^{\mu\nu}\,F_{\mu\nu}) + \overline{\psi}\,(i\not{D} - m)\,\psi \tag{B1}$$

where $F^{\mu\nu} = \partial^\mu A^\nu - \partial^\nu A^\mu + ig[A^\mu, A^\nu]$ and $iD^\mu = i\partial^\mu - gA^\mu$. Here the guage field A^μ is a traceless 3×3 color matrix ($A^\mu \equiv \sum_a A^{a\mu}T^a$, $\mathrm{Tr}(T^aT^b) = 1/2\delta^{ab}$, $[T^a, T^b] = ic^{abc}T^c, \ldots$), and the quark field ψ is a color triplet spinor (for simplicity, we include onlly one flavor). At a given light-cone time, say $\tau = 0$, the independent dynamical fields are $\psi_\pm \equiv \Lambda_\pm\psi$ and $A^i_\perp$ with conjugate fields $i\psi^\dagger_+$ and $\partial^+A^i_\perp$, where $\Lambda_\pm = \gamma^0\gamma^\pm/2$ are projection operators ($\Lambda_+\Lambda_- = 0$, $\Lambda^2_\pm = \Lambda_\pm$, $\Lambda_+ + \Lambda_- = 1$) and $\partial^\pm = \partial^0 \pm \partial^3$. Using the equations of motion, the remaining fields in $\mathcal{L}$ can be expressed in terms of ψ_+, $A^i_\perp$:

$$
\begin{aligned}
\psi_- &\equiv \Lambda_- \psi = \frac{1}{i\partial^+}\left[i\vec{D}_\perp \cdot \vec{\alpha}_\perp + \beta m\right]\psi_+ \\
&= \tilde{\psi}_- - \frac{1}{i\partial^+}\, g\vec{A}_\perp \cdot \vec{\alpha}_\perp \psi_+ \,, \\
A^+ &= 0 \,, \\
A^- &= \frac{2}{i\partial^+} i\vec{\partial}_\perp \cdot \vec{A}_\perp + \frac{2g}{(i\partial^+)^2}\left\{\left[i\partial^+ A^i_\perp, A^i_\perp\right] + 2\psi^\dagger_+ T^a \psi_+ T^a\right\} \\
&\equiv \tilde{A}^- + \frac{2g}{(i\partial^+)^2}\left\{\left[i\partial^+ A^i_\perp, A^i_\perp\right] + 2\psi^\dagger_+ T^a \psi_+ T^a\right\} \,,
\end{aligned}
\tag{B2}
$$

with $\beta = \gamma^o$ and $\vec{\alpha}_\perp = \gamma^o \vec{\gamma}$.

To quantize, we expand the fields at $\tau = 0$ in terms of creation and annihilation operators,

$$
\begin{aligned}
\psi_+(x) &= \int_{k^+>0} \frac{dk^+ d^2k_\perp}{k^+ 16\pi^3} \sum_\lambda \Big\{ b(\underline{k},\lambda)\, u_+(\underline{k},\lambda)\, e^{-ik\cdot x} \\
&\qquad + d^\dagger(\underline{k},\lambda)\, v_+(\underline{k},\lambda)\, e^{ik\cdot x}\Big\} \,, \quad \tau = x^+ = 0 \\
A^i_\perp(x) &= \int_{k^+>0} \frac{dk^+ d^2k_\perp}{k^+ 16\pi^3} \sum_\lambda \Big\{ a(\underline{k},\lambda)\, \epsilon^i_\perp(\lambda)\, e^{-ik\cdot x} + c.c.\Big\} \,, \quad \tau = x^+ = 0 \,,
\end{aligned}
\tag{B3}
$$

with commutation relations ($\underline{k} = (k^+, \vec{k}_\perp)$):

$$
\begin{aligned}
\left\{b(\underline{k},\lambda),\ b^\dagger(\underline{p},\lambda)\right\} &= \left\{d(\underline{k},\lambda),\ d^\dagger(\underline{p},\lambda')\right\} \\
&= \left[a(\underline{k},\lambda),\ a^\dagger(\underline{p},\lambda')\right] \\
&= 16\pi^3\, k^+\, \delta^3(\underline{k}-\underline{p})\, \delta_{\lambda\lambda'} \,, \\
\{b,b\} = \{d,d\} &= \ldots = 0 \,,
\end{aligned}
\tag{B4}
$$

where λ is the quark or gluon helicity. These definitions imply canonical commutation relations for the fields with their conjugates ($\tau = x^+ = y^+ = 0, \underline{x} = (x^-, x_\perp), \ldots$):

$$
\begin{aligned}
\left\{\psi_+(\underline{x}),\ \psi^\dagger_+(\underline{y})\right\} &= \Lambda_+\, \delta^3(\underline{x}-\underline{y}) \,, \\
\left[A^i(\underline{x}),\ \partial^+ A^j_\perp(\underline{y})\right] &= i\delta^{ij}\, \delta^3(\underline{x}-\underline{y}) \,.
\end{aligned}
\tag{B5}
$$

As described in the third section, the creation and annihilation operators define the Fock state basis for the theory at $\tau = 0$, with a vacuum $|0\rangle$ defined such that $b|0\rangle = d|0\rangle = a|0\rangle = 0$. The

evolution of these states with τ is governed by the light-cone Hamiltonian, $H_{LC} = P^-$, conjugate to τ. Combining Eqs. (B1) and (B2), the Hamiltonian is readily expressed in terms of ψ_+ and $A^i_\perp$:

$$H_{LC} = H_0 + V \ , \tag{B6}$$

where

$$\begin{aligned} H_0 &= \int d^3x \left\{ \mathrm{Tr}\left(\partial^i_\perp A^j_\perp \partial^i_\perp A^j_\perp\right) + \psi^\dagger_+ \left(i\partial_\perp \cdot \alpha_\perp + \beta m\right) \frac{1}{i\partial^+} \left(i\partial_\perp \cdot \alpha_\perp + \beta m\right) \psi_+ \right\} \\ &= \sum_{\substack{\lambda \\ \text{colors}}} \int \frac{dk^+ \, d^2k_\perp}{16\pi^3 \, k^+} \left\{ a^\dagger(\underline{k},\lambda)\, a(\underline{k},\lambda) \frac{k_\perp^2}{k^+} + b^\dagger(\underline{k},\lambda)\, b(\underline{k},\lambda) \right. \\ &\quad \left. \times \frac{k_\perp^2 + m^2}{k^+} + d^\dagger(\underline{k},\lambda)\, b(\underline{k},\lambda) \frac{k_\perp^2 + m^2}{k^+} \right\} + \text{constant} \end{aligned} \tag{B7}$$

is the free Hamiltonian and V the interaction:

$$\begin{aligned} V = \int d^3x \ \Big\{ & 2g \ \mathrm{Tr}\left(i\partial^\mu \widetilde{A}^\nu \left[\widetilde{A}_\mu, \widetilde{A}_\nu\right]\right) - \frac{g^2}{2} \mathrm{Tr}\left(\left[\widetilde{A}^\mu, \widetilde{A}^\nu\right]\left[\widetilde{A}_\mu, \widetilde{A}_\nu\right]\right) \\ & + g\overline{\widetilde{\psi}} \ \widetilde{\not{A}} \widetilde{\psi} + g^2 \, \mathrm{Tr}\left(\left[i\partial^+ \widetilde{A}^\mu, \widetilde{A}_\mu\right] \frac{1}{(i\partial^+)^2} \left[i\partial^+ \widetilde{A}^\nu, \widetilde{A}_\nu\right]\right) \\ & + g^2 \overline{\widetilde{\psi}} \ \widetilde{\not{A}} \frac{\gamma^+}{2i\partial^+} \ \widetilde{\not{A}} \widetilde{\psi} - g^2 \overline{\widetilde{\psi}} \gamma^+ \left(\frac{1}{(i\partial^+)^2} \left[i\partial^+ \widetilde{A}^\nu, \widetilde{A}_\nu\right]\right) \widetilde{\psi} \\ & + \frac{g^2}{2} \, \overline{\psi} \gamma^+ \, T^a \psi \frac{1}{(i\partial^+)^2} \overline{\psi} \gamma^+ \, T^a \psi \Big\} \ , \end{aligned} \tag{B8}$$

with $\widetilde{\psi} = \widetilde{\psi}_- + \psi_+$ ($\to \psi$ as $g \to 0$) and $\widetilde{A}^\mu = (0, \widetilde{A}^-, A^i_\perp)$ ($\to A^\mu$ as $g \to 0$). The Fock states are obviously eigenstates of H_0 with

$$H_0 \left|n : k_i^+, k_{\perp i}\right\rangle = \sum_i \left(\frac{k_\perp^2 + m^2}{k^+}\right)_i \left|n : k_i^+, k_{\perp i}\right\rangle \ . \tag{B9}$$

It is equally obvious that they are not eigenstates of V, though any matrix element of V between Fock states is trivially evaluated. The first three terms in V correspond to the familiar three and four gluon vertices, and the gluon-quark vertex [Fig. 19(a)]. The remaning terms result from substitutions (B2), and represent new four-quanta interactions containing instantaneous fermion and gluon propagators [Fig. 19(b)]. All terms conserve total three-momentum $\underline{k} = (k^+, \vec{k}_\perp)$, because of the integral over $\underline{x}$ in V. Furthermore, all Fock states other than the vacuum have total $k^+ > 0$, since each individual bare quantum has $k^+ > 0$ [Eq. (B3)]. Consequently the

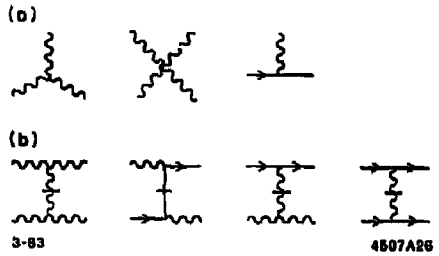

Fig. 19. (a) Basic interaction vertices in QCD.
(b) "Instantaneous" contributions.

Fock state vacuum must be an eigenstate of V and therefore an eigenstate of the full light-cone Hamiltonian.

Light-Cone Perturbation Theory

We define light-cone Green's functions to be the probability amplitudes that a state starting in Fock state $|i\rangle$ ends up in Fock state $|f\rangle$ a (light-cone) time τ later

$$\begin{aligned} \langle f|i\rangle\ G(f,i;\tau) &\equiv \langle f|e^{-iH_{LC}\tau/2}|i\rangle \\ &= i\int \frac{d\epsilon}{2\pi}\, e^{-i\epsilon\tau/2}\, G(f,i;\epsilon)\,\langle f|i\rangle\ , \end{aligned} \tag{B10}$$

where Fourier transform $G(f,i;\epsilon)$ can be written

$$\begin{aligned} \langle f|i\rangle\ G(f,i;\epsilon) &= \left\langle f\left|\frac{1}{\epsilon - H_{LC} + i0_+}\right|i\right\rangle \\ &= \left\langle f\left|\frac{1}{\epsilon - H_{LC} + i0_+} + \frac{1}{\epsilon - H_0 + i0_+} V \frac{1}{\epsilon - H_0 + i0_+}\right.\right. \\ &\quad \left.\left. + \frac{1}{\epsilon - H_0 + i0_+} V \frac{1}{\epsilon - H_0 + i0_+} V \frac{1}{\epsilon - H_0 + i0_+} + \ldots \right| i\right\rangle . \end{aligned} \tag{B11}$$

The rules for τ-ordered perturbation theory follow immediately from the expansion in (B9) when $(\epsilon - H_0)^{-1}$ is replaced by its spectral decomposition in terms of Fock states:

$$\frac{1}{\epsilon - H_0 + i0_+} = \sum_{n,\lambda_i} \int \tilde{\prod} \frac{dk_i^+\, d^2k_{\perp i}}{16\pi^3\, k_i^+}\ \frac{|n:\underline{k}_i,\lambda_i\rangle\ \langle n:\underline{k}_i,\lambda_i|}{\epsilon - \sum_i (k^2+m^2)_i/k_i^+ + i0_+} \tag{B12}$$

where in (B9) the sum becomes a sum over all states n intermediate between two interactions. To calculate $G(f,i;\epsilon)$ perturbatively then, all τ-ordered diagrams must be considered, the contribution from each graph computed according to the following rules:

1. Assign a momentum k^μ to each line such that the total $k^+, k_\perp$ are conserved at each vertex, and such that $k^2 = m^2$, i.e., $k^- = (k^2 + m^2)/k^+$. With fermions associate an on-shell spinor [from Eq. (B2)]

$$u(\underline{k}, \lambda) = \frac{1}{\sqrt{k^+}} \left(k^+ + \beta m + \vec{\alpha}_\perp \cdot \vec{k}_\perp \right) \begin{cases} \chi(\uparrow) & \lambda = \uparrow \\ \chi(\downarrow) & \lambda = \downarrow \end{cases}$$

or

$$v(\underline{k}, \lambda) = \frac{1}{\sqrt{k^+}} \left(k^+ - \beta m + \vec{\alpha}_\perp \cdot \vec{k}_\perp \right) \begin{cases} \chi(\downarrow) & \lambda = \uparrow \\ \chi(\uparrow) & \lambda = \downarrow \end{cases}$$

where $\chi(\uparrow) = 1/\sqrt{2}\,(1,0,1,0)$ and $\chi(\downarrow) = 1/\sqrt{2}\,(0,1,0,-1)^T$. For gluon lines, assign a polarization vector $\epsilon^\mu = (0,\ 2\vec{\epsilon}_\perp \cdot \vec{k}_\perp/k^+,\ \vec{\epsilon}_\perp)$ where $\vec{\epsilon}_\perp(\uparrow) = -1/\sqrt{2}\,(1,i)$ and $\vec{\epsilon}_\perp(\downarrow) = 1/\sqrt{2}\,(1,-i)$.

2. Include a factor $\theta(k^+)/k^+$ for each internal line.

3. For each vertex include factors as illustrated in Fig. 20. To convert incoming into outgoing lines or vice versa replace

$$u \leftrightarrow v\,, \qquad \overline{u} \leftrightarrow -\overline{v}\,, \qquad \epsilon \leftrightarrow \epsilon^*$$

in any of these vertices.

4. For each intermediate state there is a factor

$$\frac{1}{\epsilon - \sum_{\text{interm}} k^- + i0_+}$$

where ϵ is the incident P^-, and the sum is over all particles in the intermediate state.

5. Integrate $\int dk^+ d^2k_\perp/16\pi^3$ over each independent k, and sum over internal helicities and colors.

6. Include a factor -1 for each closed fermion loop, for each fermion line that both begins and ends in the initial state (i.e. $\overline{v} \ldots u$), and for each diagram in which fermion lines are interchanged in either of the initial or final states.

As an illustration, we give a representative contribution

$$\frac{1}{\epsilon - \sum_{i=b,d} \left(\frac{k_i^2 + m^2}{k^+} \right)_i} \cdot \frac{\theta(k_a^+ - k_b^+)}{k_a^+ - k_b^+}$$

$$\times \frac{g^2 \sum_\lambda \overline{u}(b)\, \epsilon^*(\underline{k}_a - \underline{k}_b, \lambda)\, u(a)\, \overline{u}(d)\, \not{\epsilon}(\underline{k}_a - \underline{k}_b, \lambda)\, u(c)}{\epsilon - \sum_{i=b,c} \left(\frac{k_i^2 + m^2}{k^+} \right)_i - \frac{(k_{1a} - k_{1b})^2}{k_a^+ - k_b^+}} \cdot \frac{1}{\epsilon - \sum_{i=a,c} \left(\frac{k_i^2 + m^2}{k^+} \right)_i}$$

(times a color factor) to the $q\overline{q} \to q\overline{q}$ Green's function. (The vertices for quarks and gluons of

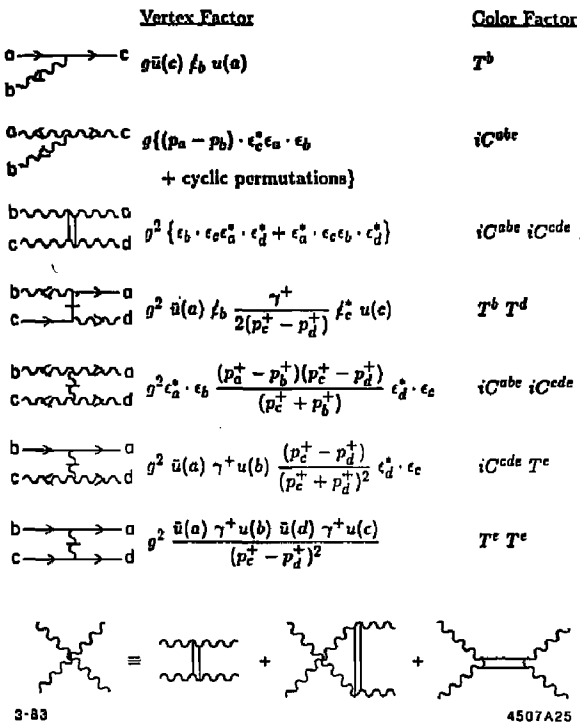

Fig. 20. Graphical rules for QCD in light-cone perturbation theory.

definite helicity have very simple expressions in terms of the momenta of the particles.) These same rules apply for scattering amplitudes, but with propagators omitted for external lines, and with $\epsilon = P^-$ of the initial (and final) states.

Finally, notice that this quantization procedure and perturbation theory (graph by graph) are manifestly invariant under a large class of Lorentz transformations:

1. boosts along the 3-direction — i.e. $p^+ \to Kp^+$, $p^- \to K^{-1}p^-$, $p_\perp \to p_\perp$ for each momentum;
2. transverse boosts — i.e. $p^+ \to p^+$, $p^- \to p^- + 2p_\perp\cdot Q_\perp + p^+Q_\perp^2$, $p_\perp \to p_\perp + p^+Q_\perp$ for each momentum ($Q_\perp$, like K, is dimensionless);
3. rotations about the 3-direction.

It is these invariances which lead to the frame independence of the Fock state wave functions. A comparison between τ-ordered and time-ordered perturbation theory is given in Table I.

Table I. Comparison Between Time-Ordered and τ-Ordered Perturbation Theory

Equal t	Equal $\tau = t + z$
$k^0 = \sqrt{\vec{k}^2 + m^2}$ (particle mass shell)	$k^- = \frac{k_\perp^2 + m^2}{k^+}$ (particle mass shell)
$\sum \vec{k}$ conserved	$\sum \vec{k}_\perp$, k^+ conserved
$M_{ab} = V_{ab} + \sum_c V_{ac} \frac{1}{\sum_a k^0 - \sum_c k^0 + i\epsilon} V_{cc}$	$M_{ab} = V_{ab} + \sum_c V_{ac} \frac{1}{\sum_a k^- - \sum_c k^- + i\epsilon} V_{cb}$
$n!$ time-ordered contributions	$k^+ > 0$ only
Fock states $\psi_n(\vec{k}_i)$	Fock states $\psi_n(\vec{k}_{\perp i}, x_i)$
$\sum_{i=1}^n \vec{k}_i = \vec{P} = 0$	$x = \frac{k^+}{P^+}$, $\sum_{i=1}^n x_i = 1$, $\sum_{i=1}^n \vec{k}_{\perp i} = 0$ $(0 < x_i < 1)$
$\mathcal{E} = P^0 - \sum_{i=1}^n k_i^0$	$\mathcal{E} = P^+ \left(P^- - \sum_{i=1}^n k_i^- \right)$
$= M - \sum_{i=1}^n \sqrt{k_i^2 + m_i^2}$	$= M^2 - \sum_{i=1}^n \left(\frac{k_\perp^2 + m^2}{x} \right)_i$

REFERENCES

1. G. P. Lepage, S. J. Brodsky, T. Huang and P. B. Mackenzie, CLNS–82/522, published in Banff Summer Institute 81 (1981).

APPENDIX C

FACTORIZATION PROPERTIES OF THE DEUTERON FORM FACTOR

From the standpoint of quantum chromodynamics the deuteron is a complex dynamical system. At large distances the deuteron is evidently well described as a $J = 1$, $I = 0$, $Q = 1$ composite of two nucleon clusters with binding energy ~ 2.2 MeV, together with small admixtures of $\Delta\Delta$ and virtual meson components. However, at short distances, in the region where all six quarks overlap within a distance $R = 1/Q \to 0$, one can show rigorously that the deuteron state in QCD necessarily has "fractional parentage" $(1/9)\,np$, $(4/45)\,\Delta\Delta$, and $(4/5)$ "hidden color" (nonnuclear) components.[1,2] In fact, at any momentum scale the deuteron cannot be described solely in terms of standard nuclear physics degrees of freedom, and in principle, any physical or dynamical property of the deuteron is modified by the presence of such non-Abelian components. In particular, the standard "impulse approximation" form for the deuteron form factor

$$F_d(Q^2) = F_d^{\text{body}}(Q^2)\, F_N(Q^2) \quad , \tag{C1}$$

where F_N is the on-shell nucleon form factor, cannot be precisely valid at any momentum transfer scale $Q^2 = -q^2 \neq 0$ because of hidden color components. More important, even if only the nucleon–nucleon component were important, Eq. (C1) cannot be reliable for composite nucleons since the struck nucleon is necessarily off-shell[3] in the nuclear wave function: $|k'^2 - k^2| \sim \frac{1}{2}Q^2$ (see Fig. 14). Thus in general one requires knowledge of the nucleon form factors $F_N(q^2, k^2, k'^2)$ for the case in which one or both nucleon legs are off-shell. In QCD such amplitudes have completely different dynamical dependence compared to the on-shell form factors.

Although Eq. (C1) has been used extensively in nuclear physics as a starting point for the analysis of nuclear form factors,[4] its range of validity has never been seriously questioned. Certainly in the non-relativistic domain where target recoil and off-shell effects can be neglected, the charge form factor of a composite system can be computed from the convolution of charge distributions. However, in the general situation, the struck nucleon must transfer a large fraction of its momentum to the spectator system, rendering the nucleon state off-shell. As we shall show here, the region of validity of Eq. (C1) for the deuteron is very small:

$$Q^2 > 2 M_d\, \epsilon_d$$

i.e., $Q \lesssim 100$ MeV. However, in this region the nucleon form factor does not deviate significantly from unity, so Eq. (C1) is of doubtful utility.

The form factor $F_d(Q^2)$ is, by definition, the probability amplitude for the deuteron to stay intact after absorbing momentum transfer Q. If the deuteron is taken as a lightly-bound cluster

of two nucleons, then the form factor contains the probability amplitudes for each nucleon to remain intact after absorbing momentum transfer $\sim q^\mu/2$. Thus, it is natural to factorize F_d in the form[5]

$$F_d(Q^2) = f_d(Q^2)\ F_N^2(Q^2/4) \qquad , \tag{C2}$$

which defines the "reduced" form factor $f_d(Q^2)$. As shown in Chapter 3, QCD predicts $Q^2\ f_d(q^2) \cong$ const [modulo logarithmic modifications due to the running coupling constant anomalous dimensions of the nuclear wave function], which is in excellent agreement with experiment for $1 \leq Q^2 \lesssim 4$ GeV^2 (see Fig. 11). Thus it is interesting to understand the origin of the reduced form factor factorization, Eq. (C2), from a fundamental point of view and to verify for which regime, if any, the standard impulse approximation form, Eq. (C1), is valid or useful.

To study these questions, we will construct a simple covariant and gauge-invariant dynamical model of the deuteron which allows an analysis of the effects of nucleon compositeness in the nuclear wave function:

$$\mathcal{L}_I = g\ \phi_d\ \phi_N\ \phi_N + h\ \epsilon_{ijk}\ \phi_N\ q^i\ q^j\ q^k \qquad . \tag{C3}$$

Here g and h are the coupling constants of a deuteron to two nucleons and a nucleon to three quarks, respectively, and ϵ_{ijk} represents the SU(3) color singlet coupling. The quarks carry the electromagnetic current. This model gives an effective deuteron wavefunction with a factorized two-nucleon structure (see Sec. 2.1),

$$\Psi_d = \psi_d^{\text{body}}\ \times\ \psi_N\ \times\ \psi_N\ . \tag{C4}$$

Within the framework of this simple model, which neglects hidden color components, we derive the cluster decomposition[6] property of the deuteron wave function and identify a transition region between forms (C1) and (C2).

In QCD the deuteron is a color-singlet composite of six quarks. Using light-cone quantization, one can define a consistent Fock state basis at equal $\tau = t + z/c$ which defines the deuteron in terms of $|6q\rangle$, $|6q+g\rangle$, $|6q+q\bar{q}\rangle$ components. Only one of the five $|6q\rangle$ color singlet configurations corresponds to the usual $|NN\rangle$ nucleon-nucleon clustering. However, since the binding energy of the deuteron is very small, we shall assume that the $|6q\rangle = |NN\rangle$ configuration is by far dominant in the natural kinematic domain of the wavefunction. This structure is represented in its simplest form by the lagrangian of Eq. (C3). The resulting deuteron wavefunction is illustrated in Fig. 21.

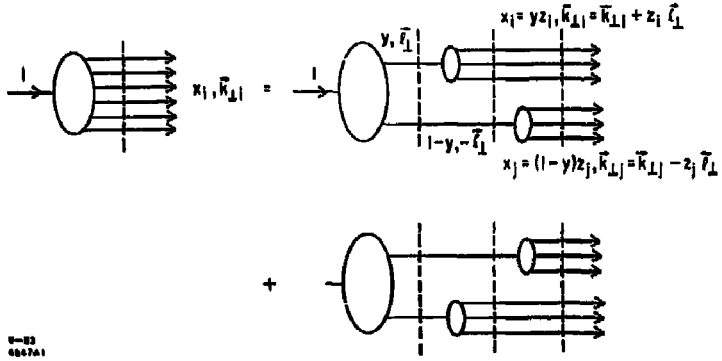

Fig. 21. The diagrammatic kernel equation of the relativistic deuteron wave function on the light-cone frame. The effective ϕ^3-type interaction [see Eq. (C3)] provides the clustering of two separate nucleons.

In terms of the light-cone variables

$$x_i = \frac{(k^0 + k^z)i}{p^0 + p^z}\,, \quad \sum_{i=1}^{6} x_i = 1, \quad \sum_{i=1}^{6} \vec{k}_{\perp i} = 0$$

the wave function has the form of a convolution:[7]

$$\left(M^2 - \sum_{i=1}^{6} \frac{\vec{k}_{\perp i}^2 + m_i^2}{x_i}\right) \Psi_d(x_i, \vec{k}_{\perp i}) = \frac{g}{M^2 - \dfrac{\vec{\ell}_\perp^2 + M_N^2}{y(1-y)}} \frac{1}{y} \frac{1}{1-y}$$

$$\times h^2 \left(\frac{1}{M^2 - \dfrac{\vec{\ell}_\perp^2 + M_N^2}{(1-y)} - \sum_{i=1}^{3} \dfrac{\vec{k}_{\perp i}^2 + m_i^2}{x_i}} + \frac{1}{M^2 - \dfrac{\vec{\ell}_\perp^2 + M_N^2}{y} - \sum_{j=4}^{6} \dfrac{\vec{k}_{\perp j}^2 + m_j^2}{x_j}} \right), \tag{C5}$$

where M, M_N and m_i are the masses of the deuteron, the nucleon, and the quarks, respectively, and the momentum-conserving delta function fixes $y = \sum_{i=1}^{3} x_i$ and $\vec{\ell}_\perp = \sum_{i=1}^{3} \vec{k}_{\perp i}$. If we define the function $\epsilon(y, \vec{\ell}_\perp)$,

$$\epsilon(y, \vec{\ell}_\perp) = M^2 - \frac{\vec{\ell}_\perp^2 + M_N^2}{y(1-y)} \quad , \tag{C6}$$

then $\epsilon(y, \vec{\ell}_\perp)$ measures the deuteron off-shell light-cone energy $\epsilon = p^+ \cdot \sum_{i=1}^{6} k_i^-$. The zero-binding energy limit implies $\epsilon(y, \vec{\ell}_\perp) \to 0$. In the $\epsilon(y, \vec{\ell}_\perp) \to 0$ limit, $y \to 1/2$ and $\vec{\ell}_\perp \to 0$ since $M^2 \to 4M_N^2$. Thus we obtain approximate delta function behavior of $\epsilon^{-1}(y, \vec{\ell}_\perp)$ near the zero

binding energy limit:

$$\epsilon^{-1}(y,\vec{\ell}_\perp) \sim \delta\left(y-\frac{1}{2}\right)\delta^2(\vec{\ell}_\perp) \quad . \tag{C7}$$

In this limit, the factor inside the parenthesis of the right hand side of Eq. (2.1) is given by

$$\frac{M^2-\sum_{i=1}^{6}\frac{\vec{k}_{\perp i}^2+m_i^2}{x_i}}{\left(M^2-\frac{\vec{\ell}_\perp^2+M_N^2}{(1-y)}-\sum_{i=1}^{3}\frac{\vec{k}_{\perp i}^2+m_i^2}{x_i}\right)\left(M^2-\frac{\vec{\ell}_\perp^2+M_N^2}{y}-\sum_{j=4}^{6}\frac{\vec{k}_{\perp j}^2+m_j^2}{x_j}\right)} \quad . \tag{C8}$$

The numerator of the right hand side of Eq. (2.4) is cancelled by the factor on the left hand side of Eq. (2.1) so that in $\epsilon(y,\vec{\ell}_\perp)\to 0$ limit $\Psi_d(x_i,\vec{k}_{\perp i})$ is given by

$$\begin{aligned}\Psi_d(x_i,\vec{k}_{\perp i}) =& \frac{g}{M^2-\frac{\vec{\ell}_\perp^2+M_N^2}{y(1-y)}}\ \frac{1}{y}\ \frac{h}{M^2-\frac{\vec{\ell}_\perp^2+M_N^2}{(1-y)}-\sum_{i=1}^{3}\frac{\vec{k}_{\perp i}^2+m_i^2}{x_i}} \\ &\times\frac{1}{1-y}\ \frac{h}{M^2-\frac{\vec{\ell}_\perp^2+M_N^2}{y}-\sum_{j=4}^{6}\frac{\vec{k}_{\perp j}^2+m_j^2}{x_j}} \quad .\end{aligned} \tag{C9}$$

If we change to the variables:

$$\begin{aligned} z_i &= \frac{x_i}{y} \quad , \quad \vec{k}'_{\perp i} = \vec{k}_{\perp i} - z_i\,\vec{\ell}_\perp \qquad (i=1,2,3) \\ z_j &= \frac{x_j}{1-y} \quad , \quad \vec{k}'_{\perp j} = \vec{k}_{\perp j} - z_j\,\vec{\ell}_\perp \qquad (j=4,5,6) \quad , \end{aligned} \tag{C10}$$

then for $\epsilon\to 0$ Eq. (2.5) is reduced to

$$\Psi_d(x_i,\vec{k}_{\perp i}) = \frac{g}{M^2-\frac{\vec{\ell}_\perp^2+M_N^2}{y(1-y)}}\ \frac{h}{M_N^2-\sum_{i=1}^{3}\frac{\vec{k}'^2_{\perp i}+m_i^2}{z_i}}\ \frac{h}{M_N^2-\sum_{j=4}^{6}\frac{\vec{k}'^2_{\perp j}+m_j^2}{z_j}} \quad . \tag{C11}$$

This is the expected factorized form of the deuteron wave function since the last two terms of the right hand side of Eq. (2.8) are the nucleon wave functions $\psi_N(z_i,\vec{k}'_\perp)$ and $\psi_N(z_j,\vec{k}'_\perp)$. The light-cone variables z_i and $\vec{k}'_{\perp i}$ are the light-cone momentum fractions and the transverse momenta in the hadron relative to the struck nucleon. The first term of the right hand side of Eq. (2.8) is the "body" wave function $\psi_d^{\rm body}(y,\vec{\ell}_\perp)$. This proves the factorization of the deuteron wave function in the zero binding energy limit:

$$\Psi_d(x_i,\vec{k}_{\perp i}) \;=\; \psi_d^{\rm body}(y,\vec{\ell}_\perp)\ \psi_N(z_i,\vec{k}'_{\perp i})\ \psi_N(z_j,\vec{k}'_{\perp j}) \quad . \tag{C12}$$

The form factor of the deuteron is given exactly in terms of the light-cone Fock state expansion by the Drell–Yan formula, Eq. (2.2).[8] In the last section we demonstrated the factorization of

$\Psi_d(x_i, \vec{k}_{\perp i})$ for small $\epsilon(y, \vec{\ell}_\perp)$. If $|\vec{q}_\perp|$ is the order of $|\vec{\ell}_\perp|$ or $|\vec{k}_{\perp i}|$, then $\psi^*\left(x_i, \vec{k}_{\perp i} + (\delta_{ia} - x_i)\,\vec{q}_\perp\right)$ is factorized in the same way as $\psi(x_i, \vec{k}_{\perp i})$ since $\epsilon(y, \vec{\ell}_\perp + (1-y)\vec{q}_\perp)$ is almost the same as $\epsilon(y, \vec{\ell}_\perp)$. Thus for small q^2 the factorization of $\sum_{a=1}^{6} \Psi_d^*\left(x_i, \vec{k}_{\perp i} + (\delta_{ia} - x_i)\,\vec{q}_\perp\right)$ is given by

$$\sum_{a=1}^{6} \Psi_d^*\left(x_i, \vec{k}_{\perp i} + (\delta_{ia} - x_i)\,\vec{q}_\perp\right) = \psi_d^{*\,\mathrm{body}}\left(y, \vec{\ell}_\perp + (1-y)\vec{q}_\perp\right)$$

$$\times \left[\sum_{a=1}^{3} \psi_N^*\left(z_i, \vec{k}'_{\perp i} + (\delta_{ia} - z_i)\,\vec{q}_\perp\right)\, \psi_N^*(z_j, \vec{k}'_{\perp j}) \right. \tag{C13}$$

$$\left. + \sum_{a=4}^{6} \psi_N^*(z_i, \vec{k}'_{\perp i})\, \psi_N^*\left(z_j, \vec{k}'_{\perp j} + (\delta_{ja} - z_j)\,\vec{q}_\perp\right)\right] .$$

This result becomes invalid when $|\vec{q}_\perp|$ is much larger than $|\vec{\ell}_\perp|$ since $\epsilon(y, \vec{\ell}_\perp + (1-y)\vec{q}_\perp)$ is then non-negligible. Thus Eq. (2.10) becomes

$$\begin{aligned} F_d(\vec{q}_\perp^{\,2}) \;=\; & \int_0^1 \frac{dy}{y(1-y)} \int \frac{d^2\vec{\ell}_\perp}{16\pi^3}\, \psi_d^{*\,\mathrm{body}}\left(y, \vec{\ell}_\perp + (1-y)\vec{q}_\perp\right)\, \psi_d^{\mathrm{body}}(y, \vec{\ell}_\perp) \\ & \times \left[\sum_{a=1}^{3} e_a \int [dx]_i \int [d^2\vec{k}'_\perp]_i\, \psi_N^*\left(z_i, \vec{k}'_{\perp i} + (\delta_{ia} - z_i)\,\vec{q}_\perp\right)\, \psi_N(z_i, \vec{k}'_{\perp i}) \right. \\ & \times \int [dx]_j \int [d^2\vec{k}'_\perp]_j\, \psi_N^*(z_j, \vec{k}'_{\perp j})\, \psi_N(z_j, \vec{k}'_{\perp j}) \\ & + \sum_{a=4}^{6} \int [dx]_i \int [d^2\vec{k}'_\perp]_i\, \psi_N^*(z_i, \vec{k}'_{\perp i})\, \psi_N(z_i, \vec{k}'_{\perp i}) \\ & \times e_a \int [dx]_j \int [d^2\vec{k}'_\perp]_j\, \psi_N^*\left(z_j, \vec{k}'_{\perp j} + (\delta_{ja} - z_j)\,\vec{q}_\perp\right)\, \psi_N(z_j, \vec{k}'_{\perp j}) \Big] \\ = \; & \sum_N F_N(\vec{q}_\perp^{\,2})\, F_d^{\mathrm{body}}(\vec{q}_\perp^{\,2}) \quad , \end{aligned} \tag{C14}$$

where the body form factor $F_d^{\mathrm{body}}(\vec{q}_\perp^{\,2})$ is defined by

$$F_d^{\mathrm{body}}(\vec{q}_\perp^{\,2}) \;=\; \int_0^1 \frac{dy}{y(1-y)} \int \frac{d^2\vec{\ell}_\perp}{16\pi^3}\, \psi_d^{*\,\mathrm{body}}\left(y, \vec{\ell}_\perp + (1-y)\vec{q}_\perp\right)\, \psi_d^{\mathrm{body}}(y, \vec{\ell}_\perp) \,. \tag{C15}$$

Equation (2.15) is the same form as Eq. (C1). This proves the impulse approximation at small $|\vec{q}_\perp|$.

When $|\vec{q}_\perp|$ becomes large, $|\vec{q}_\perp| \gg |\vec{\ell}_\perp|$ or $|\vec{k}_{\perp i}|$, the impulse approximation breaks down since $|\epsilon\left(y, \vec{\ell}_\perp + (1-y)\vec{q}_\perp\right)|$ becomes large and $\Psi_d^*\left(x_i, \vec{k}_{\perp i} + (\delta_{ia} - x_i)\,\vec{q}_\perp\right)$ cannot be factorized in the same way as $\psi(x_i, \vec{k}_{\perp i})$. The quarks of the deuteron must interact so that a large fraction of $\vec{q}_\perp$ can be transferred from the quark which absorbs $\vec{q}_\perp$ to a quark of the other nucleon. Since the exchanged gluon is a color octet, quarks must be interchanged between the nucleons in order to satisfy the color selection rules.

Taking a and b as the indices of two interchanged quarks, we obtain for large $\vec{q}_\perp^{\,2}$:

$$\sum_{a=1}^{6} \Psi_d\left(x_i, \vec{k}_{\perp i} + (\delta_{ia} - x_i)\,\vec{q}_\perp\right) = \left(\sum_{a=1}^{3}\sum_{b=4}^{6} + \sum_{a=4}^{6}\sum_{b=1}^{3}\right) \frac{x_a}{x_a - 1}$$

$$\times\ \frac{1}{\vec{q}_\perp^{\,2}}\, V\left(x_i,\ (\delta_{ia} - x_i)\vec{q}_\perp;\ x_j,\ \{y\delta_{ja} + (1-y)\delta_{jb} - x_j\}\,\vec{q}_\perp\right) \tag{C16}$$

$$\times\ \psi_N\left(x_i, \vec{k}'_{\perp i} + (\delta_{ia} - x_i)y\vec{q}_\perp\right)$$

$$\times\ \psi_N\left(x_j, \vec{k}'_{\perp j} + (\delta_{bj} - x_j)(1-y)\vec{q}_\perp\right)\ \psi_{NR}^d(\vec{0}) \quad ,$$

where the kernel V can be obtained by calculating the diagrams shown in Fig. 22. The weak binding of the deuteron forces $y \sim \frac{1}{2}$. On the average we expect the struck and interchanged quark to have roughly the same x. With this approximation we obtain the factorization of the form factor from Eq. (2.10):

$$F(\vec{q}_\perp^{\,2}) = \frac{C}{\vec{q}_\perp^{\,2}}\,|\psi_{NR}^d(\vec{0})|^2$$

$$\times \left[\sum_{a=1}^{3}\int [dx]_i\,[d^2\vec{k}'_\perp]_i\ \psi_N^*\left(x_i, \vec{k}'_{\perp i} + (\delta_{ia} - x_i)\,\frac{\vec{q}_\perp}{2}\right)\ \psi_N(x_i, \vec{k}'_\perp)\right. \tag{17}$$

$$\left.\times \sum_{b=4}^{6}\int [dx]_j\,[d^2\vec{k}'_\perp]_j\ \psi_N^*\left(x_j, \vec{k}'_{\perp j} + (\delta_{jb} - x_j)\,\frac{\vec{q}_\perp}{2}\right)\psi_N(x_j, \vec{k}'_\perp) + (a \leftrightarrow b)\right]$$

$$= f_d(\vec{q}_\perp^{\,2})\ F_N^2\left(\vec{q}^{\,2}/4\right) \quad ,$$

where the reduced form factor $f_d(\vec{q}_\perp^{\,2})$ is defined by

$$f_d(\vec{q}_\perp^{\,2}) = \frac{C}{\vec{q}_\perp^{\,2}}\,|\psi_{NR}^d(\vec{0})|^3 \quad , \tag{C18}$$

and C is determined by value of the kernel V. More generally, we iterate the wavefunction wherever large momentum transfer is required and in this way build up the entire T_H contribution

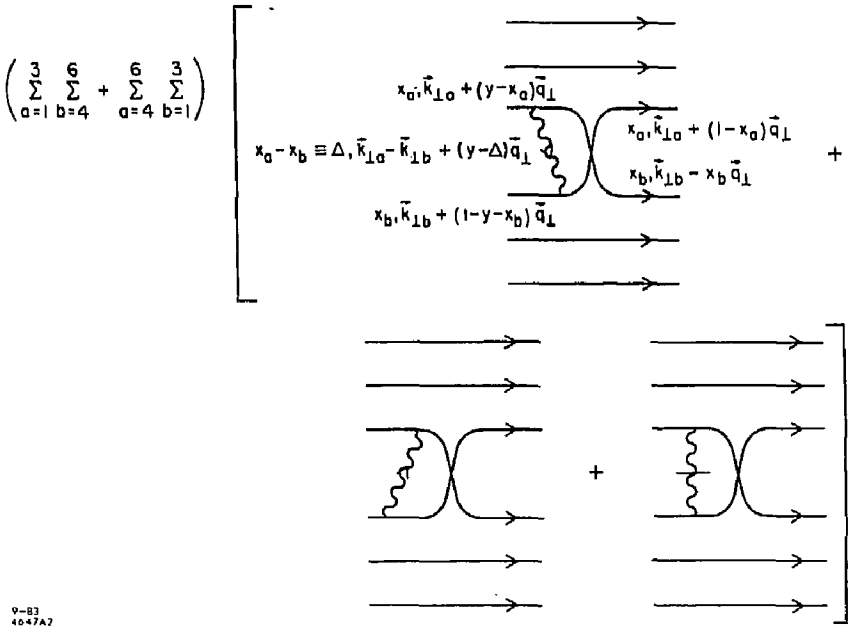

Fig. 22. The lowest order diagrams of the quark interchange model. By the constraint for the deuteron to be loosely bounded after absorbing $\vec{q}_\perp$, the momenta of each constituent are fixed.

to the form factor, as in Eq. (C6). Equation (2.2) is thus the same form as Eq. (C2). This proves the transition of the form factor at large $|\vec{q}_\perp|$ ($|\vec{q}_\perp| \gg |\vec{\ell}_\perp|$ or $|\vec{k}_{\perp i}|$) from the impulse approximation form to the reduced form.

In the full QCD analyses, the iteration of the gluon exchange kernel leads to a logarithmically-evoluting distribution amplitude which replaces $\psi^d_{NR}(\vec{0})$. At large Q^2 the gluon exchange kernel generates other color singlet configuration of six quarks, so that the approximation that the deuteron only consists of a nucleon pair breaks down. The complete calculation of the deuteron form factor thus requires the inclusion of these other components. The reduced form factor prediction is useful for incorporating non-leading power law corrections, but it does not include the hidden color contributions of the deuteron wavefunction (see Fig. 23).

The factorization of light-cone wavefunctions leads, as we have shown, to various forms of factorization for the nuclear form factor. At low $Q^2 < 2M_d\epsilon_d$, the usual impulse approximation result is valid. The region of validity of this form though is limited to momentum transfers smaller than the inverse size of the nucleus. In this case, the struck nucleon can remain nearly on-shell by virtue of the nuclear Fermi motion. For larger Q^2, the kinematics the struck nucleon is forced off-shell and the traditional form of factorization becomes useless. Fortunately, in this domain the

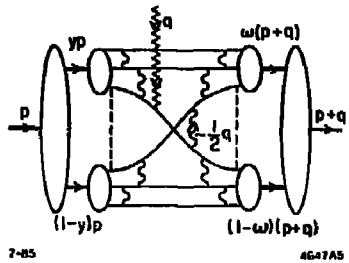

Fig. 23. QCD analysis of the reduced form factor. The gluon exchange contributions to the deuteron wavefunction lead to hidden color components and are not included.

reduced form factor result becomes valid, replacing the impulse approximation as a valid starting point for QCD phenomenology.

REFERENCES

1. S. J. Brodsky, C.–R. Ji and G. P. Lepage, *Phys. Rev. Lett.* **51**, 83 (1983).
2. M. Harvey, *Nucl. Phys.* **A352**, 301 (1981); **A352**, 326 (1981).
3. For a general discussion of off-shell nucleon form factors, A. M. Bincer, *Phys. Rev.* **118**, 855 (1960).
4. S. A. Gurvitz, *Phys. Rev.* **C22**, 725 (1980); R. D. Amado, M. P. Lockher and M. Simonius, *Phys. Rev.* **C17**, 403 (1978). In these References, it is argued that exchange current contributions can compensate for the off-shell nucleon corrections to the impulse formula (C1). The analyses are based on a soft gaussian like interactions and are invalid for the power-law forms of QCD. In fact exchange current contributions take the form of the reduced form factor result (C2). See Blankenbecler and Gunion, *Phys. Rev.* **D4**, 718 (1971).
5. S. J. Brodsky and B. T. Chertok, *Phys. Rev. Lett.* **37**, 269 (1976); *Phys. Rev.* **D14**, 3003 (1976); S. J. Brodsky and J. Hiller, *Phys. Rev. Lett.* **C28**, 475 (1983).
6. J. Namyslowski, *Proc. of the 9th Int. Conf. on Few Body Problems, Eugene, Oregon*, 1980.
7. D. Kusno, *Phys. Rev.* **D26**, 3276 (1982); D. Kusno and M. J. Moravcsik, *Phys. Rev.* **D20**, 2734 (1981); D. Kusno and K. R. Wiharti, *Fisika UI–82/4* (1982): In these papers the truncated n–p–d vertex function is simplified to a constant g in the present analysis.
8. S. D. Drell and T. M. Yan, *Phys. Rev. Lett.* **24**, 181 (1970).